SOUTHERN HEMISPHERE EARLY-TYPE STARS AT INTERMEDIATE AND HIGH GALACTIC LATITUDES

David Kilkenny

A Thesis Submitted for the Degree of PhD
at the
University of St Andrews

1973

SOUTHERN HEMISPHERE EARLY - TYPE STARS

AT

INTERMEDIATE AND HIGH GALACTIC LATITUDES

by

David Kilkenny

A dissertation submitted for the degree of Ph.D. at the University of St. Andrews

St. Andrews September 1973

Declaration

Except where reference is made to the work of others, the research described in this thesis and the composition of the thesis are my own work. No part of this work has been submitted for a higher degree at this or any other University. Under Ordinance General No. 12, I was admitted to the Faculty of Science of the University of St. Andrews as a research student on the 1st October 1969, to carry out photometric and spectroscopic observations of early-type stars at intermediate galactic latitudes, with the general aim of investigating the distribution and motions of these stars. I was accepted as a candidate for the degree of Ph.D. on the 1st October 1970, under Resolution of the University Court, 1967, No.1

24.SEP.73

Certificate

I certify that David Kilkenny has spent nine terms in research work at the University Observatory, St. Andrews, that he has fulfilled the conditions of Ordinance General No.12 and Senate Regulations under Resolution of the University Court,1967, No.1, and that he is qualified to submit the accompanying dissertation in application for the degree of Ph.D.

Contents

Abstract

A survey of early-type stars at intermediate galactic latitudes was carried out in the southern hemisphere winters of 1970 and 1971. The observing programme was limited to negative declinations and covered a range in right ascension of approximately 12^h to 20^h. At the Royal Observatory, Cape Town, in 1970, UBV photoelectric measurements were made of 56 stars for which no UBV data existed and 20 stars which had been observed on one or two previous occasions, the intention being to obtain four separate measures of each star. In 1971, the Bochum University telescope at the E.S.O. site in Chile was used for Hβ photoelectric photometry of over 200 intermediate and high latitude stars. Shortly afterwards, spectra for radial velocity determination and MK classification were obtained with the two-prism spectrograph and 74" reflector of Radcliffe Observatory, Pretoria. Work was concentrated upon some 60 stars not previously observed with spectroscopic equipment and selected on the basis of blue colour or possible high luminosity from photometric considerations. A few southern standard stars and stars from earlier Radcliffe programmes were re-observed as control or overlap stars. Chapters II - IV describe the observational procedures and reduction methods. Tables in chapter V contain results from the 1970-71 programmes plus UBV and spectroscopic data for intermediate and high latitude stars from various other sources.

The remaining chapters are concerned with analysis and discussion of the observations. Chapter VI summarises some optical and radio determinations of the spiral structure of the Galaxy and compares the spatial distribution of the programme stars with these results. The possibility that early-type stars may be formed well away from the galactic plane is considered by comparison of

kinematic and evolutionary lifetimes of some stars at appreciable distances from the plane. In chapter VII, intermediate and high latitude stars are shown to participate in the differential rotation of the Galaxy and detailed analysis of the space motions of a number of high velocity stars leads to the conclusion that some may have sufficient energy to escape from the galactic system. The radial velocities of interstellar Ca II lines are shown in chapter VIII to be as expected for material in the solar neighbourhood involved in differential galactic rotation. An apparent deviation from circular motion, reported by observers investigating H II regions, is also present in the Ca II gas. Constants in the cosecant equation of interstellar reddening are re-determined and show an apparently significant difference between northern and southern galactic hemispheres.

Appendix I describes attempts to simulate the effect of Hβ filters in order to explain the curvature in the transformations from instrumental to standard photometric systems. Appendix II gives details of the method used to compute stellar space velocities from proper motions and radial velocities and includes a short Fortran IV programme which implements the operations described.

Illustrations

Illustrations (cont.)

Tables

CHAPTER I

INTRODUCTION

Most of the work on galactic spiral structure as defined by optical surveys of young objects, has for obvious reasons dealt with areas of sky close to the equatorial plane of the Galaxy. As a consequence, the equatorial regions have been extensively surveyed, at least as far as small and medium size telescopes are concerned. This is one reason for the present survey of early-type stars at intermediate galactic latitudes but there are several other considerations.

A recent northern hemisphere study by Kepner (1970) has demonstrated that spiral arms delineated by the distribution of neutral hydrogen appear to extend to one or two kiloparsecs from the galactic plane. It is therefore of some interest to discover whether or not the early-type stars away from the plane show any tendency to follow similar spiral structure to that traced by young objects near the plane. If intermediate latitude stars are linked to the spiral arms, this could prove useful for investigating distant galactic structure. A few degrees on either side of the galactic equator, the obscuration caused by interstellar gas and dust becomes very much less than in the equatorial regions and it is possible to observe distant stars which are not heavily reddened. In particular, it was hoped to observe stars related to the -II or Norma-Scutum spiral arm without the problem of heavy obscuration caused by material of the -I or Sagittarius arm.

Finally, surveys of blue stars at higher latitudes have often discovered unusual objects. Thackeray and Wesselink (1952) found the helium star HD 168476 and surveys by Feast and Thackeray (1963) and Hill (1971) have located apparently normal early-type stars with high radial velocities which cannot be attributed to the effect of differential galactic rotation.

1. The observing programme

The basis of the programme was a list of stars selected from the Henry Draper Catalogue (Cannon and Pickering, 1918-24). Dr. P.W. Hill made available a magnetic tape containing data for all O- and B-type stars in the HD catalogue plus a library of access and sort programmes to retrieve and print the data. Thus a list was compiled of O-B5 stars fainter than seventh magnitude and in the latitude range $7^{\circ}<b<15^{\circ}$, together with a secondary list of B8-9 stars in the same range. The lower latitude limit was chosen to be above the normal upper limit for near-equatorial surveys and also above the worst of the obscuring material. The upper limit is roughly equal to the lower limit of completion of a high latitude early-type star survey carried out by Hill (1970). To the basic O-B5 list were added several faint stars not classified by the HD survey but with spectral types from the Cape Photographic Catalogue for 1950 (Stoy, 1966). These stars are referred to by "CPD" numbers from the Cape Photographic Durchmusterungen (Gill and Kapteyn, 1899). Also included in the primary observing list were a few B8-9 stars which were possible giants or supergiants. Such stars might have HD catalogue comments "narrow lines" for example. Excluded from the programme were known variable or binary stars and emission-line stars. To eliminate the latter, an unpublished survey by Henize of Hα-emission objects in the southern hemisphere was used and I am grateful to Dr. A.D. Thackeray for allowing me to consult the Radcliffe copy of this catalogue. Shortly afterwards, the compilation by Wackerling (1970) was published and provided a useful check for emission stars.

It was originally intended to make UBV and Hβ measurements at the

Royal Observatory, Cape Town in the southern winter of 1970. The data thus obtained would then be used to select the bluest and most luminous stars for priority of observation with Radcliffe spectrographic equipment in 1971. The 1970 Hβ programme was severely curtailed by poor weather and late delivery of the interference filters but, fortunately, observing time was made available by the Ruhr-Universität Bochum on their 24-inch telescope at the European Southern Observatory site in Chile. This permitted Hβ measurements to be made of all the intermediate latitude programme stars together with high latitude stars from the survey by Hill (1970) and other sources.

2. General Aims

Photometric and spectroscopic reductions and results are described in chapters II - V. The UBV photometry is used to determine and correct for the effect of interstellar extinction on the V-magnitudes of the programme stars. The Hβ-index provides a measure of the absolute magnitude of each star which in turn gives a distance estimate when combined with the corrected V-magnitude. Spectra were principally for radial velocity measurement of stellar and interstellar features but also yield an estimate of absolute magnitude by way of the MK classification system, and furnish a means of checking for binary or emission stars. With stellar distances we can investigate the space distribution of the programme stars and from radial velocities a study of certain kinematical effects can be made. If reliable proper motions exist, which is not often the case with early-type stars, space velocity components and total space motions can be calculated.

The use of Hβ photometry for absolute magnitude determination has advantages over MK-type luminosities in that the former uses a continuous rather than a discrete calibration and is, or should be, virtually free from personal systematic errors. Of course there are disadvantages with the photometric method; erroneous results will be obtained for multiple stars and stars with any trace of emission in the Hβ absorption line. The latter should be largely eliminated by rejecting stars listed in Hα surveys and the problem of multiple stars can be reduced by rejecting velocity variables. However, it is not certain that we can remove all errors from these sources. Abt and Osmer (1965) have shown that rotational broadening of the Hβ line should not cause appreciable errors provided the narrow interference filter has a half width of about 30Å or more.

CHAPTER II

UBV PHOTOMETRY

In the period May to August of 1970, the Large Telescope User's Panel allocated 26 nights on the 40-inch reflector (the "Elizabeth" telescope) of the Royal Observatory Cape of Good Hope, to be used for UBV and Hβ photometry of early-type stars. The UBV photometry and reductions are described in this chapter, the Hβ photometry in the next.

1. Instrumentation

The Elizabeth telescope of the Cape Observatory has been briefly described by Stoy (1964). It is a 40-inch (1.02m) reflector on a cross-axis mount and had a focal ratio of f/20 when observations were made at the Cassegrain focus. The telescope was simple to operate and could be set with accuracy such that it was never necessary to use the attached finding telescopes. On almost every occasion the programme star to be observed was found in the area of sky accessible with the field eyepiece of the photometer. The accuracy and ease-of-setting of the telescope did much to minimise time loss between observations. The Elizabeth telescope has now been moved to the new South African Astronomical Observatory site near Sutherland in the Karroo region of Cape Province and is now f/15 at the Cassegrain focus.

The photometer at the Cassegrain focus, prior to the removal of the telescope, was of conventional design. The field eyepiece mentioned previously had a field of view of about ten minutes of arc in diameter. A second eyepiece behind the diaphragm wheel enabled a star to be positioned more precisely in the diaphragm centre, having been approximately centred on the crosswires of the field eyepiece. A range of diaphragm sizes was available. For UBV photometry, the filter slide carried the following filters:

For V	2 mm.	Omag 302
B	4 mm.	Schott GG 13 + 1 mm. Schott BG 12
U	1 mm.	Schott UG 2 + 1.3 mm. glass

The photomultiplier was a quartz-window E.M.I.6256A in a cooled housing. The 1.3 mm. of glass had been added to the ultra-violet filter so that the conversion from the instrumental (U-B) to the Johnson-Morgan, or standard, (U-B) would be more nearly linear. The standard UBV photometric system is based on the glass envelope R.C.A.1P21 photomultiplier which provides a short wavelength cut-off in the ultra-violet, unlike the quartz EMI tube. Cousins (1967a) has given a more detailed discussion of the efforts to reproduce the standard system.

The photometer was used with a D.C. integrator which had a choice of integration times of 10, 30 or 60 seconds; the 30-second integration was used for all UBV measurements. The integrated output was displayed on a digital voltmeter and printed on a paper strip for a more permanent record. A differentiator and chart recorder were available for continuous monitoring of the observations.

2. Standard Stars

Cousins (1967a) has published a list of UBV photometry for 900 stars brighter than fifth magnitude and south of $+10^{\circ}$ declination, compiled from lists published by a number of observatories. The UBV system defined by these stars is believed to be constant over the southern sky and is very close to the standard system. Unfortunately, these stars were too bright to be observed with the Elizabeth telescope-photometer combination and so standard stars had to be sought elsewhere. Many of the stars in the Harvard E-regions observed by Cousins and Stoy (1962) are suitable for use as standards. The original paper lists V, (B-V) and $(U-B)_c$, the latter colour being a Cape (U-B) in which the U filter was a Corning 9863; the transformation from $(U-B)_c$ to the standard U-B is not a single-valued relation. A later paper by Cousins (1967b) gives (U-B) on the standard system for most of the stars from the original paper. In accordance with Cousins' recommendations, the (B-V) and (U-B) colours were adopted unaltered and the V magnitudes of stars used as standards were adjusted by + $0^m.005$ to bring the photometry onto the same system as "Mean magnitudes and colours of bright stars south of $+10^\circ$ declination".

The E-regions are centred on -45° declination but the programme stars are spread between about -75° declination and the celestial equator, consequently it was not always convenient to use E-region standards. It was desirable to have standard stars located reasonably near programme stars (in projection on the celestial sphere) so that standard and programme stars could be observed at approximately equal zenith distances and, of lesser importance, so that little time was lost setting the telescope and dome. Additional standards were selected from Royal Observatory Bulletins 64 and 121 (Cousins and Stoy, 1963; Cousins, Lake and Stoy, 1966) which give V and (B-V) for about 7000 southern stars and (U-B) for roughly a third of them. Again the V magnitudes of stars selected were adjusted by $+0^m.005$ but the (B-V) and (U-B) colours were corrected by the amounts shown in Table 1, a private communication from Dr. Cousins. For stars from R. Obs. Bull. 64 with $(U-B) < -0.50$ the equation

$$\Delta(U-B) = -0.019 + 0.096(B-V) - 0.038(U-B)$$

was used to derive corrections to published values of (U-B).

Table 1

Corrections to published colours in R. Obs. Bull. 64 and 121

Inclusive limits of (B-V)			△(B-V)	△(U-B)
-0.535	to	-0.485	+0.01	-0.05
-0.48		-0.435	+0.01	-0.045
-0.43		-0.385	+0.01	-0.04
-0.38		-0.33	+0.01	-0.035
-0.325		-0.28	+0.01	-0.03
-0.275		-0.225	+0.01	-0.025
-0.22		-0.175	+0.01	-0.02
-0.17		-0.155	+0.01	-0.015
-0.15		-0.12	+0.005	-0.015
-0.115		-0.07	+0.005	-0.01
-0.065		-0.055	+0.005	-0.005
-0.05		-0.02	0.0	-0.005
-0.015		+0.035	0.0	0.0
+0.04		+0.085	0.0	+0.005
+0.09		+0.095	0.0	+0.01
+0.10		+0.14	-0.005	+0.01
+0.145		+0.19	-0.005	+0.015
+0.195		+0.24	-0.005	+0.02
+0.245		+0.295	-0.005	+0.025
+0.30		+0.30	-0.005	+0.03
+0.305		+0.40	-0.005	+0.025
+0.405		+0.50	-0.005	+0.02
+0.505		+0.595	-0.005	+0.015
+0.60		+0.695	0.0	+0.01
+0.70		+0.79	0.0	+0.005
+0.795		+0.845	0.0	0.0
+0.85		+0.89	+0.005	0.0
+0.895		+0.99	+0.005	-0.005
+0.995		+1.025	+0.005	-0.01
+1.03		+1.245	+0.005	-0.005
+1.25		+1.305	0.0	-0.005
+1.31		+1.58	0.0	0.0
+1.585		+1.645	0.0	+0.005
+1.65		+1.86	-0.005	+0.005

Stars to be used as standards were chosen from the lists detailed above so as to be in, or reasonably close to, the areas of sky containing the programme stars. Special care was taken to choose stars with good (U-B) measures as several of the E-region stars have their listed (U-B) colours followed by a colon or double-colon indicating unreliability (Cousins 1967b). Many of the stars selected were of early-type, according to HD classification, although later types were also used. Figures 1 and 2 show the distribution of the standard stars by magnitude and spectral type. It was difficult to find faint stars with good UBV measures, hence the concentration of stars between sixth and seventh magnitude. There were few good standards of very early type, although figure 3, the two-colour diagram for the selected stars, shows that at least some of them must be earlier than is indicated by the Harvard spectral types. As might be expected, most of them appear to be only slightly reddened.

3. Observation and Reduction

The Cape methods of observation and reduction for general photometry in U, B and V were fairly closely followed (Cousins, 1966). The pattern of observation was to make every third star a standard star. For the first standard star, several integrations would be made, usually on the B filter, and the digitised output from the strip printer checked for variability. If the series of measurements showed more than 2% variability, the observing programme was not started; the variation was often the result of very thin cirrus cloud. If the "check" integrations proved satisfactory, observations were made in the sequence: standard, two programme stars, standard, two programme stars, and so on, as noted above. In general, a different standard star was observed each time to minimise the possibility of systematic

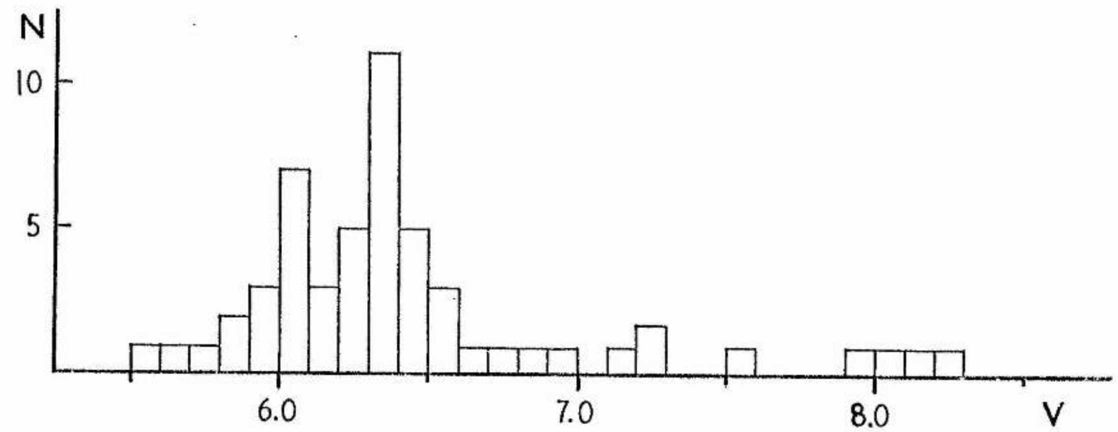

Fig. 1 Magnitude distribution of standard stars

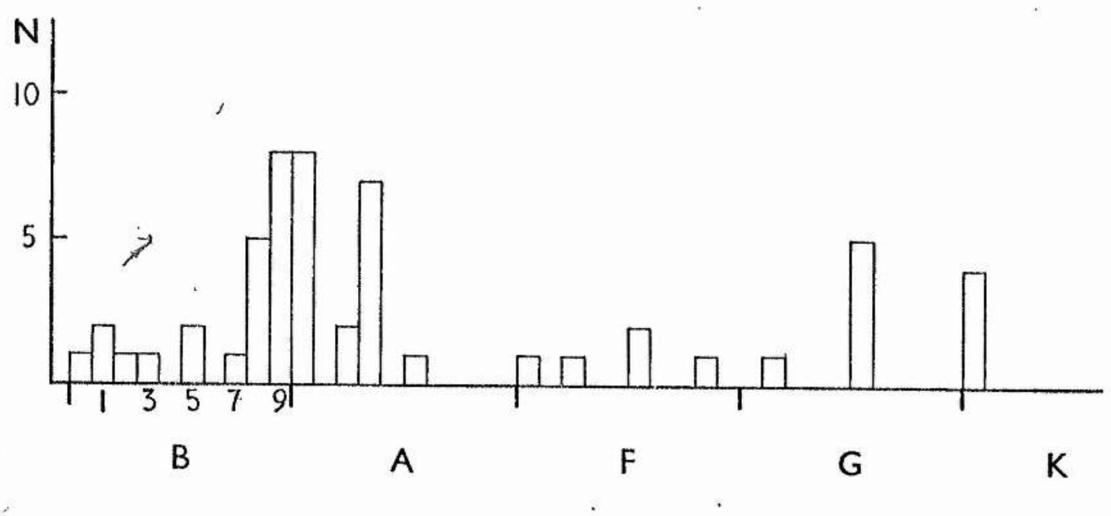

Fig. 2 Spectral type distribution of standard stars

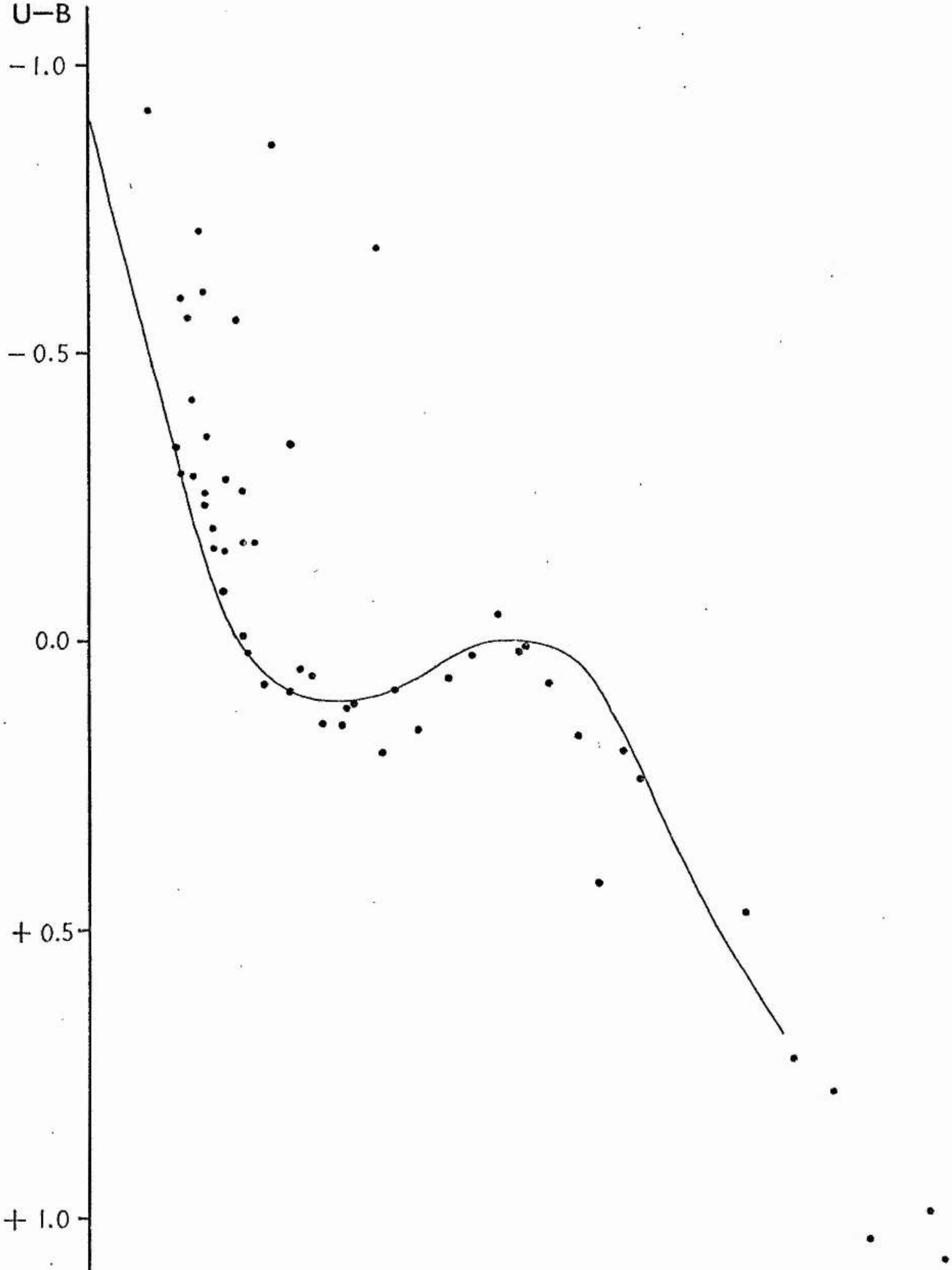

Fig. 3 Standard star colours. Unreddened line from Johnson (1958).

errors. The chart recorder output was checked frequently and if traces showed signs of variability, other than the usual trace "noise", a further series of "check" integrations were made.

For individual stars, sky measures were made in B and V, star measures in V, B and U, and finally sky measures in U and B. For a given filter, sky and star were observed at the same gain, though it was often necessary to increase the gain setting for star and sky measured through the U filter. This sequence of measures is efficient in that it requires few changes of filter. V and U measures for the star are as close as possible to the sky measures through these filters, and B (star) is symmetrically placed between two B integrations of the sky which can be averaged to give B (sky). Each of the seven integrations of the sequence was made for 30 seconds, a total of $3\frac{1}{2}$ minutes integration time for a given star. With a little experience, it was possible to observe about eight or nine stars per hour, generally less than half the total time spent on each star being necessary for setting the telescope and dome, checking the star field and so on.

It is normal practice in Cape general photometry to observe stars at roughly equal altitudes, usually at 30° or 40° zenith distance (Cousins, 1966). This was not always possible in the present programme, for example, stars further south than declination -75° are still more than 40° from the Cape zenith at upper transit. Generally, programme stars were observed at zenith distances smaller than 40° and, wherever possible, the programme stars and the standard stars close to them on the observing list were observed at similar altitudes.

Whilst the various integrations were in progress on a given star, a note was made in the observing book of the star number (HR, HD or CPD) and integrator gain setting, or settings. A clinometer, conveniently calibrated in units of sec z (natural secant of zenith distance), had been attached to the side of the telescope. The clinometer reading and local sidereal time of mid-observation were noted and logged during the B (star) integration.

UBV measurements were made on ten nights or part-nights, in a total of only 57 hours observing. This rather poor record, about 30% of the allocated time, was due almost entirely to the poor weather during the Cape winter. The prevailing south-easterly wind, which in summer creates goodtransparency, if less than perfect seeing, tends to carry rain clouds in winter. With the wind from the north or north-west, photoelectric photometry was made rather risky by thin smoke from the industrial areas of Cape Town. Time lost because of instrumental failure was negligible. The strip printer occasionally malfunctioned so that a check had to be kept on the printed output to ensure that it matched the digital voltmeter reading. In spite of the poor weather, some 367 UBV observations of programme and standard stars were made. Excluding standard stars, 225 observations were obtained for 76 stars, of which 56 had not been previously observed on St. Andrews intermediate-latitude programmes. Most of the remaining 20 programme stars had been observed only once or twice by Dr. van Breda or Dr. Hill. Fourteen of the "new" stars were faint CPD stars, many of which turned out to be very blue, for example, nine were more blue than (U-B)= -0.75 before correction for interstellar reddening.

During a short visit to the Cape in July of 1971, about a dozen programme stars, mostly from the CPD, were observed but the poor weather prevented any really useful work. The 1971 observations were made and reduced in exactly the same manner as the 1970 set and any future reference to 1970 data will also include the 1971 UBV observations.

The first stages of the preliminary reductions were carried out with an Olivetti desk computer and a Cape programme used to reduce all

40-inch observations. Instrumental magnitudes u, b and y were calculated from the digitised output of the strip printer by the usual expression

$$\text{magnitude} = \text{constant} - 2.5\log_{10}E$$

where E = star measure - sky measure for a given filter. A different constant was used for each gain step to bring all measurements to the same gain. Next, v, b-y and u-b were corrected to the zenith using mean extinction coefficients

$$k_y = 0.20 \qquad k_{b-y} = 0.15 \qquad k_{u-b} = 0.30$$

With standard and programme stars observed at similar altitudes, it is not usually necessary to measure actual coefficients for a given night (Cousins, 1966). V^1, $(B-V)^1$ and $(U-B)^1$ were computed using the colour equations

$$\begin{aligned} V^1 &= y + 0.03(b-y) \\ (B-V)^1 &= (b-y) + 0.04(b-y) \\ (U-B)^1 &= (u-b) \end{aligned}$$

which were mean Cape equations in general use for the 40-inch reductions. The constant term usually added to the right-hand side of each equation, that is the "zero-point" required to bring the measurements onto the standard system, is taken care of by the next step of the reduction. Table 2 shows how this was effected. The first three columns of the table are star number, underlined in the case of standards, amplifier gain and natural secant of zenith distance. The next three columns give the instrumental magnitudes and colours, corrected for colour equation and to one air mass. Columns 7 to 9 list ΔV, $\Delta(U-B)$ and $\Delta(B-V)$, the differences between standard and instrumental magnitudes and colours for the standard stars. Shifted to the right in each of these columns are the interpolated zero-points for the programme stars. These differences are added to the corresponding programme star magnitude and colours to give the last three columns which are preliminary values of V, (U-B) and (B-V) on the standard

Table 2

Sample preliminary reductions for observations of 25/26 April 1970

						Zero points			Preliminary UBV		
Star	Gain	Sec z	V^1	$(U-B)^1$	$(B-V)^1$	ΔV	$\Delta(U-B)$	$\Delta(B-V)$	V	(U–B)	(B–V)
115967	1	1.30	4.022	1.038·	–0.669	2.02	–1.38	+0.76			
115149	1	1.18·	4.022·	1.365·	–0.310	2.04	–1.38·	+0.74·			
105139	1	1.23	5.509·	0.717·	–0.730·	2.04·	–1.38·	+0.74·	7.55·	–0.67	+0.01·
107788	1	1.06	6.670	0.521	–0.824·	2.04·	–1.38·	+0.75	8.71·	–0.86·	–0.07·
118285	1	1.34	4.282	1.122·	–0.741·	2.05	–1.38·	+0.75			
109399	1	1.27	5.577	0.515	–0.739·	2.05·	–1.38	+0.74	7.63	–0.86	0.00
111290	1	1.25	5.722	0.583	–0.737	2.05·	–1.37	+0.73·	7.77·	–0.78·	0.00
116579	1	1.30	4.566	1.139·	–0.781	2.06	–1.36·	+0.72·			
112843	2	1.27	7.471	0.675	–0.633	2.06	–1.36·	+0.72·	9.53	–0.69	+0.09
114441	1	1.07	5.967·	0.598·	–0.598	2.06	–1.36·	+0.72	8.03	–0.76·	+0.12
117025	1	1.16	4.046·	1.416·	–0.616·	2.06	–1.36·	+0.72			

UBV system. By observing many standards, the constant of transformation or zero-point in the colour equation is allowed to vary slightly and thus should remove any long period fluctuations in the atmospheric conditions or equipment sensitivity.

As shown in Table 2, for initial calculations three decimal places were retained but for the final stages only two are really significant. The dot or "pip" following the last decimal place indicates that the next figure, appropriately rounded, would be a five.

4. Corrections and smoothing

Before the preliminary UBV results could be smoothed, certain corrections were required. A private communication was received from the Cape observatory describing amendments to the colour equations. Cape observations of standard stars on the 40-inch telescope had been re-reduced in groups, based on the state of the telescope mirrors between November 1965 and July 1971, and small alterations to the colour equations for certain periods were found to be necessary. For the period in which observations were made for this dissertation, corrections of +0.02(b-y) to (u-b) and -0.01(b-y) to (b-y) were required. The new colour equations were then

$$\begin{aligned} V &= y + 0.03(b-y) \\ (B-V) &= (b-y) + 0.03(b-y) \\ (U-B) &= (u-b) + 0.02(b-y) \end{aligned}$$

On the natural system, (b-y) was not numerically greater than unity so the largest correction applied was $0^m.02$.

In a private communication, Dr. Cousins noted results of (U-B) extinction coefficients computed from photoelectric scans of stellar spectra (Willstrop, 1965). From these coefficients, Dr. Hill derived a relation between the extinction in (U-B) and (B-V), (U-B) colours. The relation is non-linear and a result of the increase in Balmer series absorption from O- to A-type stars. The derivation is only described briefly here, since the work was done by Dr. Hill.

Stock (1969) has given the following empirical formulae for the Balmer depression in unreddened or slightly reddened stars:

$$D = (U-B) + 0.784 - 1.285(B-V) \qquad \text{for } (B-V) \leq 0.60$$
$$D = (U-B) + 1.203 - 1.983(B-V) \qquad (B-V) > 0.60$$

With data from 23 class III – V unreddened stars and using a method similar to that described by Hardie (1965), Hill derived

$$k_{U-B} = 0.321 - 0.005(U-B) - 0.04D$$

and substituting for the Balmer depression gives

$$k_{U-B} = 0.051(B-V) - 0.045(U-B) + 0.290 \qquad (B-V) \leq 0.60$$
$$k_{U-B} = 0.079(B-V) - 0.045(U-B) + 0.273 \qquad (B-V) > 0.60$$

The second equation was applicable to a few of the later type stars used as standards. The UBV colours of standards are well defined and k_{U-B} could be computed directly. For programme stars, preliminary colours had been calculated as described in II.3, using the value $k_{U-B} = 0.30$. From these colours a corrected k_{U-B} was determined and the (U-B) colours were revised. The procedure could be used iteratively but in practice it was found that since none of the stars had been observed at low altitudes, the corrections were very small. Revised colours, corrected to the zenith were calculated from

$$\text{Revised } (U-B)^1 = (U-B)^1 - \Delta k.\Delta X$$

where $\Delta X = \sec z - 1$ and $\Delta k = k_{U-B} - 0.30$. The correction was made to $(UBV)^1$ colours so that the last step of the preliminary reduction, the zero-point interpolation, could be re-calculated. The largest value of Δk was less than 0.03 and for a zenith distance of 40°, $\sec z \simeq 1.3$ hence $\Delta X = 0.3$, and corrections should be $0^m.01$ or less. Most stars were observed at zenith distances less than 40° and so corrections were not necessary in many cases and only as great as

$0^m.01$ in a few. Errors may occur for heavily reddened stars or supergiants where k_{U-B} will be uncertain, but such errors will be insignificant unless $\Delta k.\Delta X$ is large.

A few of the stars observed in 1970 had also been in earlier St. Andrews programmes by van Breda and Hill in 1968 and 1969 respectively. All observers had used the same telescope, equipment and method of reduction, although the colour equations were slightly different for the three sets of data. In addition, some of the 1968 observations had been made at rather low altitudes so corrections to k_{U-B} were greater than $0^m.01$. Comparisons between the sets of observations were fairly satisfactory and considerable improvement had been made to the (U-B) data by application of the extinction coefficient corrections. For the preliminary data, the mean difference $\overline{D(U-B)}$, where for a given star

$$D(U-B) = (U-B)_{1970} - (U-B)_{1968,\ 1969}$$

was found to be $-0^m.030 \pm 0.017$ (s.d.) whereas for the corrected data, $\overline{D(U-B)} = -0^m.009 \pm 0.020$ (s.d.).

In the smoothing process, programme stars with good UBV photometry were used as "secondary standards". The criteria used to select such stars were that a star should have at least four separate observations of V, (B-V) and (U-B) and that the standard error of these observations should be less than or equal to $0^m.01$ for all three quantities. Twenty seven stars were found to satisfy these criteria. The quantities ΔV, $\Delta(B-V)$ and $\Delta(U-B)$ were re-calculated for secondary standards as well as the original standards, and the Δ differences for the programme stars were not interpolated directly. Instead, running means of five standards, primary and secondary, were used to derive new ΔV, $\Delta(B-V)$ and $\Delta(U-B)$ for each standard star, including the secondary standards. For example, ΔV for the third standard was taken to be the mean of the first five standards, ΔV for the fourth standard was the mean of standards two to six, and so on. New Δ differences for the programme stars could now be interpolated from the running mean differences. The new values of ΔV, $\Delta(B-V)$ and $\Delta(U-B)$ were then used to re-compute V, B-V and U-B for all stars.

The magnitudes and colours of the primary standards were subtracted from the catalogue values to give mean differences for each night. These "night corrections" were rounded to the nearest $0^m.005$ and applied to all programme stars, including those used as secondary standards. Table 3 shows the actual mean differences $\overline{\Delta}_N$ for each night; n is the number of standards involved.

Table 3

Night corrections to UBV photometry

Date	$\overline{\Delta}_N(V)$	$\overline{\Delta}_N(B-V)$	$\overline{\Delta}_N(U-B)$	n
24/25. iv .70	-0.002	0.000	-0.002	3
25/26. iv .70	+0.006	-0.002	+0.006	9
9/10. v .70	+0.003	+0.001	-0.001	6
12/13. v .70	+0.002	-0.004	+0.002	17
1/2 . vi. 70	0.000	+0.001	+0.003	21
13/14. vi. 70	-0.002	-0.001	-0.002	16
14/15. vi .70	0.000	+0.002	-0.005	4
26/27. vi. 70	+0.002	-0.002	-0.001	8
27/28. vi .70	+0.001	0.000	-0.001	14
14/15.vii.70	-0.001	+0.002	+0.000	15
18/19.vii.71	+0.003	+0.001	-0.001	8

The underlined quantities indicate where corrections were applied. As can be seen, with appropriate rounding, the largest correction added or subtracted on any night was $0^m.005$.

5. Errors

The internal errors of the magnitudes and colours derived from 1970 data were calculated using σ, the standard deviation of a single observation:

$$\sigma = \sqrt{\frac{\sum_{i} \sum_{j} (x_{ij} - x_i)^2}{n - m}}$$

where x_{ij} = j^{th} measure of V, B-V or U-B for the i^{th} star

x_i = mean value of V, B-V or U-B for the i^{th} star

m = total number of stars

n = total number of observations.

Table 4 shows the internal errors for the preliminary and revised photometry. Using all stars with more than one observation and discounting possible variables, n = 181 and m = 57

Table 4

Internal errors of UBV photometry

	σ(V)	σ(B-V)	σ(U-B)
Preliminary	±0.020	±0.013	±0.011
Revised	±0.015	±0.011	±0.011

The smoothing process improved the errors in V considerably and in (B-V) to a lesser extent. A small improvement was made to σ(U-B) but only in the fourth decimal place and therefore of little significance. The standard deviations of the mean values of V, B-V and U-B for each star were calculated using Bessel's formula for a sample from an infinite population:

$$\sigma' = \sqrt{\frac{\sum_{i} (\bar{x}_i - x_i)^2}{n - 1}}$$

Applying the criterion for variability that $\sigma' \geqslant 3\sigma$ it was found that the stars eliminated from the computation of σ on the grounds of probable variability, were in fact variable in V if not in (B-V) or (U-B).

6. Interstellar Extinction

It would be impossible to detail more than a fraction of the work which has been done on the various aspects of the interstellar scattering of light, but some of the papers relevant to the effect of "reddening" on the intrinsic colours and magnitudes of early-type stars will be discussed.

When Johnson and Morgan (1953) defined the UBV system they also discussed the location of unreddened stars in the (U–B)/(B–V) diagram and the effect of reddening on stellar colours. They described a method for determining the reddening of OB stars from observed colours by defining

$$Q = (U-B) - \frac{E_{U-B}}{E_{B-V}} \cdot (B-V)$$

where $E_{U-B} = (U-B) - (U-B)_o$ and $E_{B-V} = (B-V) - (B-V)_o$ are the "colour excesses" or differences between observed and intrinsic colours. The quantity Q is independent of interstellar reddening but dependent on spectral type. E_{U-B}/E_{B-V} is the gradient of the "reddening line" on the two-colour diagram. In other words, a selection of stars with identical intrinsic colours $(B-V)_o$, $(U-B)_o$ but different amounts of reddening should form a line with slope E_{U-B}/E_{B-V} passing through the point $(B-V)_o$, $(U-B)_o$ on the two-colour diagram. Johnson and Morgan gave a value of 0.72 ± 0.03 (p.e.) for the gradient of the reddening line. In principle then, given the observed colours of a star it is possible to determine intrinsic colours when spectral type is known and hence the colour excesses. If the spectral type is not known, it may be estimated by the "Q-method" since Johnson and Morgan calibrated Q in terms of spectral type. If the ratio of absorption in (B–V) to absorption in V is known then it is possible to remove the effect of interstellar absorption on the V-magnitude of a given star as follows:

$$\text{Absorption in } V = A_V = R.\ E_{B-V}$$

$$\text{Absorption free V-magnitude } V_o = V - A_V$$

and R is usually called the ratio of total to selective absorption.

In practice it is not quite so simple. Johnson and Morgan (1953) realised that stars of the same spectral type but different luminosity classes did not necessarily have the same intrinsic colours, and Hiltner and Johnson (1956) investigating the reddening line for O stars found that the data could be represented by

$$E_{U-B} = 0.72\ E_{B-V} - 0.05\ E^2_{B-V}$$

that is, the reddening line is slightly curved. They also investigated reddening in the region of h and X Persei, finding a value for R of 3.0±0.3, and noted that reddening of stars in the Cygnus rift was not consistent with other regions of the sky. Studies by Walker (1957) and Lindholm (1957) showed that the gradient of the reddening line varied with spectral type. In view of these complications, Johnson (1958) re-examined the Q-method and, assuming a value of 0.05 for the curvature coefficient, tabulated values for the gradient. He also gave values for the intrinsic colours of O – AO stars of luminosity classes V, III, II, Ia and Ib. A recent survey by FitzGerald (1970) of some 7000 stars, including 2500 OB stars in the U.S. Naval Observatory Photoelectric Catalogue (Blanco et al., 1968), gives intrinsic colours for all "normal" spectrum/luminosity classes and lists the gradient of reddening lines as a function of MK type and $(U-B)_o$. FitzGerald found the curvature coefficient to be 0.05, in accord with earlier results.

To remove the effect of interstellar extinction on the programme star magnitudes, it is necessary to determine $(B-V)_o$ for each star, then the colour excess and hence the extinction in V. There are several practical problems. It is important to have good intrinsic colours and to be able to assign intrinsic colours to each programme star as accurately as possible since any error in E_{B-V} will be multiplied by the factor R. Finally, and perhaps most important, the value of R must be known.

Figure 4 shows the intrinsic colours for O – A0 stars. Unbroken lines are from data by Johnson (1958) and the various symbols represent FitzGerald's (1970) data. Agreement is good for luminosity classes V – II and, for this programme, Johnson's apparently smoothed values have been adopted with small modifications. The class V line has been extended slightly at the upper end in accordance with FitzGerald's results for O5 – O7 stars and where Johnson's results for class III stars become uncertain, the class III line has been assumed identical to the class V line. This is supported by the FitzGerald data, which is also used for class II stars later than B5. Modifications are indicated by broken lines in fig. 4. For supergiants there is another problem in that Johnson used two classes, Ia and Ib, with class Iab presumably merged with these. Again the FitzGerald data were used to modify the intrinsic colour lines given by Johnson. The resultant lines can be seen in fig. 4 where it is apparent that classes Iab and Ib are similar. The Ia colours given by Johnson are adopted although there is some disagreement with FitzGerald's results in the range $-0.7 > (U-B)_o > -0.9$.

Having fixed intrinsic colour lines, the next step is to determine $(B-V)_o$ for each programme star. It is common practice, when an MK-type is available for a star, to take the intrinsic colours from a tabulation such as those discussed above. This is somewhat unsatisfactory because the intrinsic colours quoted are mean values for a particular type of star and there will be a certain amount of scatter within each type. Also, any systematic errors in the classification will affect the intrinsic colours. As an illustration, programme stars classified B3V are plotted in fig. 5 together with part of the class V intrinsic

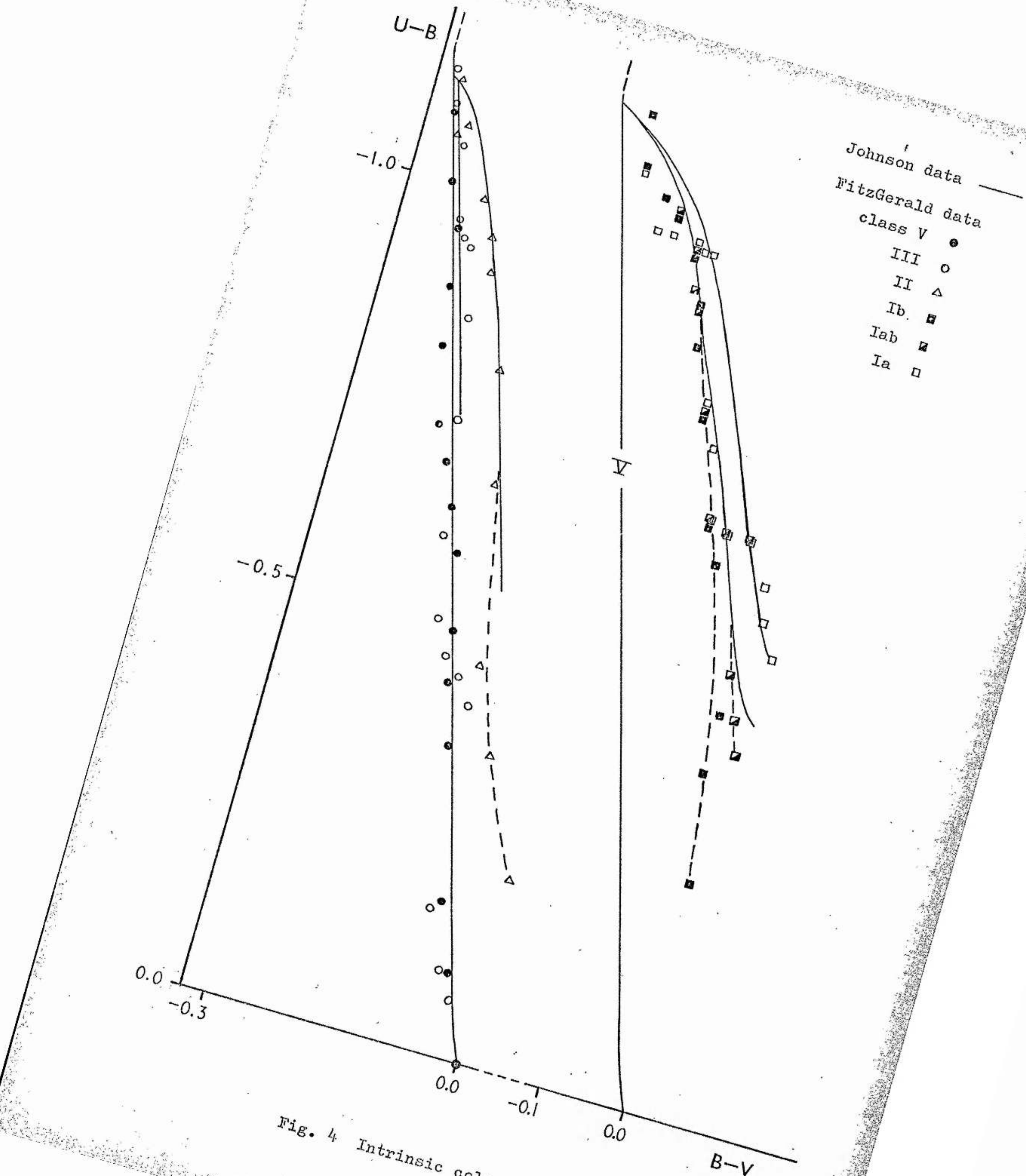

Fig. 4 Intrinsic colours for O – AO stars.

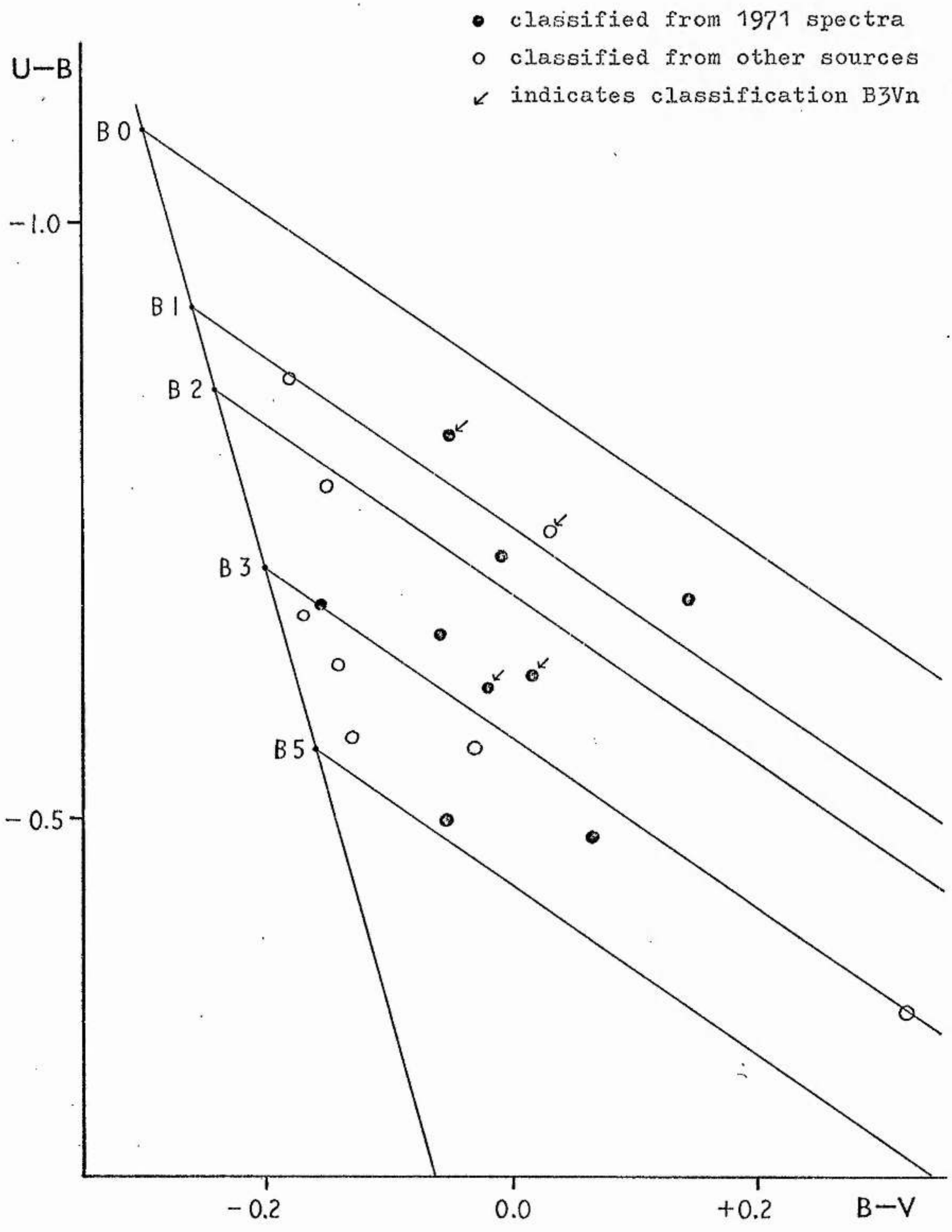

Fig. 5 Two colour diagram for B3V programme stars.

colour line and several approximate reddening lines. The stars seem to lie mostly in the region of the B1 and B3 reddening lines. Spectra of B1V and B3V stars are similar as far as hydrogen and He I lines are concerned; B1 stars are usually obvious by the presence of faint OII blends at 4415-17, 4317-20 and 4070-76 Å. It is possible that the stars above the B2 line in fig. 5 are in fact of class B1 but rotation effects have rendered the faint features invisible at the dispersions used. This systematic effect would introduce errors of up to $0^m.07$ in $(B-V)_o$ if all the fig. 5 stars were assumed to be B3V and to have $(B-V)_o = -0^m.2$. Ignoring the stars above the B2 reddening line, the scatter of stars about the B3 line and the assumption of $(B-V)_o = -0^m.2$ would still introduce errors of up to $0^m.03$. Both random and systematic errors will be multiplied by a factor of 3.2 when A_v is derived.

In the revision of the Q-method, Johnson (1958) gives an equation for calculating the $(B-V)_o$ colour of a star directly from the observed (B-V), (U-B) colours. In effect, the equation gives the $(B-V)_o$ intercept of a reddening line with the intrinsic colour line for class V stars. The method is only valid for main sequence stars earlier than A0 but it indicates how intrinsic colours of any early-type star might be found without accurate knowledge of spectral type, provided the star is fairly "normal". If a (B-V)/(U-B) graph is drawn with intrinsic colour lines for each luminosity class and to this is added a series of reddening lines drawn from published values for gradient and curvature, then if the position of a reddened star in the two colour diagram is known, its position on the intrinsic colour line can be found by projection parallel to the nearest reddening line. In this way it is hoped to reduce errors introduced by spectral classification and, apart from luminosity errors, the accuracy of the reddening correction is dependent on the determination of the reddening lines. Both Johnson (1958) and

FitzGerald (1970) give tables for reddening line gradients which are in good agreement for O and early B spectral classes. Maximum discordance occurs at about $(B-V)_0 = -0^m.1$, roughly B8, where there is a difference of 0.1 between the two sets of results. If, as an example, we assume $E_{B-V} = 0.5$, then an error of 0.1 in the reddening line gradient will induce an error of 0.02 in $(B-V)_0$. For the present programme, this estimate is pessimistic since most of the stars are earlier than B5 and very few have $E_{B-V} > 0.3$. Hence, for stars which are not heavily reddened, there is justification for believing the graphical method of estimating intrinsic colours to be superior to the method of assuming colours to fit a spectral type. Figure 6 is an example of the graphs used to determine $(B-V)_0$. The intrinsic colour line is taken from fig. 4 and the gradients of reddening lines are from FitzGerald (1970) who conveniently lists gradient as a function of $(U-B)_0$. The curvature coefficient is the generally accepted value of 0.05.

A problem remains in that the determination of $(B-V)_0$ is still dependent on the luminosity class and, as can be seen from fig. 4, an error in classification between say II and III, could lead to an error of $0^m.05$ in $(B-V)_0$. There does not seem to be a simple way around this problem, although the fact that class III and V stars have very similar intrinsic colours does reduce the probability of large errors. In practice, absolute magnitudes from β-indices were occasionally useful where MK luminosity classes were uncertain.

The final hurdle is determination of R, the ratio of total to selective absorption. There are three basic methods:

(i) from the apparent increase in diameters of open clusters with distance, caused by an increase of apparent photometric distance due to extinction.

(ii) from variable extinction effects in a cluster. Comparisons of apparent magnitudes and colours can be made between stars

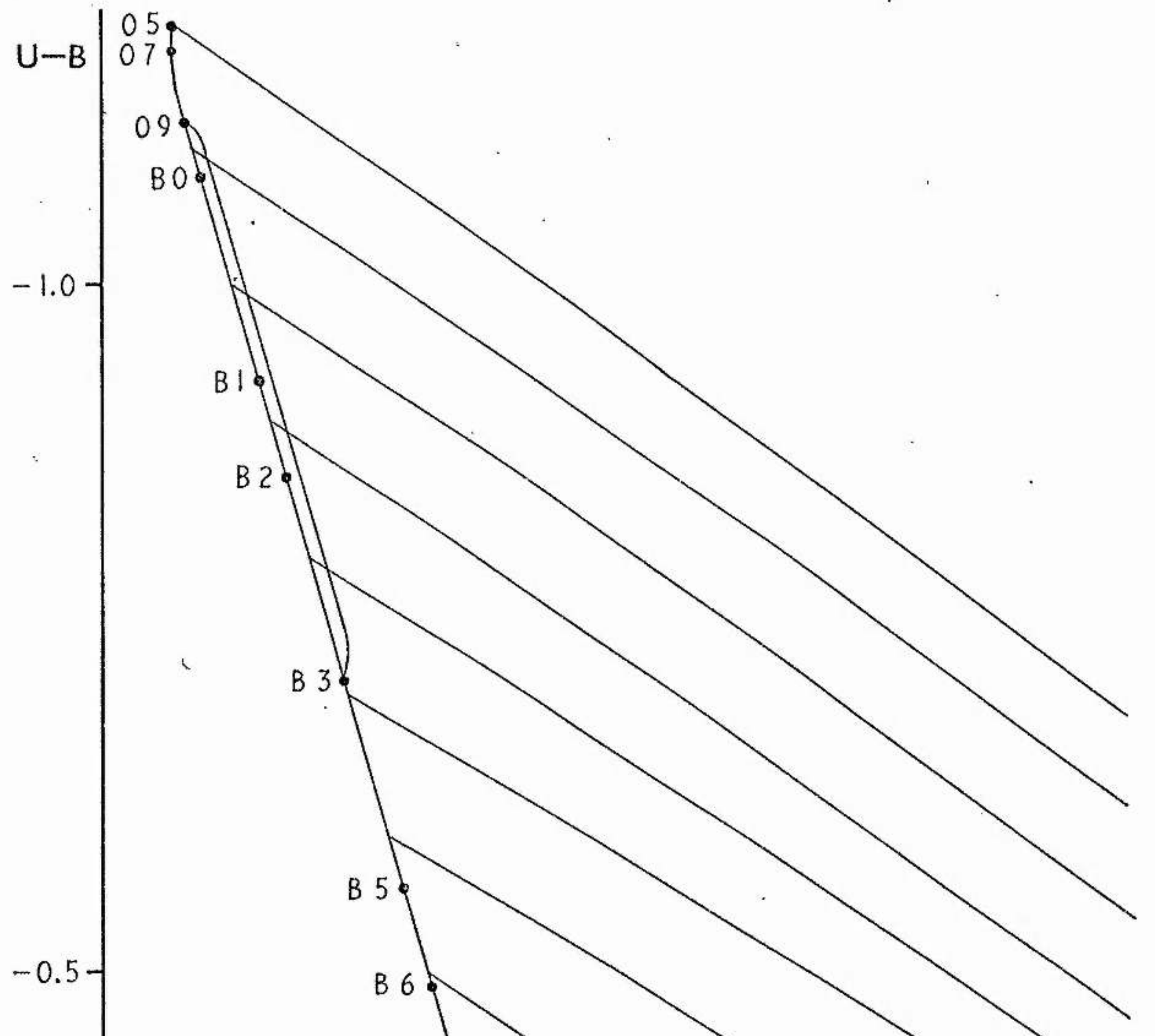

Fig. 6 Intrinsic colours and reddening lines for class III-V stars.

of the same absolute magnitude.

(iii) from the colour differences between reddened and apparently unreddened stars over a range of colours.

Early research by Morgan, Harris and Johnson (1953) and Whitford (1958) on colour differences gave $R = 3.0 \pm 0.2$. Johnson (1968) considered all three methods and suggested that $R = 3$ should be regarded as a minumum value and that R may be as large as 6 in some regions. Schmidt-Kaler (1967, 1971) has reviewed the argument against higher values for R. Briefly, a value of $R = 3$ has been shown to cause no systematic differences between photometric and geometric distances of clusters; the inclusion of non-members in variable extinction studies of clusters can produce erroneously high values of R; finally, circumstellar shells around M supergiants and some early-type stars can result in infra-red excesses in the application of the colour difference method and hence spurious results for R. Schmidt-Kaler (1967) finds the most probable value for the ratio of total to selective extinction to be $R = 3.2$ with regional variations of less than ± 0.5. Since this result seems to be the best available at the present time, it was used to calculate extinction corrections for the programme stars. It is not expected that any large variations in R will affect programme stars as these do not lie in regions of high obscuration. Small regional variations should be negligible because measured values of E_{B-V} are not large.

CHAPTER III

Hβ PHOTOMETRY

On the original observing plan, the Hβ photometry was to be carried out at the Cape along with the UBV programme. Unfortunately, late delivery of the interference filters, combined with poor weather at the Cape in July and August, severely restricted the accumulation of data. Professor Schmidt-Kaler of the Astronomisches Institut der Ruhr-Universität Bochum, had suggested making an application for observing time on the Bochum telescope at the European Southern Observatory site on Cerro La Silla in Chile. Bochum University kindly allocated seven nights, later extended to thirteen nights, in May 1971.

1. Instrumentation

Details of the Cape 40-inch telescope and instrumentation were given in Chapter II. The UBV filter slide was simple to remove and replace by a slide carrying narrow and intermediate band filters for Hβ photometry. This, and the use of ten second instead of thirty second integrations, were the only instrumental changes.

The Bochum installation, telescope and instrumentation have been described by Schmidt-Kaler and Dachs (1969) and some notes are reproduced here. The telescope was a standard Boller and Chivers Cassegrain reflector of 24-inches (61 cm.) aperture and focal ratio f/15. Declination and right ascension drives had slewing, setting and guiding speeds which made the telescope easy to move from star to star quickly and convenient for careful setting. A "finder" attached to the main telescope gave a field of view of $1\frac{1}{2}^{\circ}$ diameter. The photometer was based on a design by Dachs and was of fairly conventional design. The filter wheel, diaphragm slide, Fabry lens and cold box were "plug-in" units which could be quickly removed and exchanged for similar units. For Hß photometry, an EMI 9502A photomultiplier was used, mounted in a Products for Research TE-200 cold box which, when filled with a solid carbon dioxide/isopropyl alcohol mixture, maintained the tube at $-70^{\circ}C$ for about six hours. A good supply of CO_2 was provided each night and the cold box was filled 1 – 2 hours before observations were started and was refilled every four hours during the night to ensure a safety margin. The amplifier used with the photometer was a Keithley 416 picoammeter which had a 4160 remote input head on the telescope. Output was recorded on a Phillips PM8000 potentiometric recorder.

Interference filters used at the Cape and La Silla observatories were manufactured by Baird-Atomic Inc. Details of the characteristics will be given later when the filters will be discussed and compared with regard to the transformations from the instrumental to the standard system.

2. Standard stars

The fundamental reference for Hß standard stars is the list published by Crawford and Mander (1966) of stars observed at Kitt Peak National Observatory. Most of these stars are in the northern hemisphere and are distributed around the sky so that only a few were accessible for the present programme. A later list by Crawford, Barnes and Golson (1970) contains ß-indices for nearly 400 southern bright stars of B-, A- and F-type, many of which are well-observed and suitable for use as standards. Over 100 OB stars were selected as potential standards, mainly from the latter list, but all primary standards likely to be easily accessible were included.

3. Observation and reduction

For observations made at the Cape, with digitised output, the procedure described by Crawford and Mander (1970) was followed. Denoting observations through narrow and intermediate filters by N and W respectively, the sequence was NNWWNN on the star followed by NW on the sky. Since each observation was of ten seconds duration, the time required to make a sequence of observations on a given star was about one minute, including moving the telescope from star to sky. Because of the short time involved, it was possible to use rather poor nights, not suitable for UBV photometry, even though only a single channel photometer was used. Star and sky measurements were made at the same gain for a given filter, although narrow and intermediate filter measures of the same star were not necessarily on the same amplifier gain setting. Sky measures were made after every star and generally the variation was small unless conditions were poor. Standard stars were observed after every four or five programme stars and usually two standards were observed at the beginning and end of the programme on any given night.

Averages $\bar{N}$ and $\bar{W}$ were taken and the sky reading subtracted from them. Any gain difference between narrow and intermediate filters was removed and the natural or instrumental system β-index was calculated from

$$\beta' = 2.5 \log_{10}(\bar{W}/\bar{N})$$

If the overall variation in the four N values or two W values was more than 2%, the value of β' was enclosed in brackets in the reduction book to indicate a result of doubtful quality.

By the time the Hβ filters reached the Cape, only the first half of the night was usable as programme stars were at large zenith distances after midnight; this was a small problem compared with the persistent bad weather. Observations were attempted on six nights but the total of useful observing time was only seventeen hours, during which 113 observations were made on 62 programme stars.

The La Silla procedure was similar to that used at the Cape except that the output was a pen recorder and so the observing sequence was NWN on the star and NW on the sky. Each measurement was continued until a reasonable trace was produced, usually about a centimetre in length, although for fainter stars the traces were made longer. Standard stars were not observed as frequently as at the Cape but the atmospheric conditions were so good throughout the night that the average number of standards measured nightly was greater at La Silla than at the Cape.

Median lines were carefully ruled through the traces in the usual way; $\bar{W}$ was then the height of the W (star) trace above W (sky) and $\bar{N}$ was the average of the two N traces with N (sky) as zero line for measurement. Natural system β-indices were calculated as for the Cape data. Out of $12\frac{1}{2}$ nights, one was slightly cloudy and unsuitable for photometry, on another the wind was too severe for the dome to be left open. Excluding standard stars, 803 observations were made on 233 stars. These were not all intermediate latitude stars as the programme included stars from Dr. Hill's high latitude programme. The observing was shared between Dr. Hill and myself.

Preliminary reductions of β'-indices from instrumental to standard system were effected by using standard stars in a least-squares solution of the linear equation

$$\beta = a + b\beta'$$

A separate transformation was computed for each night. Cape solutions and some of the La Silla transformations were evaluated with the aid of a desk calculator, then a short computer programme was written, checked against the original calculations and used to compute the remaining transformations. This programme proved useful for the further reductions because any dubious standards, poor observations and the like, could be removed and new transformations computed very easily. Examples of transformations are shown in fig. 7. Preliminary internal errors for each set of observations were derived using the equation quoted in II.5 for the standard deviation of a single observation and were as follows

	σ	n (observations)	m (stars)
Cape	±0.013	65	27
La Silla	±0.023	722	200

excluding variable stars and stars with only one observation. A significant part of the error in each case is almost certainly due to variable stars or faint stars with rather poor quality observations. These will be discussed in the section on errors.

4. Data improvement

In addition to the rather large internal errors in the preliminary results, there appeared to be a significant difference between measurements of the same star at the two observatories. The overlap data was rather poor, both in quality and number of stars involved, and so it was decided to try to improve all the data before attempting to remove any differences. A list was made of the poor and apparently discrepant results and these were checked by re-measuring traces in the case of the La Silla data and re-calculating averages for the Cape data. This done, the ß-indices were re-computed. A number of apparently good measurements were included to act as "controls". By checking the measuring and calculations, a few small alterations were made but the most useful result of the process was the discovery of several errors of a gross kind, both of measurement and of computation.

The next step was to re-examine the standard stars and the transformations from instrumental to standard system. Any standards

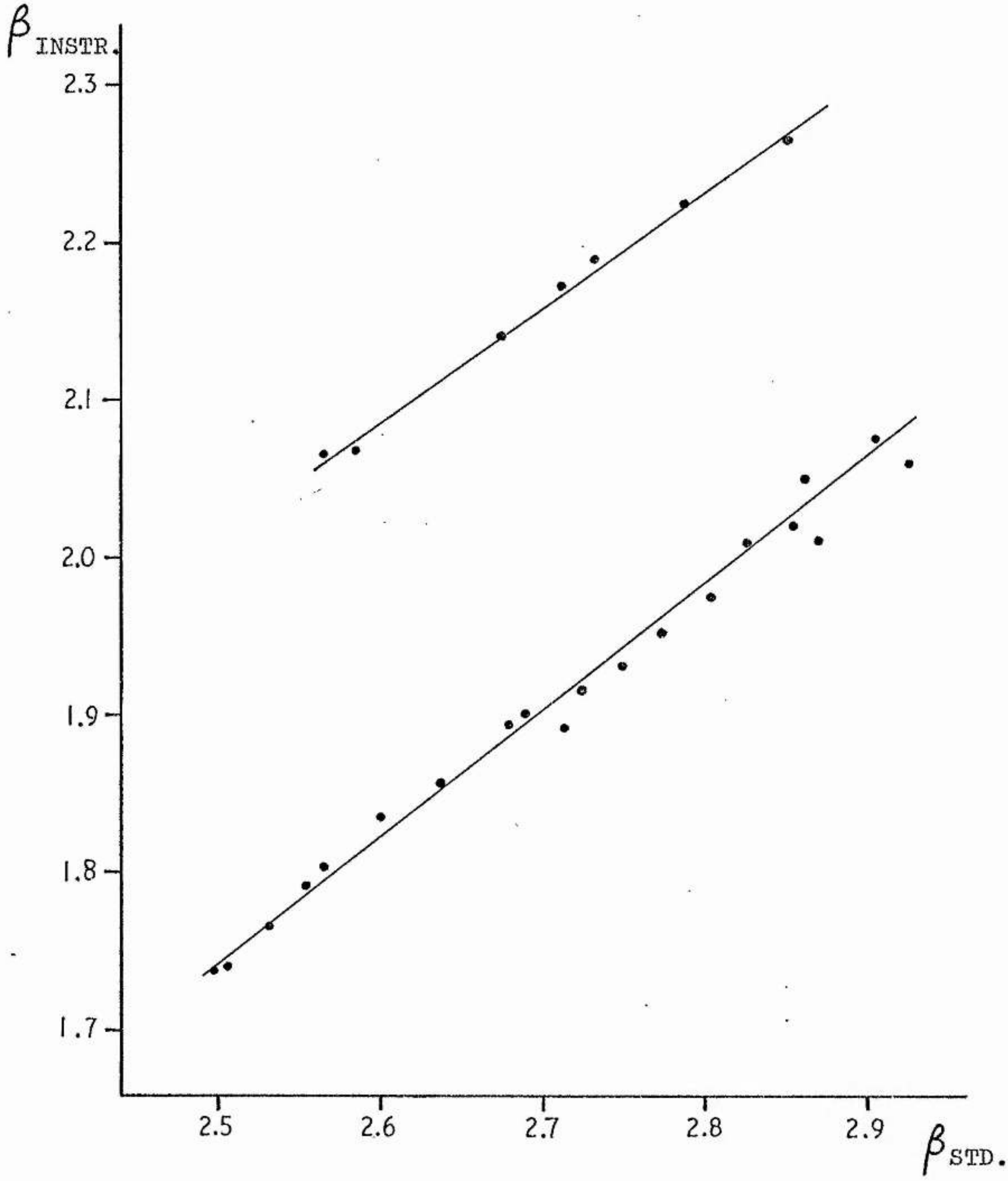

Fig. 7 Examples of instrumental to standard transformations.
Upper transformation for Cape, 0/1 Aug 70
Lower transformation for La Silla, 9/10 May 71

which might have been affected by transparency variations or which were otherwise suspect were removed and new transformations were computed. Final results for gradients and zero-points of the transformations are listed in Table 5. As a check on the transformations, the instrumental system ß-indices (ß') for the standard stars were converted into standard system data. Thus for each night a set of "calculated standard" values was obtained for the standards observed. The differences

$$\Delta\beta = \beta\,(\text{standard}) - \beta\,(\text{calculated standard})$$

were derived for each night and plotted against ß (instrumental). These graphs seemed to show that a curvature term was present in the transformations, but not in the same sense for the two observatories. Rather than fit a curve to individual graphs, in which it must be admitted there was a good deal of scatter, it was decided to try to obtain an average correction curve for each set of observations. For each standard used, the mean value of $\Delta\beta$ was plotted against the mean value of ß (instrumental) and the resultant graphs are shown in figs. 8 and 9. The numbers used as data points indicate the number of measurements forming the mean point. In each case the curves were hand drawn through the weighted means of groups of data points. No attempt was made to fit polynomials to the points but the hand-drawn curves appear to represent the general trends reasonably well. From the graphs, tables of corrections were drawn up so that each programme star measurement, supposedly on the standard system, could be easily corrected according to the value of the instrumental ß-index.

It is important to remove the curvature effect; having done so, it is perhaps of interest to consider the possible causes of non-linearity. The strongest contender is the difference between the two sets of filters and the filters used to define the standard system.

Table 5

Night Transformations from natural to standard system

Date	a (zero-pt.)	b (gradient)	n (stars)
23/24. vi .70	0.032 ± 0.079 (s.e.)	1.224 ± 0.037 (s.e.)	7
25/26. vi .70	0.109 ± 0.100	1.193 ± 0.046	11
0/1 .vii.70	-0.027 ± 0.105	1.260 ± 0.049	6
4/5 .vii.70	0.103 ± 0.135	1.197 ± 0.064	9
9/10.vii.70	0.069 ± 0.051	1.215 ± 0.051	16
7/8 . v .71	0.354 ± 0.122	1.245 ± 0.066	15
8/9 . v .71	0.325 ± 0.073	1.255 ± 0.039	20
9/10. v .71	0.295 ± 0.057	1.263 ± 0.030	18
10/11. v .71	0.253 ± 0.084	1.287 ± 0.044	18
11/12. v .71	0.235 ± 0.052	1.296 ± 0.028	20
12/13. v .71	0.285 ± 0.050	1.272 ± 0.026	21
13/14. v .71	0.239 ± 0.096	1.289 ± 0.051	12
15/16. v .71	0.237 ± 0.148	1.289 ± 0.077	8
16/17. v .71	0.188 ± 0.078	1.318 ± 0.041	19
18/19. v .71	0.213 ± 0.075	1.309 ± 0.039	22

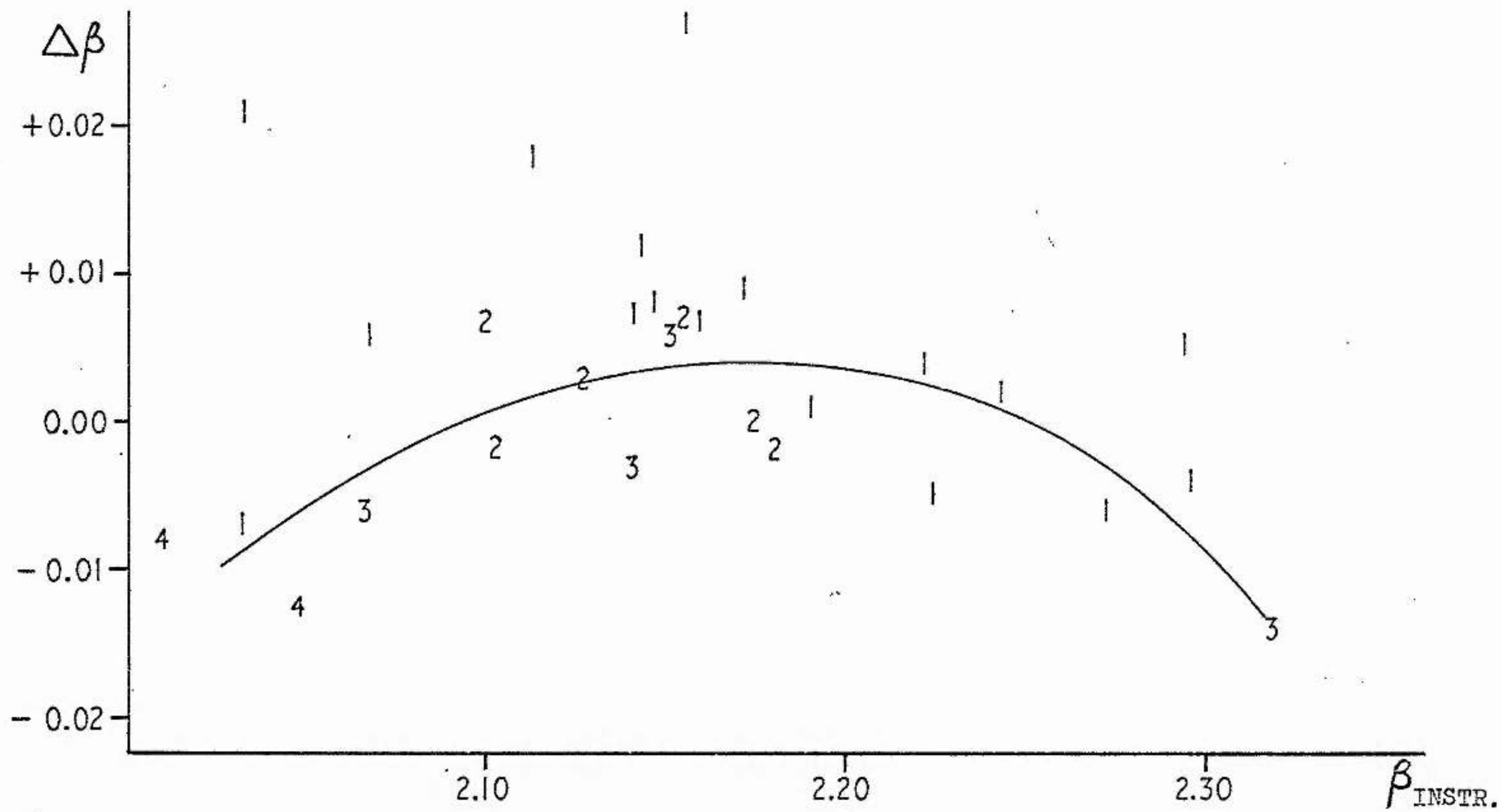

Fig. 8 Mean curvature in Cape transformations.

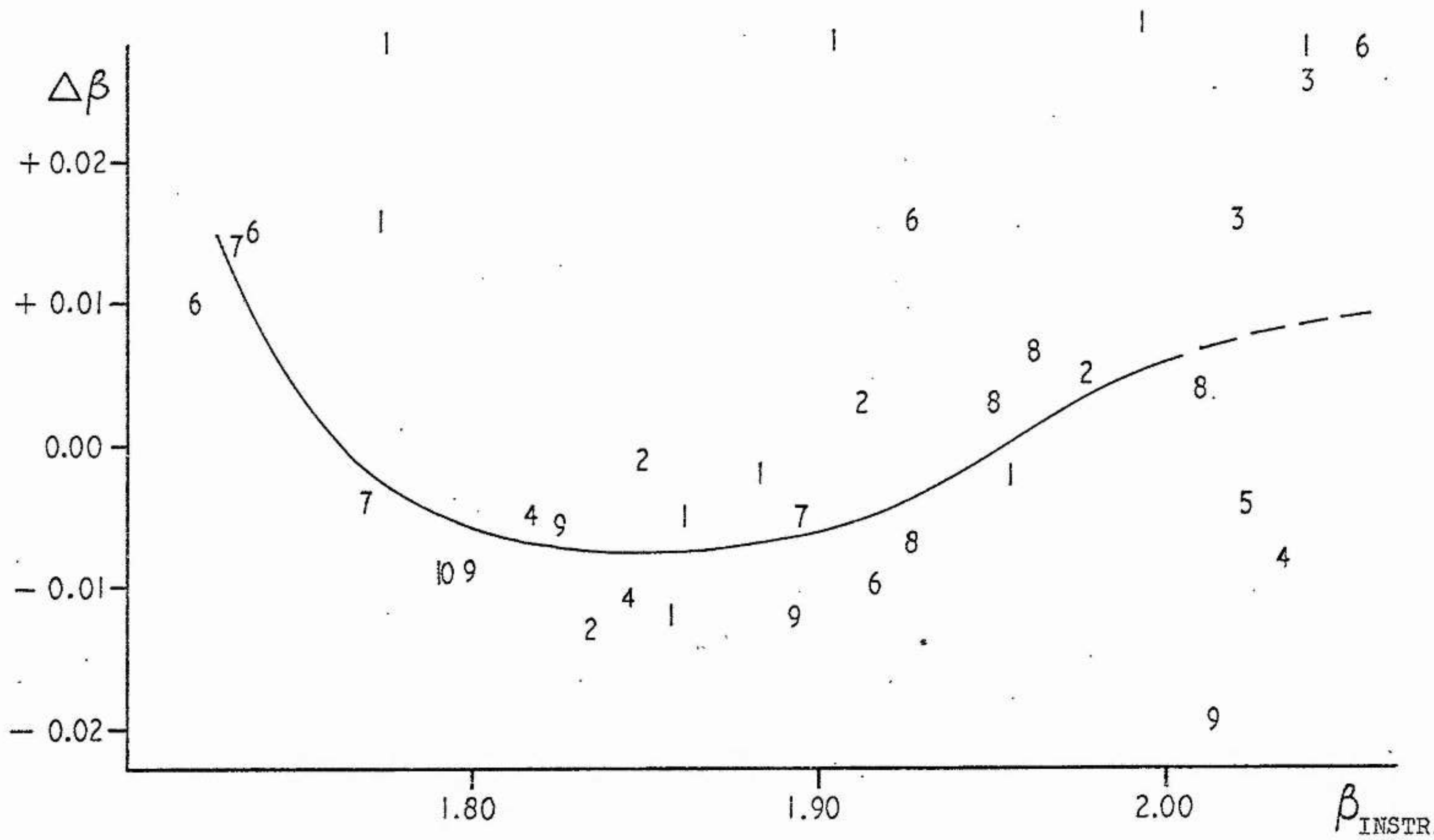

Fig. 9 Mean curvature in La Silla transformations.

Table 6 lists the main characteristics of filters used at the Cape and La Silla observatories and one of the sets used by Crawford (1964) at Kitt Peak.

Table 6

Hβ filter characteristics

		Peak wavelength	Width at ½-peak transmission	Peak transmission
Kitt Peak	W	4850 Å	136 Å	71%
	N	4858	29	58
Cape	W	4900	212	84
	N	4866	31	76
La Silla	W	4848	98	58
	N	4857	28	49

The Cape filters have a higher peak transmission percentage than the La Silla filters with the Kitt Peak set in between. The narrow band filters are all similar but the Cape intermediate band is over twice as wide as that used at La Silla with the Kitt Peak filter between the two extremes. Investigation of the transmission curves reveals that the He I line at 4922 Å may affect the intermediate band filter of each system in a different way. On the La Silla filter, the helium line can have little effect, falling at about 5% transmission. On the Kitt Peak filter it lies at 36% transmission and on the Cape filter at roughly 83% in the relatively flat region of best transmission. Figure 10 shows the transmission curves of the intermediate band filters from the three systems and the location of Hβ and He I 4922. These are schematic drawings which show the flat plateaux of maximum transmission as rather less "noisy" than is actually the case. If the helium line affects the Cape filter, what effect should this have on

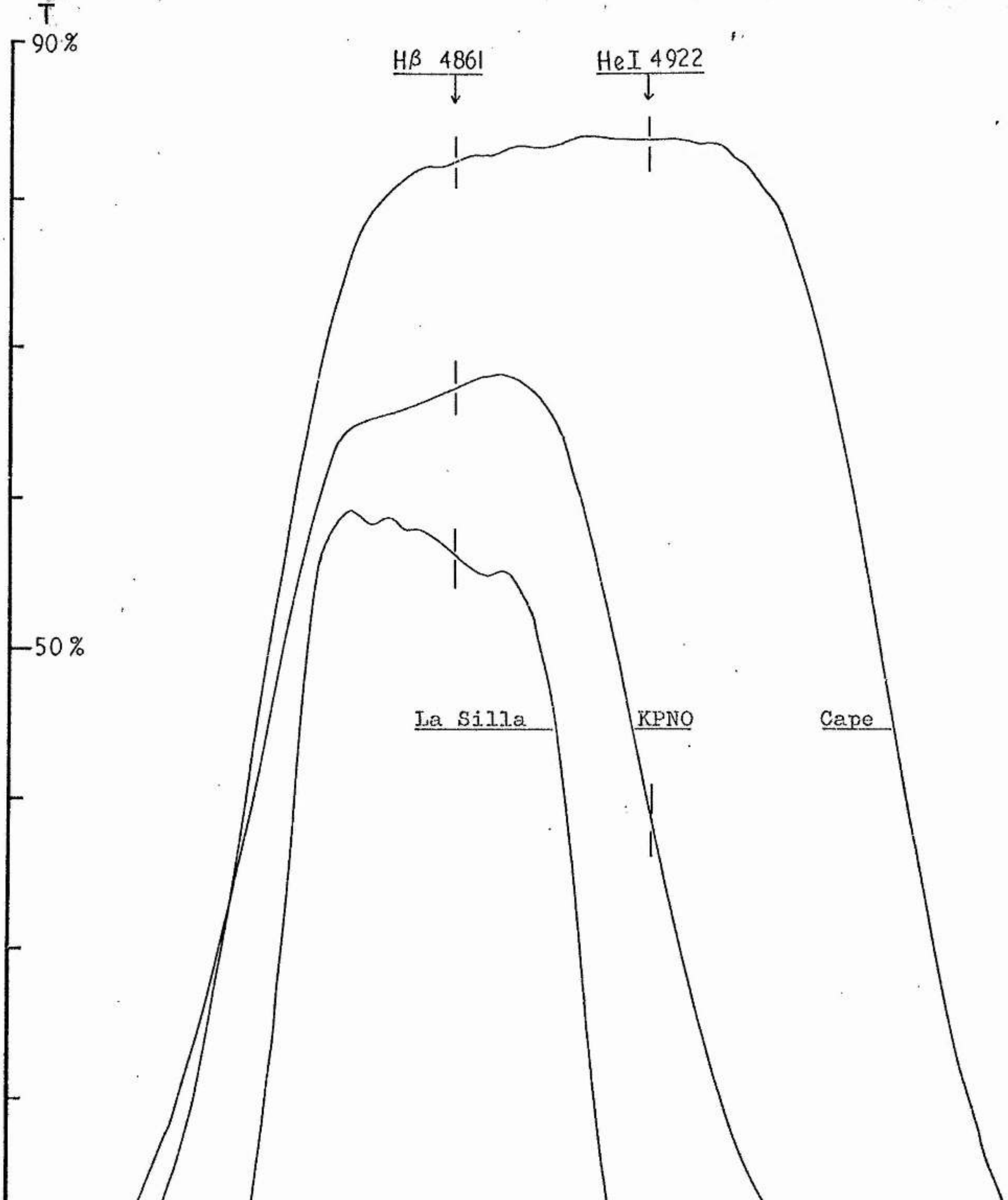

Fig. 10 Transmission curves for intermediate band filters.

a β-index? For a standard star, the natural system β-index will be smaller than if the helium line were not present, since $\beta = 2.5 \log (W/N)$ and W is reduced by He I absorption in a range of about $2.60 < \beta < 2.75$. However the curvature induced in the transformations by this effect would be in the opposite sense to that observed. This qualitative conclusion was supported by numerical calculations described in Appendix I. It was found by simulation of filter and spectrum that the helium line should not affect the La Silla transformations but should curve the Cape transformations very slightly in the opposite direction to the observed curvature.

A second possibility considered was the effect on the instrumental β-index when the Hβ absorption line has a non-negligible effect on the intermediate band filter. Simulated line profiles were convoluted with filter transmission curves (see Appendix I) and the observed curvature was reproduced moderately well. The size of the "theoretical" effect was less than that actually seen but it seems likely that the major part of the curvature is due to the difference in bandwidth of the intermediate filters of the three systems.

With corrections for curvature applied, the overlap stars, observed at both observatories, were re-considered. The differences $\Delta\beta$ were re-calculated and a few stars suspected of variability were rejected as were four stars for which the difference depended on only one poor quality measurement at one of the sites. For the remaining stars, the mean difference was found to be $+0^{m}.001$ which is small compared with the standard error of a single observation. To calculate the mean, $\Delta\beta$ for each star was weighted according to the minimum number of observations made at either site. The residuals are plotted against β (Cape) in fig. 11 and although the scatter is quite large it seems that more points lie above the zero line as β increases; the weighted least

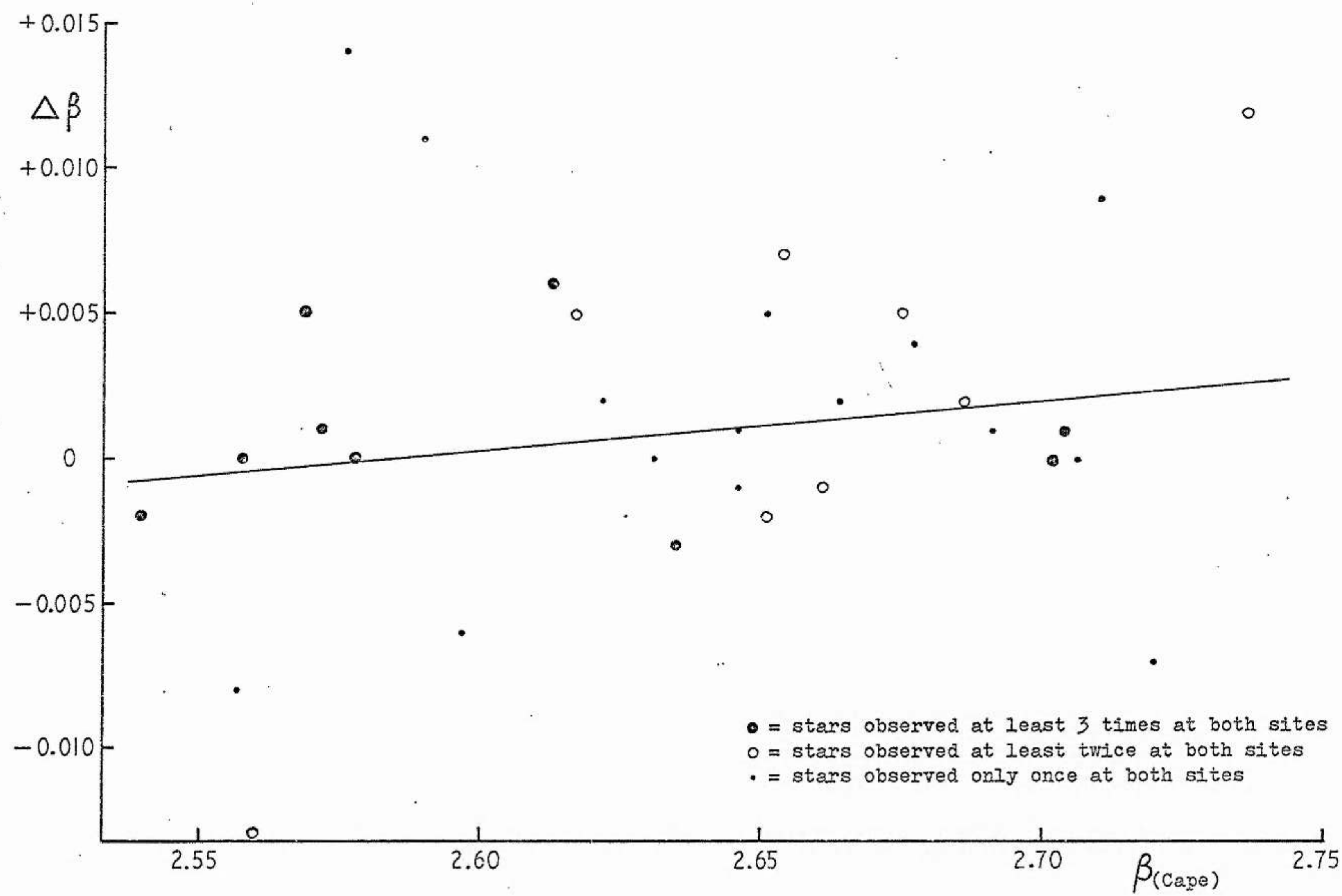

Fig. 11 Residuals β(Cape) − β(La Silla) plotted against β(Cape).

squares solution verifies this.

The residual difference between the two sets of data is difficult to explain since one would expect any systematic effects to be removed in the transformations, unless there is a consistent difference between standard and programme stars. As far as the pen recorder data were concerned, traces of standard stars were all fairly noise free because the standards were all bright stars whereas many programme stars were faint and had high noise levels. It is thus possible that systematic personal errors could have occurred in judging the median level of a noisy trace and such errors should be reduced when the ratios of intermediate to narrow band measures were taken. Six programme stars near the celestial equator were observed by Dr. Hill during a visit to Kitt Peak in 1972. Comparing his measures with La Silla measures produced the mean result ß(KPNO) - ß(La Silla) = +0.004. There was insufficient data to determine how well the KPNO - La Silla relationship matches that for Cape - La Silla but there is some similarity and in the absence of better data it seemed preferable to correct the La Silla results to the Cape data rather than vice versa. Supporting this decision is the better precision of the Cape data, as indicated by the standard deviations, and the possibility that the difference is caused by personal errors in reduction of the chart recorder output. The following small corrections were applied to La Silla ß-indices

range	correction
$\beta \leq 2.560$	$- 0^m.001$
$2.560 < \beta \leq 2.615$	0.0
$2.615 < \beta \leq 2.670$	+ 0.001
$2.670 < \beta \leq 2.725$	+ 0.002
$2.725 < \beta$	+ 0.003

These are taken from the least squares solution in fig. 11. The two sets of data were then combined.

5. Errors

In section 3 of this chapter it was noted that the standard deviation of a single observation for the Cape and La Silla Hβ measurements were $\pm 0^m.013$ and $\pm 0^m.023$ respectively. In the last section, attempts to improve the data were described; checking apparently discrepant results, checking night transformations and removing curvature from the transformations. None of these would affect individual measurements greatly, except the discovery of mistakes in measuring or computation, although all might contribute to reducing the scatter in the β-index of a given star. When the preliminary standard deviations were calculated it seemed likely that some variable stars had been included in the analysis simply because only the most obviously variable were rejected. As an interim criterion it was decided to call any star for which the range of separate measures of the β-index exceeded $0^m.05$ a variable star. This is reasonable considering the preliminary standard deviations and the fact that the total range of β is only about $0^m.4$. Error analysis gave the following results

	σ	observations	stars	variable
Cape	$\pm 0^m.009$	60	25	7
La Silla	$\pm 0^m.014$	644	180	29

Comparing these results with the preliminary σ, two more Cape stars and twenty more La Silla stars have been excluded as variable.

After combination of the data, the result $\sigma = \pm 0.013$ was derived. Then for each star, the standard deviation σ' was calculated by Bessel's formula as in Chapter II. Any star for which $\sigma' \geqslant 3\sigma$ was assumed to be variable and any star for which $2\sigma \leqslant \sigma' < 3\sigma$ has been marked in the data tables with a colon to indicate probable variability. Six stars designated as variable by the criterion 'range of $\beta > 0^m.05$' were not variable by the test $\sigma' > 2\sigma$. These six were included in a final analysis for σ but did not affect the preliminary determination.

Details are:

	σ	observations	stars	variables
Initial	$\pm 0^m.013$	689	178	33
Final	$\pm 0^m.013$	720	184	27

and the final result is unlikely to be changed by further analysis.

Investigation of the La Silla variable stars showed many of them to be amongst the faintest stars observed in this programme. The total number of programme stars in V-magnitude intervals of $0^m.5$ were counted and the percentage of variables was calculated for each interval. Results are illustrated in the graph and histogram of fig. 12. It is clear that for stars brighter than 10^m the percentage of variables is small and fairly constant. Fainter than 10^m the percentage increases suddenly to over 50%. It seems certain that many of the fainter stars described as "variable" might be better termed "uncertain" in the sense that they are fainter than the level above which the instrumentation and observer can produce consistent results.

Figure 13 is a plot of σ' against apparent V-magnitude for all programme stars observed more than once. Since the La Silla data comprises over 90% of the total, it is not surprising that fig. 13 reflects the results of fig. 12. The small crosses in fig. 13 are mean points for each half magnitude interval, excluding points above the 2σ line. There is a very slight tendency for σ' to decrease towards the brighter magnitudes, even if the mean point of $V = 6.0$ is ignored. There does not appear to be any correlation between variability in β and small variations in V although the sample of stars is too small for definite conclusions.

6. Absolute magnitudes from β-indices

The photoelectric method of measuring the strength of Hβ has been in use for a number of years and several attempts have been made to calibrate β-index in terms of stellar absolute magnitudes. In this

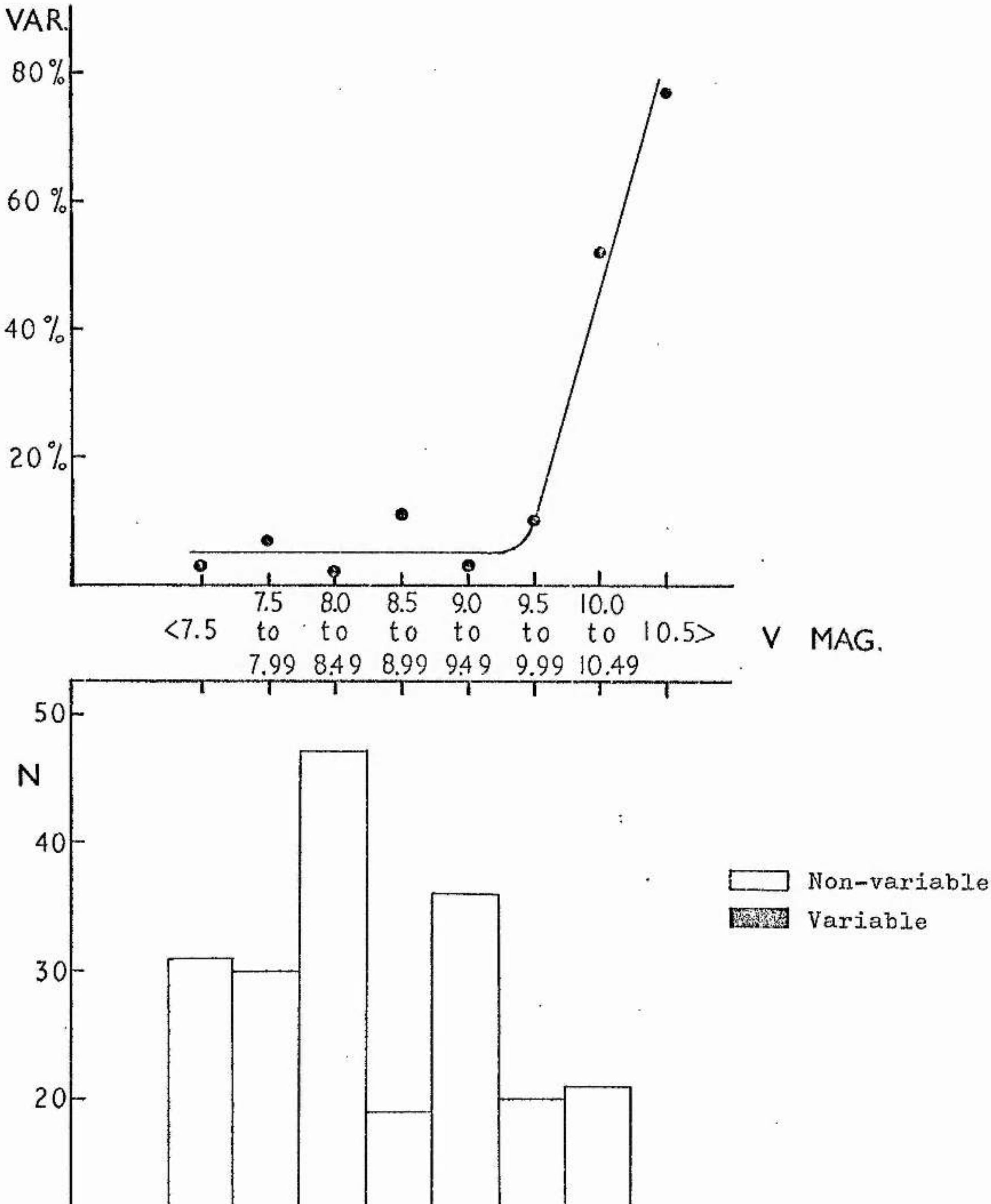

Fig. 12 Analysis of La Silla variable stars. The graph illustrates the percentage of 'variables' in each half magnitude interval ; the histogram shows relative numbers of stars involved.

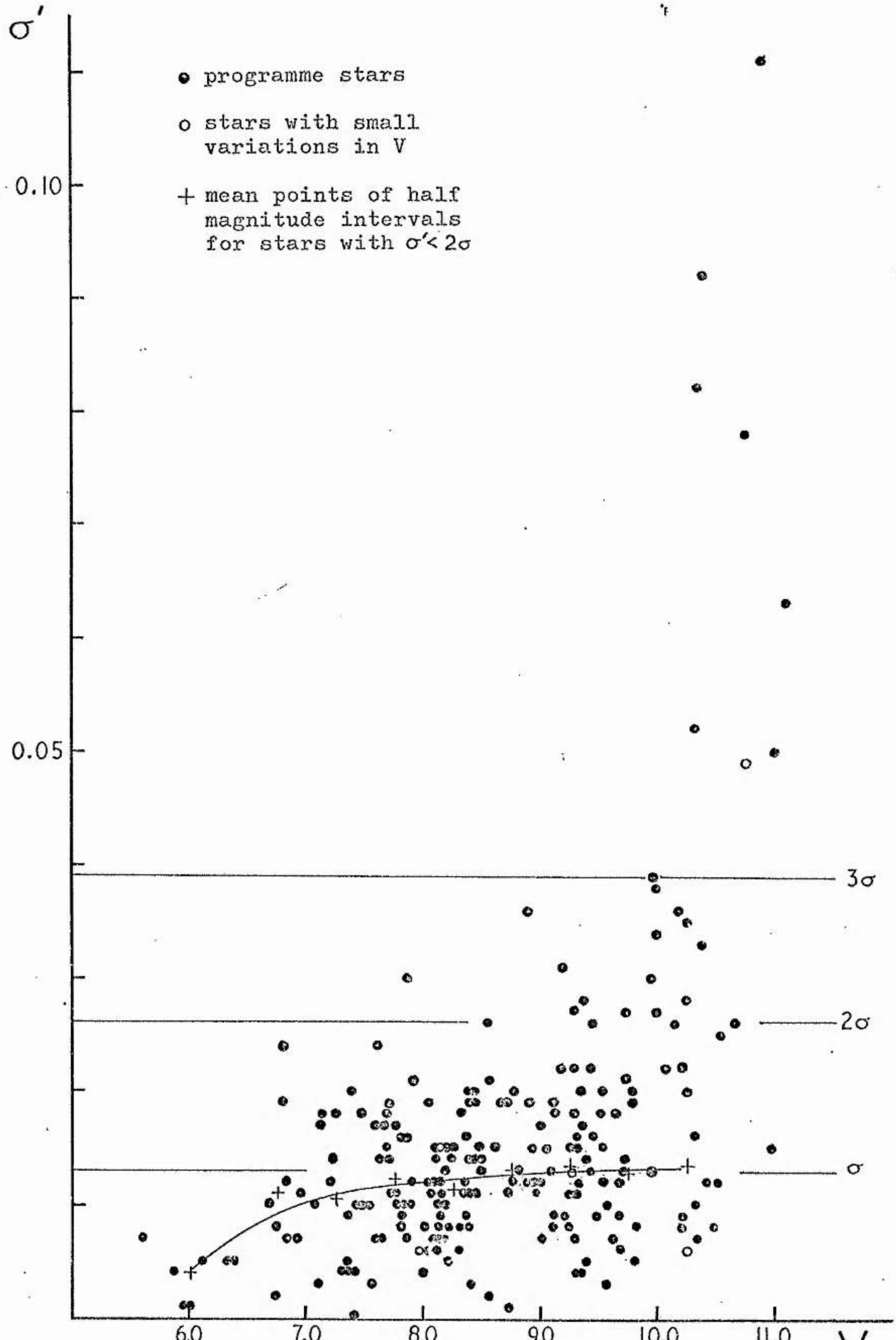

Fig. 13 Standard deviation of β-index against V-magnitude for programme stars.

section, the calibrations presently available will be briefly described and compared.

In a study of association II Sco, the Upper Scorpius region of the Sco-Cen aggregate, Hardie and Crawford (1961) derived two calibrations of ß, the first using all stars measured and the second using "single" or non-multiple stars. Not surprisingly, there was a small but significant difference between the two calibrations, the result for single stars agreeing quite well with more recent work. Both calibrations were based on the mean distance of stars in II Sco from work by Bertiau (1958).

A preliminary $ß/M_V$ relation was presented by Graham (1964) at the I.A.U./U.R.S.I. symposium on the Galaxy and Magellanic clouds. In this calibration Graham used 165 early-type stars, mainly from young clusters and associations. Stars with well-determined MK types were chosen and their absolute magnitudes taken from the MK luminosity calibration by Johnson and Iriarte (1958). Curves of best fit were computed for stars of luminosity classes I - IV and V and all classes together. Graham found a small difference between curves for classes I - IV and class V although the scatter of points about the mean curves in his fig. 1 seems to be quite large. Using the calibration, Graham (1967) derived distances for seven southern star clusters and Sco-Cen and found that distance moduli from his Hß photometry agreed well with results by various authors using different methods.

An indirect approach was made by Fernie (1965) who used published Hγ data and the fact that well-defined relationships exist between the equivalent width of Hγ and Crawford's ß-index. As examples, Bappu et al. (1962) demonstrated that their photoelectrically measured Γ can be accurately transformed to ß and Crawford (1958) has shown that provided ß is less than about 2.85, a linear, well-defined transformation can be made from Hγ equivalent widths to the Hß index. Taking stars with ß-indices and

$H\gamma$ data from Bappu et al. (1962), Beer (1962) or Petrie (1953a, 1956, 1958, 1962), Fernie derived transformations from the various $H\gamma$ -indices to the ß-index of Crawford. These transformations were used to calculate ß-indices for stars in seven galactic clusters and, with published cluster distance moduli, Fernie was able to determine the absolute magnitudes of the cluster stars. The M_V/β calibration thus formed was, with the exception of O stars, independent of spectral type. The six O stars in Fernie's data lie on average $+1^m.0$ from the calibration curve. Apparently no attempt was made to differentiate between luminosity classes in the analysis and so Fernie's calibration curve was re-plotted with different symbols for class I - II, III - IV and V after the manner of Graham's fig. 1 (1964). It was apparent that most of the class III - IV stars were above the mean curve; measurement showed the mean difference to be $-0^m.3$. The effect is not as large as that found by Graham (1954) and seems to be systematic rather than to increase with decreasing absolute magnitude. Comparison is rather difficult because Graham only plots a sample of his total material and in the Fernie data there are only fourteen giants which is rather a small sample to base quantitative conclusions upon.

The most recent M_V/β relation, presented by Crawford (1972), was based on much more material than other authors have had available and will probably be considered as the definitive calibration for the foreseeable future. Crawford first determined the shape of the relation for zero-age main sequence A and F stars in several clusters with a main sequence fitting procedure similar to that described by Blaauw (1963) for correlating M_V and $(B-V)_0$. Age or evolution corrections were applied, based on information from uvby photometry. Next, the zero-point was fixed by fitting the AF star curve to nearby stars with trigonometric parallaxes. The relation between ß and apparent magnitude,

V_o, for B stars in clusters was determined and the V_o scale converted to an absolute magnitude scale by forcing agreement on distance moduli for B and AF stars in the Pleiades, α Per and IC 4665 clusters. The calibration thus derived was based on stars from over twenty clusters and on many nearby field stars. Crawford indicates that stellar rotation appears to have no effect and age or evolution effects are smaller than in previous cluster fitting attempts.

Figure 14 shows the various calibration curves described. For β greater than about 2.58, the Hardie and Crawford (1961), Fernie (1965) and Crawford (1972) curves are in good agreement; Graham's (1964) curve is systematically half a magnitude above the other three. The difference is difficult to explain without access to the data involved. It may be that Graham had a larger proportion of evolved stars, though this seems unlikely as his stars were selected from young associations and clusters. The Hardie and Crawford (1961) calibration which did not exclude multiple stars is close to Graham's calibration for $\beta > 2.65$ but there is no obvious reason why he might have included more unresolved binaries than other authors.

For evaluating absolute magnitudes of programme stars it was decided to use Crawford's 1972 calibration since this represents by far the most exhaustive study. Using programme stars as a check, absolute magnitudes $M_V(\beta)$ were plotted against $M_V(S)$ derived from Blaauw's (1963) calibration of MK types. Fig. 15 is the result. There appears to be a systematic difference of about half a magnitude between the two determinations of M_V although the scatter in the diagram is considerable. The straight line is at 45° to the axes; open circles represent 1971 classifications and filled circles represent MK types from other sources, mostly Radcliffe publications.

In II.6 an account was given of attempts to remove the effect of

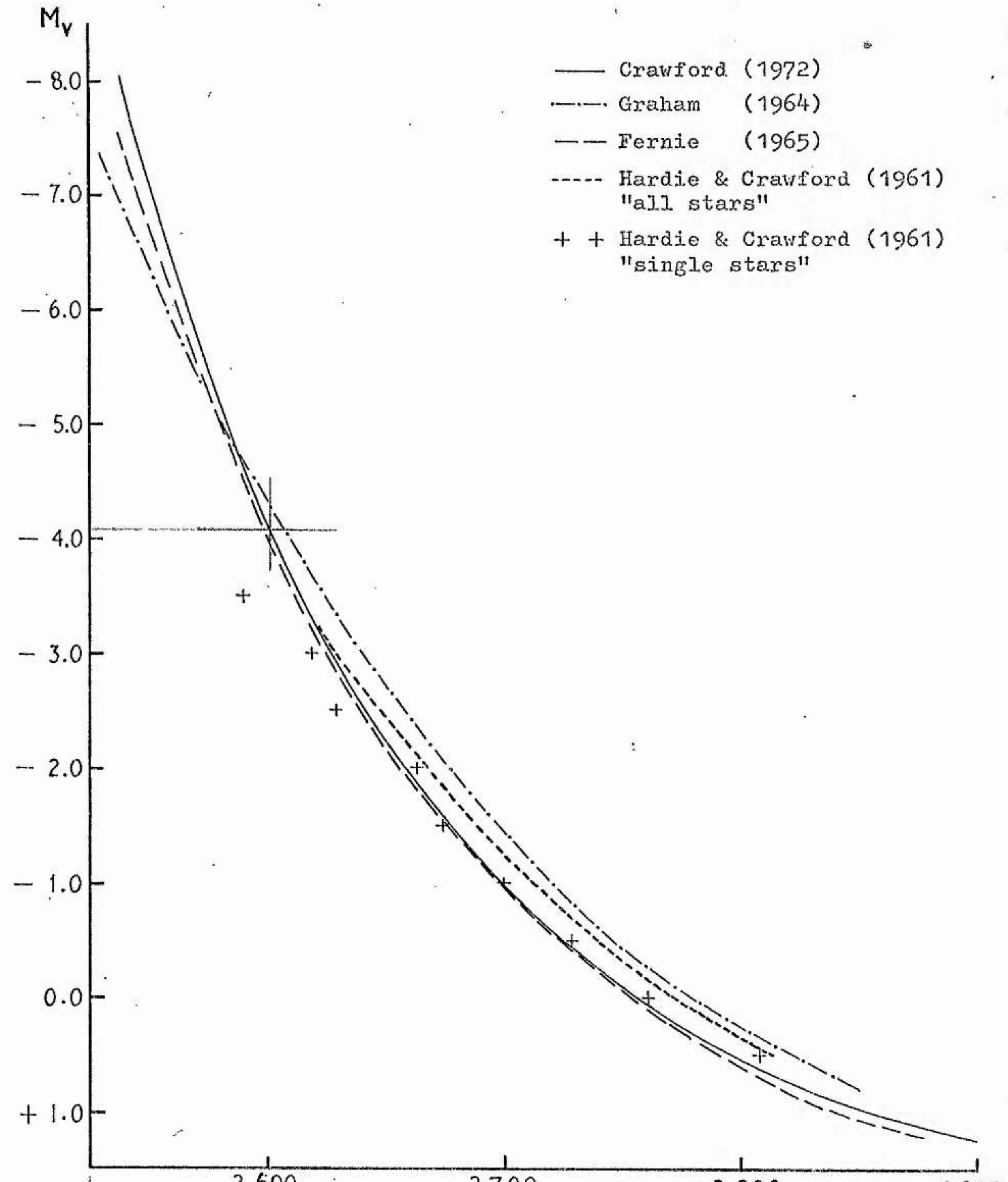

Fig. 14 Calibration of β-index in terms of absolute magnitude. For the sake of clarity, the Hardie & Crawford line for non-multiple stars is shown as separate points rather than a smooth curve.

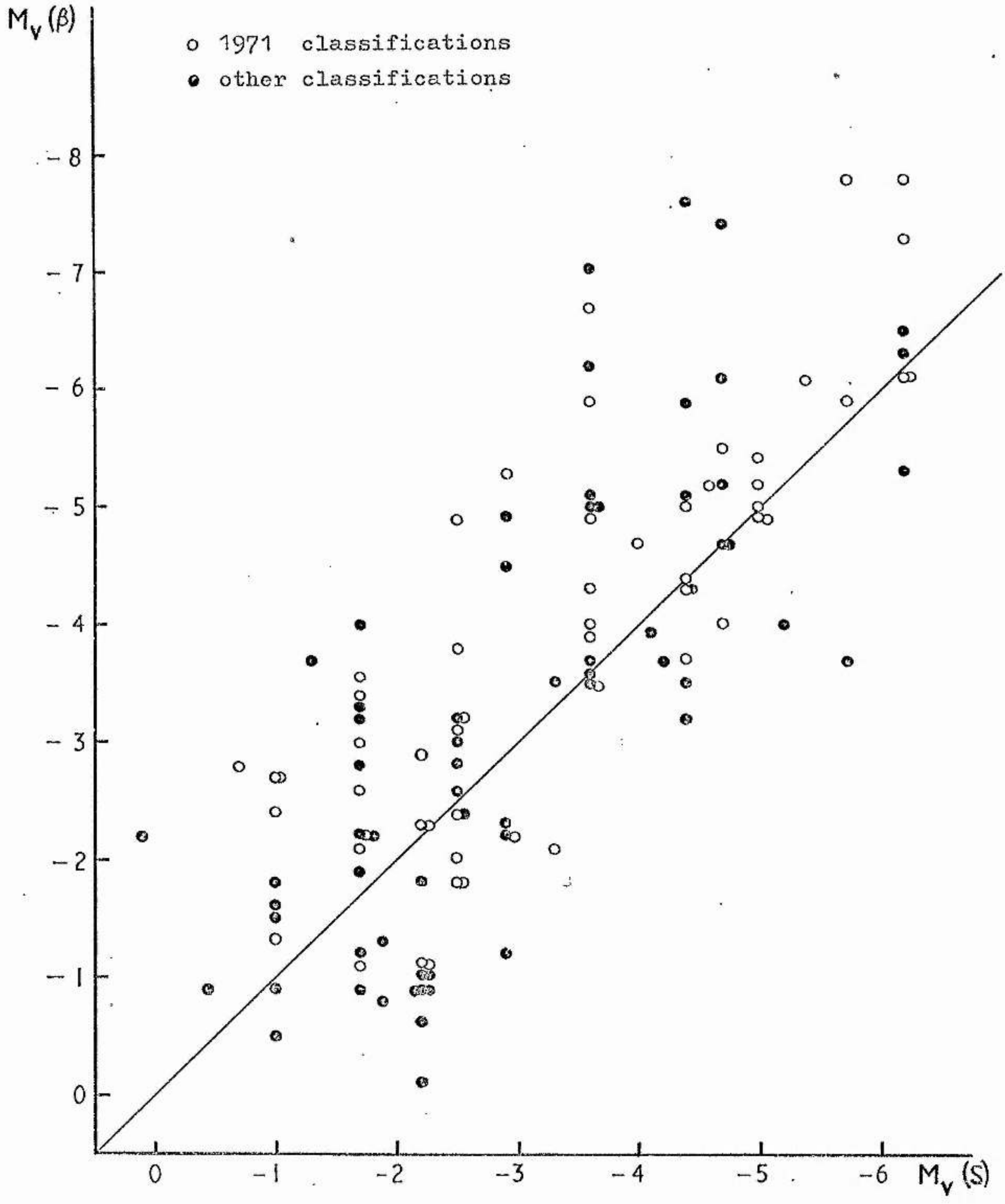

Fig. 15 Comparison of absolute magnitudes from β -indices and MK types
(a) Using visually classified spectral types

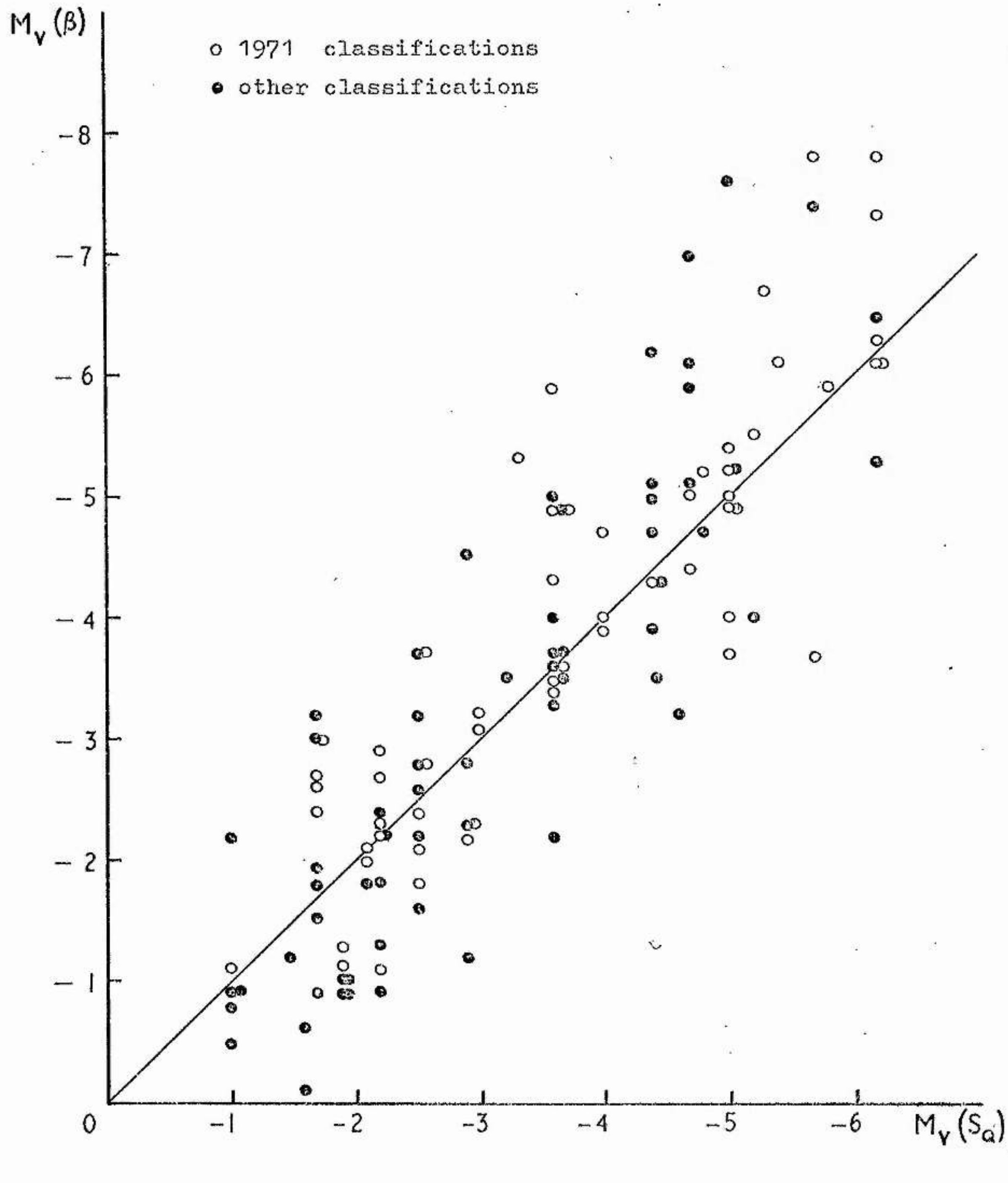

Fig. 16 Comparison of absolute magnitudes from β -indices and MK types
(b) Using ' Q-method ' spectral types

interstellar reddening on the programme star colours and magnitudes. There were indications that spectral classification can result in quite large errors in the assumed intrinsic colours of a star, if for example, the spectral lines are nebulous. To reduce possible classification errors in fig. 15, spectral types were re-determined from observed colours using the Q-method in the graphical form described in II.6. Luminosity classes had to be assumed correct as there was no simple way of determining them independently of both visual classifications and photoelectric Hβ measurements. Stars represented in fig. 15 are re-plotted in fig. 16 with the difference that the M_v of the abscissa are evaluated from Q-method spectral types, designated $M_v(S_Q)$. It is evident that both systematic difference and scatter are smaller in the latter diagram. Expressed numerically, for 119 stars,

$$\text{Mean} \quad M_v(\beta) - M_v(S) = -0^m.40 \pm 0^m.11 \quad (\text{s.e.})$$

$$\text{Mean} \quad M_v(\beta) - M_v(S_Q) = -0^m.14 \pm 0^m.09 \quad (\text{s.e.})$$

The mean difference between $M_v(\beta)$ and $M_v(S_Q)$ is largely due to the more luminous stars which seem to deviate from the 45° line in fig. 16. In particular, if six stars for which $M_v(\beta) > -7$ are removed, then the mean difference becomes -0.06 ± 0.08.

Undoubtedly errors remain in the luminosity classifications which, if systematic, could produce the observed effect. On the other hand, small systematic errors in the β-indices would become more noticeable at higher luminosities due to the shape of the M_v/β calibration curve. Trace emission in Hβ cannot be entirely ruled out although known Hα-emission stars were excluded from the analysis.

Several high latitude stars observed on the Hβ programme had been classified on the MK system from Radcliffe spectra. Some of these stars were independently assessed by two or three classifiers;

MK-types were compared by Hill (1970) who provided a list of the independent classifications. The resulting absolute magnitude comparisons are illustrated in fig. 17. In each pair of graphs, $M_V(\beta)$ is compared with $M_V(S)$ on the left and $M_V(S_Q)$ on the right. Straight lines are all at 45° to the axes. Results for classifier 2 are inconclusive as the data sample is small; results for classifiers 1 and 3 show a very definite improvement in the correlation when S_Q spectral types are used. The greatest improvements tend to occur for stars above the 45° line, in the range $-2 > M_V(\beta) > -5$. I am indebted to Dr. Hill for the data plotted in fig. 17.

Figures 15-17 imply that systematic errors, independent of classifier, may be inherent in absolute magnitudes determined directly from MK types. Since virtually all available spectral classification was performed with Radcliffe spectra, it is not possible to determine whether or not the observed effect is sensitive to the instrumentation. Use of spectroscopic absolute magnitudes without consideration of photometric information would seem to be unsatisfactory, with the danger of systematic errors in quantities dependent on spectroscopic parallaxes, for example, stellar distances, stellar distributions and galactic rotation constants. The difference between Graham's preliminary calibration of the β-index and later results (fig. 14) may have its origin in classification effects similar to those described above. Feast and Shuttleworth (1965) used spectroscopically determined distances in their studies of early-type objects but applied a correction to remove systematic errors due to logarithmic bias.

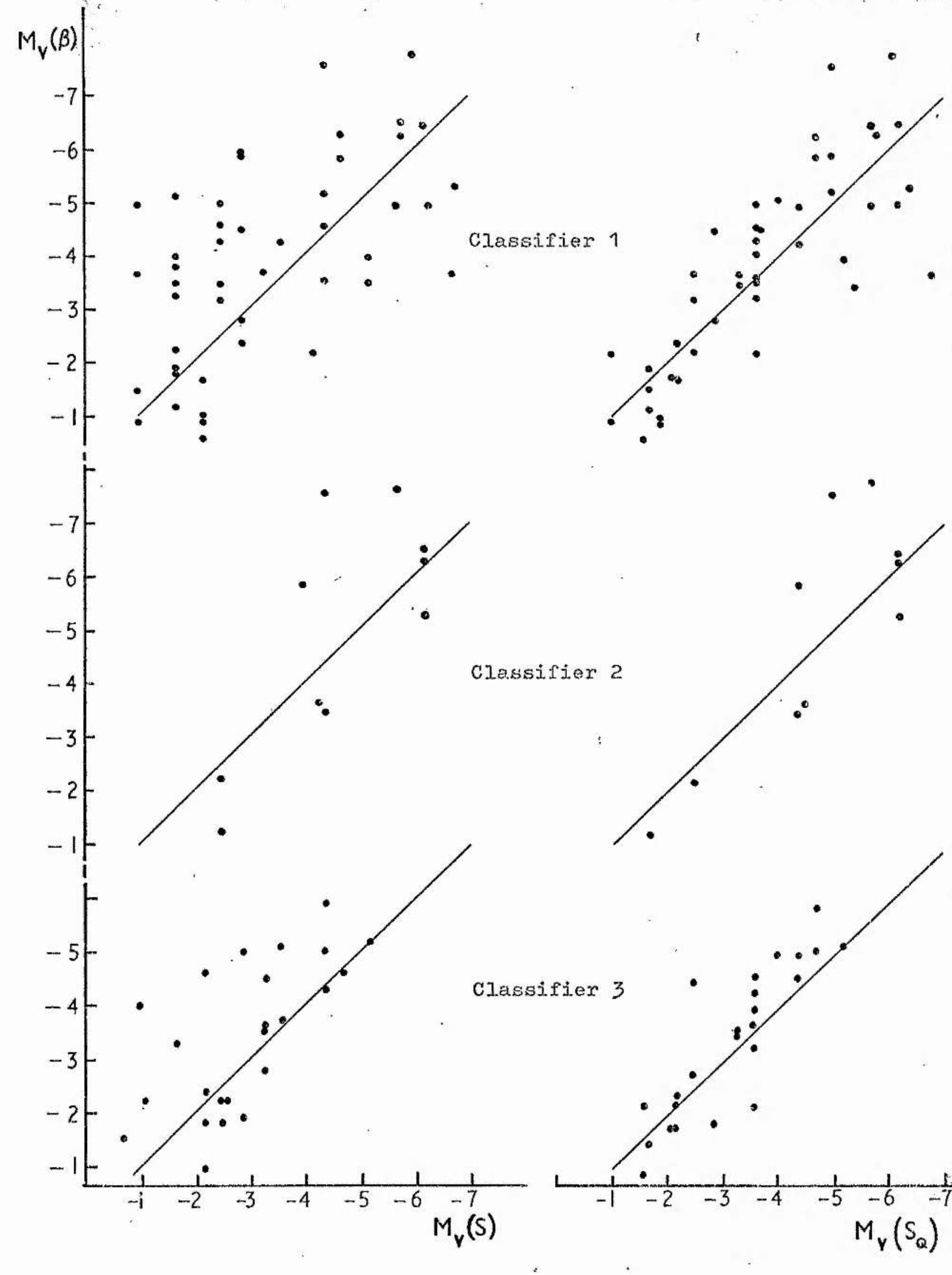

Fig. 17 Comparison of absolute magnitudes from β-indices and MK types (c) Using classifications by other observers

CHAPTER IV

SPECTROSCOPY

The final part of the observational programme was photographic spectroscopy, principally for radial velocity measurement and MK classification. Spectra were obtained with the two-prism spectrograph at the Cassegrain focus of the Radcliffe 74-inch telescope. Twelve nights were allocated by the L.T.U.P. for this project, in June, July and August of 1971.

1. The spectrograph

The construction of the Radcliffe two-prism spectrograph has been described in detail by Jackson (1951). The two 60° prisms are set for minimum deviation at 4200 Å and there are five interchangeable camera lenses with focal ratios ranging from f/8 to f/1. Only the f/3.7 "c" camera (49 Å/mm at Hγ) and f/2 "d" camera (86 Å/mm at Hγ) were used in this project as the programme stars were mostly too faint to permit efficient use of higher dispersions. The inside of the spectrograph is felt-lined for insulation and the internal temperature is regulated by a network of thermostatically controlled electrical resistance wire on the inner surface of the felt. The temperature of the spectrograph interior was noted at the beginning and end of each night and checked occasionally during the night. Internal temperature variation was less than 1°C on ten out of twelve nights and was never greater than 2°C.

The spectrograph was carefully designed to minimise distortion of the optical path caused by changing orientation of the telescope, and Feast, Thackeray and Wesselink (1955) have described tests to determine whether or not such flexure effects were significant. They concluded that "systematic errors arising from reversal of the telescope must be less than 1 km/sec." and that no significant error arises "from a change in tilt of the spectrograph in an east-west direction of about 100°".

The spectrograph slit is figured in a slight curve so that spectral lines recorded on the photographic plate are not appreciably curved. Wesselink has measured iron-arc spectra (see Feast et al., 1955) and found that corrections to measured radial velocities for slit curvature must be of the order of 0.01 km/sec. for the "c" camera. An effect of this size is completely negligible when compared with random measuring errors in early-type stars. A specially constructed mask enabled comparison spectra to be positioned close to either side of a stellar spectrum, for a choice of four stellar spectrum widths. Light from an iron-arc unit attached to the side of the spectrograph was used to produce comparison spectra. Once a plateholder had been secured in the spectrograph it could be moved perpendicular to the direction of dispersion, thus enabling up to ten d spectra or seven c spectra, together with comparison spectra, to be recorded on one 2 x 4 inch photographic plate.

Radcliffe observatory now has a new image-tube spectrograph and the two-prism spectrograph is not in general use. For several reasons it was thought preferable to use the old two-prism unit for this project. It is known to be extremely stable for radial velocity measurement and Radcliffe measurements of I.A.U. standard stars are in close agreement with the I.A.U. velocities (see, for example, Thackeray, 1966). Secondly, the Radcliffe observatory has a collection of standard spectra obtained with the c and d cameras of the two-prism spectrograph for use as comparison stars in MK classification. Finally, it was considered desirable to have continuity with published radial velocities which exist for some of the intermediate-latitude stars (Hill, 1971).

2. Observations

Stars for the radial velocity observing programme were selected on the basis of the UBV Hß measurements, priority being given to stars for which the photometry suggested high luminosity. Most of the intermediate-latitude stars for which MK spectral classification existed, had radial velocities determined by Hill (1971). Because the two-prism spectrograph has a well demonstrated stability for radial velocity work and because the available observing time was not great, it was decided not to observe many radial velocity standard stars. Instead, several intermediate and high-latitude stars previously observed by Feast, Thackeray and Wesselink (1957), Feast and Thackeray (1963) or Hill (1971) were included in the observing programme. In addition, HD 693 (Cape standard R1) was observed towards the end of the programme and HD 157457 (Cape standard R8) was used as a comparison star during a series of consecutive observations on helium star HD 168476. The Cape standards are eleven stars selected from I.A.U. recommended standards and used by Evans, Menzies and Stoy (1959) in a series of papers on fundamental data for southern stars.

For a given camera lens, photographic emulsion, slit width and star magnitude, the exposure time required was calculated using a Radcliffe device similar to a slide rule but having three slides. In practice it was found that exposure times thus calculated were too long because the primary mirror of the telescope had been re-aluminised earlier in 1971. A 30% reduction in exposure times produced acceptable spectra. Iron-arc comparison spectra were impressed on either side of each stellar spectrum before and after the stellar exposure. In other words, if a 30 second exposure was required to produce suitable iron-arc spectra, then the iron arc was allowed to run for 15 seconds before and for 15 seconds after the stellar exposure. Observing time had been allocated in blocks of three, four and five nights and focus plates were taken, using iron-arc spectra as object, at the beginning of each set of nights and on the day after each camera lens change. No significant variation in the focus of either camera lens was observed.

As described in the previous section, only the c and d lenses (49 and 86 Å/mm. respectively) were used. Radcliffe general observing notes recommend that after a lens change it is best to allow two hours before attempting to determine the position of focus of the new camera. Hence the observing programme was arranged so that any lens change required was made at the end of a night, the focus plate taken late the next day and no time was lost waiting for the newly inserted lens to reach the temperature of the spectrograph interior.

Most of the spectra were obtained with slit widths of 0.075 mm. for the c camera and 0.14 mm. for the d camera, both of which gave a projected slit width of about 0.018 mm. Some spectra were obtained on the d camera to be used for MK classification and for these the slit width was set at 0.2 mm. giving a projected slit width of 0.027 mm. This results in some loss of resolution but produces spectra more directly comparable with the MK system which is based on spectra at 120 Å/mm. (Feast and Thackeray, 1963). Where possible, c camera spectra were widened to 0.42 mm. but for fainter stars it was necessary to restrict the width to 0.2 mm. Spectra from the d camera were widened to 0.5 or 0.25 mm., the latter being necessary for a few of the faintest programme stars. The spectrum width chosen for each star depended upon the required exposure time; since only a limited amount of telescope time was available, exposures were, with one or two exceptions, kept to less than fifty minutes.

The photographic emulsion used throughout was Kodak II a O, the sensitivity of which had been increased by baking the plates for 72 hours at 50°C. The II a O emulsion is sensitive to radiation of shorter wavelengths than about 5000 Å, but the glass prisms of the spectrograph cut off most of the ultra-violet radiation, so the spectra were really only useful in the range 3900 - 5000 Å. Each exposed plate was photometrically calibrated by two exposures on a spot sensitometer, and then developed in an MQ solution which was agitated continuously during development. The plates were "fixed" for a minimum of 15 minutes and washed for at least 45 minutes.

Altogether, over 200 Cassegrain spectra were obtained for a total of 75 stars; 59d and 117c spectra were of programme stars, 29c spectra were of standard and "overlap" stars from earlier Radcliffe programmes and 10c spectra were of helium star HD 168476.

3. Radial velocity reductions

All plates were measured on a Hilger and Watts long-screw micrometer in the conventional manner. A spectrum was carefully aligned with the direction of motion of the screw and positions of stellar lines and a selection of iron-arc lines were determined, measuring from long to short wavelengths. All lines in the stellar spectrum were measured, including nebulous and interstellar Ca II lines where possible, but excluding very poor quality lines. Usually, about twenty iron-arc lines were measured, selected to give a reasonably even distribution in wavelength and to avoid very faint or very strong lines. The spectrum was then reversed and the same lines measured, starting with the shortest wavelengths and progressing to the longest. Each reading, in forward or reverse direction was an average of four settings for a stellar line or two settings for an iron-arc line, although more settings were made on nebulous or faint lines. The difference between forward and reverse readings gives a measure of displacement on the plate whilst the sum of forward and reverse readings should be constant and provides a means to guard against gross errors. Measuring a plate in both directions will tend to eliminate personal errors caused by estimating different line centres for emission and absorption lines, and cumulative errors in the micrometer screw.

Reduction of the raw data was performed with a Fortran programme (Hill, 1971) which used the well-determined Radcliffe constants λ_o, c and n_o in the Hartmann formula for prismatic dispersion

$$\lambda = \lambda_o + \frac{c}{n - n_o}$$

where n in this case is the difference between forward and reverse measurements. As with previous Radcliffe programmes, I.A.U. recommended wavelengths for OB star spectra (Pearce, 1932) and iron-arc spectra (Edlén, 1955) were adopted. The Fortran programme derived a correction curve for the Hartmann formula by fitting up to 7th order polynomials to the iron line residuals and adopting the polynomial with smallest standard deviation. The correction curves were nearly all of order 3, 4 or 5. A few manual reductions were performed but the results were not significantly different from those of the computer programme.

Although all stellar lines on a given spectrum were measured and had velocities computed, not all were used to derive the stellar radial velocity. Basic recommendations made by Petrie (1953b) were followed, with a few Radcliffe modifications. Table 7 lists the main spectral lines which, when measurable, were used to find the mean stellar velocity. All O II lines except O II 4069 were rejected as were He I 4713 and 4009. The interstellar Ca II K-line at 3933 Å was measured whenever present, but the H-line at 3968 Å was only visible on a few spectra, usually if Hε was very nebulous or absent

Table 7

Stellar lines used for radial velocity determinations

Line		Spectral types	Comments
H	4861		Spectrograph focus imperfect and emulsion sensitivity poor
	4340	B0-B8	
	4101	B0-B9	NIII 4097 implies NIII 4103 / H 4101 blend
	3970	B0-B9	CaII 3933 implies CaII 3968 / H 3970 blend; O II implies O II 3973 / H 3970 blend
He I	4921		As H 4861
	4471	B0-B9	+10 km/s for class V (Radcliffe)
	4388	B0-B8	
	4120	B0-B9	Petrie rejects on c spectra. Used if no O II present
	4026	B0-B9	+4 km/s for classes III-V (Radcliffe)
	3964	B0-B6	If resolved from H 3970 and CaII 3968
Si IV	4116		
	4089		
Si III	4569 (7)	B0-B3	
	4552	B0-B3	Petrie rejects on c dispersion spectra
Si II	4130	B3-B9	
	4128	B3-B9	
Mg II	4481	B3-B9	Blended with Al III earlier than B3
C II	4267	B0-B9	
O II	4069	B0-B3	The only O II line retained by Petrie
N II	3995	B0-B5	
He II	4686, 4541, 4199	O	He II 4541, 4199 imply blending of Balmer lines and He I 4026. In the hottest stars only He II 4541 and 4199 are unblended.

as in the case of helium star HD 168476. The corrections +10 km/s to He I 4471 in class V stars and +4 km/s to He I 4026 in class III – V stars were applied throughout, following Feast et al. (1957).

The radial velocity of a star determined directly from a spectrogram requires certain corrections. These may be conveniently divided into instrumentation corrections and corrections for the motion of the Earth. Velocity additions described above for He I 4026 and 4471 are probably due to line blending effects dependent on resolving power of the spectrograph and emulsion (Feast et al., 1957). A further instrumental effect is described by Feast and Thackeray (1963) concerning systematic errors of the d camera. The difference in measured velocities between c and d cameras was found to be related to the zenith distance of the star under observation and was attributed to systematic guiding errors occurring when the atmospheric dispersion of the star image lay across the spectrograph slit. Feast and Thackeray assumed the error to have the form

$$\Delta v\ (c - d) = k \tan z$$

where z is zenith distance. They determined a value of +10.2 for k and adopted the correction +10.2 tan z for all d camera velocities. Wallis and Clube (1968) re-examined the difference, finding $k = 9.5 \pm 1.8$ (s.e.) from bright late-type stars. In the present programme, all d camera velocities were corrected by +10.2 tan z.

When instrumental corrections have been applied, a radial velocity still contains two variable quantities, the annual and diurnal velocities, V_a and V_d, caused by the orbital motion and rotation of the Earth. These velocities must be computed for each spectrum since V_a for a given star will vary from night to night and V_d will vary during the night. The maximum range of the annual variation is -30 km/s $< V_a < +30$ km/s for a star on the ecliptic; V_d is never numerically greater than 0.5 km/s.

Herrick (1935) has given tables to assist in the evaluation of V_a and V_d, but a Fortran programme written by Jones and Wood and revised by Hill (private communication) was used to compute the "Earth corrections". A list of values of $V_a + V_d$ for all stars observed was received in a private communication from Radcliffe observatory and provided a useful check on the computations.

Mean programme star velocities were calculated with a similar weighting system to that of Feast and Thackeray (1963). Spectra taken with the c camera were given weight 1, d camera spectra weight $\frac{1}{2}$. Any poor spectra, judged by high standard error for the velocity or relatively few lines used, were given half the appropriate weight.

4. Errors

Internal error analysis was carried out in similar fashion to those for the photometric data. Results for the standard deviation of a single observation were as follows:

	σ	observations	stars
Unweighted	± 9.2 km/s	174	58
Weighted	± 8.8 km/s	141 (weight)	58

Little is gained by use of weighted residuals. The standard deviation, σ', for each star was calculated and the criteria $\sigma' \geqslant 2\sigma$ for possible variability and $\sigma' \geqslant 3\sigma$ for probable variability were applied. With $\sigma = \pm 9$ km/s, three stars included in the original analysis were found to be possible variables and were excluded from the final analysis which gave $\sigma = \pm 8.4$ km/s. For the Ca II K-line velocities a value of $\sigma = \pm 7$ km/s was found.

Internal errors are rather large and probably attributable to a combination of inexperience of the measurer and the generally poor spectra of early-type stars which tend to have few suitable lines in the 4000 – 5000 Å region. In addition, a few plates were rather underexposed which undoubtedly contributed to the scatter in some stellar velocities.

Assessment of external errors depends on half a dozen stars from previous Radcliffe programmes, observed in 1971 as overlap stars, plus two southern hemisphere standards. Mean differences are:

Stellar lines	$\overline{\Delta V}$ = −0.6 ± 0.8 (s.e.) km/s	8 stars
Ca II K-line	$\overline{\Delta V}$ = −1.7 ± 2.3 (s.e.) km/s	7 stars

which can be considered to be negligible. $\overline{\Delta V}$ for the interstellar Ca II line becomes zero if one star is removed from the analysis. A further check was possible using ten stars near the celestial equator observed by Neubauer (1943) at Lick observatory. Significant differences between Radcliffe and Lick velocities have been reported and are also found for stars of the present programme.

$\overline{\Delta V}$ (Radcliffe − Lick)	stars	source
+13.4 ± 3.2 (s.e.)	21	Feast and Thackeray (1963)
+11.4 ± 1.9	31	Feast and Thackeray (1958)
+14.3 ± 1.2	3	Hill (1971)
+10.2 ± 5.2	10	This programme

5. Spectral classification

All d spectra and many c spectra were classified on a Hilger and Watts spectrum comparator at the Radcliffe observatory. Standard spectra taken by Radcliffe observers with the two-prism spectrograph were available for virtually all spectrum and luminosity sub-classes of the early-type stars. The "Atlas of stellar spectra" (Morgan et al., 1943) was used as a guide to classification. The c spectra were later re-classified at St. Andrews but, since comparison spectra were not available, the "Atlas of stellar spectra" had to provide standards. This was unsatisfactory as not all sub-classes are represented in the Atlas photographs. These later classifications were given low weight.

I am grateful to Dr. P.W. Hill for second opinions on many of the d spectra classifications.

CHAPTER V

DATA TABLES

The basic data for 197 intermediate and high latitude stars is arranged in two tables. UBV photometry, MK types and radial velocities are from a number of sources including the present programme; the Hβ photometry is all from measurements made in the 1970-71 observing programmes. Table 8 contains positional, photometric and spectroscopic information arranged in columns as follows:

(1) Star number from the Henry Draper catalogue or Cape Photographic Durchmusterungen. In the table, CPD numbers are negative, the first two digits refer to the zone and the last four to the star number within the zone.

(2), (3) R.A. and declination for the epoch 1950.0.

(4), (5) Galactic longitude and latitude computed from 1950 equatorial co-ordinates using equations given by Torgård (1961).

(6) to (8) UBV photometry in the form V magnitude and (B-V), (U-B) colours. A colon following any quantity indicates that the standard deviation for measurements of that star was more than twice the standard deviation of a single observation calculated in II.5.

(9) References for the UBV photometry. Numbered references are in a list following Table 9. No reference indicates that the photometry is based on 1970 observations alone, and '(P)' means the photometry is "provisional", being based on combinations of observations made in 1968, '69 or '70 (by van Breda, Hill or Kilkenny) for which final results were not available at time of writing.

(10) Hβ photometry on the Crawford and Mander (1966) standard system. A colon indicates that σ', the standard deviation of measurements of a given star, was greater than twice the standard deviation of a single observation, σ ,

calculated in III.5. The letter 'V' indicates $\sigma' > 3\sigma$.

(11) The number of separate observations forming the mean β-index.

(12), (13) Radial velocity, to the nearest km/s, of star and interstellar Ca II K-line respectively. A colon implies possible variability and 'V' probable or definite variability. When the interstellar velocity is noted as possibly variable, this is presumably due to measuring effects or contamination by stellar lines. The average number of plates per 1971 stellar velocity is three, although four stars in Table 8 have velocities based on only one 1971 spectrum each. These are HD 116455, 148614 and 180629 and CPD -59° 6926. The velocity of helium star HD 168476 is based on ten spectra at 49 Å/mm.

(14) Radial velocity references. No reference means the velocity is from 1971 plates only. '(B)' indicates velocities from the "Bibliography of Radial Velocities" (Abt and Biggs, 1972). A few of these were originally published by Neubauer (1943) and have been corrected by +10 km/s, following a suggestion by Feast and Thackeray (1963). This correction is in good agreement with observed differences between Neubauer data and 1971 results (see section IV.4).

(15) Spectrum/luminosity type on the MK system, with the usual suffices for emission, nebulous lines, etc. A colon implies uncertainty in the classification and a solitary 'E' refers to stars with Hα in emission (Wackerling, 1970).

(16) References for MK classifications.

Table 8

Positional, photometric and spectroscopic data

HD/CPD	ALPHA	DELTA	L	B	V	B-V	U-B	REF	BETA	N	VEL	CAII	REF	MK TYPE	REF
	h m	° ′	°	°	m	m	m				km/s	km/s			
87782	10 4.3	-34 58	268.76	16.52	8.17	-0.06	-0.38	(2)	2.745	4				B5 III	(2)
88799	10 9.5	-78 32	295.28	-18.39	9.26	+0.02	-0.43	(2)	2.725	4				B5 V	(2)
89403	10 13.9	-78 44	295.60	-18.44	7.70	-0.03	-0.62	(2)	2.627	4	+10	+9:	(7)	B2 V	(2)
91323	10 29.5	-44 13	278.30	11.59	7.19	-0.15		(9)			+17	+10	(3)	B5 III	(3)
93840	10 46.9	-46 30	282.15	11.10	7.80	-0.01	-0.90	(9)			-2	-12:	(3)	B1 I	(6)
95029	10 55.2	-51 33	285.64	7.17					2.595	3	-31	+5	(4)	B2 V	(4)
97185	11 8.3	-49 21	286.67	10.02	7.49	-0.10	-0.72	(2)	2.610	3	-12	+2	(8)	B4 V	(2)
97991	11 13.5	-3 10	262.33	51.74	7.41	-0.22	-0.91	(2)	2.615	4	+24		(8)	B1 V	(2)
97895	11 12.9	-29 13	279.07	28.87	8.77	-0.10	-0.56	(2)	2.706	4				B5 III	(2)
99205	11 21.7	-69 50	295.57	-8.52					2.591	3					
102657	11 46.4	-51 7	293.10	10.27	7.73	-0.03	-0.56	(2)	2.621	2				B3 V	(2)
103715	11 53.9	-71 22	298.59	-9.25	9.065	+0.185	-0.765		2.41	1	-23:	-8	(4)	B2 NE	(4)
-72°1184	11 56.5	-73 9	299.16	-10.94	10.68	-0.07	-0.93		2.576:	5	-217	-10		B0 III	
105071	12 3.3	-65 16	298.24	-3.08	6.32	+0.22	-0.50	(9)	2.569	3	-7	-9		B8 IA	(10)
105139	12 3.6	-69 30	299.03	-7.26	7.55	+0.005	-0.655		2.647	4	+13	+1:	(8)	B3 III	(8)
107788	12 20.6	-53 21	298.73	9.00	8.715	-0.10	-0.855		2.585	4	+14	-17		B2 V	
108230	12 23.6	-32 3	296.75	30.25	9.34	-0.16	-0.81	(2)	2.62 :	4				B5 II	(2)
108769	12 27.2	-34 13	297.92	28.16	9.05	-0.15	-0.78	(2)	2.649	4	-46	-8	(7)	B3 V	(2)
109399	12 32.1	-72 26	301.72	-9.88	7.615	+0.005	-0.86		2.568	5	-51	-7		B0.5IIIN	
109885	12 36.1	-71 20	301.96	-8.77	9.00	+0.145	-0.685		2.616	4	-29	+5		B3 V	
111079	12 44.7	-71 18	302.66	-8.73	8.445	+0.07	-0.42		2.731	4					
111290	12 46.2	-71 26	302.78	-8.86	7.765	+0.015	-0.795		2.595	4	-4	-8		B1 III	
111822	12 49.6	-52 22	303.10	10.21	7.86	-0.045	-0.935		2.589	6	-9:	-10	(3)	B0.5 III	(3)
112192	12 52.3	-42 0	303.67	20.57	6.82	-0.13	-0.67	(2)	2.677	3	+11:		(7)	B5 V N	(2)
112481	12 54.6	-49 29	303.94	13.09	8.36	+0.04	-0.74	(2)	2.610	6	-15	-13	(7)	B2 IB	(2)
112491	12 54.7	-53 49	303.87	8.75	9.615	+0.04	-0.67		2.642	4	-27	-17		B2 V	
112510	12 54.9	-54 29	303.88	8.09	9.335	+0.005	-0.47		2.654	4					
-69°1743	12 57.2	-69 56	303.71	-7.35	9.43	+0.025	-0.815		2.567	7	-31	-3		B1 V N	
112843	12 57.7	-72 20	303.68	-9.76	9.53	+0.10	-0.705		2.563	5	-43	-4:	(4)	B2 III :	(4)
113134	12 59.2	-51 30	304.63	11.05	9.12	0.00	-0.49		2.688	4					
114200	13 7.2	-70 31	304.54	-7.99	8.465	+0.105	-0.905	(P)						E	
114441	13 8.3	-55 4	305.80	7.41	8.04	+0.13	-0.76	(P)			-8:	-2	(4)	B2 V: NE	(4)
114444	13 9.1	-75 2	304.33	-12.50	10.32	-0.01	-0.79	(2)	2.551	6	-77:	-11	(7)	B2 III	(2)
116455	13 21.5	-50 37	308.27	11.64	10.345	-0.01	-0.72		V		-27	-50		B3 V	
116538	13 22.0	-51 34	308.23	10.69	7.92	-0.07	-0.90	(2)	2.535:	5	-74	-13	(7)	B2 IV N	(2)
116852	13 25.6	-78 35	304.88	-16.13					2.555	4	-47:	-5:	(4)	O9 III	(4)
117170	13 26.4	-53 44	308.59	8.45	7.635	-0.02	-0.71		2.631	4	-21:	-13	(8)	B2 V	(8)
119069	13 38.8	-45 35	312.06	16.12	8.43	-0.20	-0.98	(2)	2.579	4	-126	-13	(7)	B1 III	(2)
119109	13 40.1	-73 22	306.70	-11.15	7.465	0.00	-0.515	(P)	2.704	4	V	+6:	(8)	B7 V	(6)
119608	13 41.7	-17 40	320.35	43.13					2.554	4	+28:	+7:	(3)	B1 IB	(6)

Table 8 (cont.)

HD/CPD	ALPHA	DELTA	L	B	V	B-V	U-B	REF	BETA	N	VEL	CAII	REF	MK TYPE	REF
	h m	° ′	°	°	m	m	m				km/s	km/s			
119644	13 42.2	-65 5	312.77	16.49	8.10	-0.09	-0.52	(2)	2.643	4	+5	-12	(7)	B4 III	(2)
120086	13 44.7	-2 12	329.61	57.48	7.89	-0.18	-0.79	(2)	2.648	4	+4	-27	(7)	B3 III	(2)
120377	13 47.8	-70 30	307.91	-8.48	9.13	+0.12	-0.075		2.745	4					
120958	13 50.4	-38 48	315.89	22.25	7.6 :	-0.11:	-0.77	(2)	2.52	1	-19:	-12:	(7)	B3 V NE	(2)
121483	13 53.5	-46 7	314.51	15.03	6.95	-0.13		(9)	2.663	4	-22:	-4:	(3)	B2 V	(3)
121968	13 56.2	-2 40	333.98	55.83	10.31	-0.19	-0.89	(9)	2.56 :	4					
121983	13 56.6	-33 17	318.88	27.21	8.10	-0.10	-0.75	(2)	2.591	4	-22	-18	(7)	B3 III	(2)
122180	13 58.9	-68 58	309.24	-7.23	8.115	-0.075	-0.575	(P)	2.705	4					
122449	13 59.9	-46 34	315.48	14.30	8.12	-0.08	-0.43	(2)	2.705	6				B5 III	(2)
-70°1704	14 0.2	-70 33	308.91	-8.78	9.525	+0.065	-0.37		2.683	6					
123884	14 7.7	-17 44	328.18	40.97	9.36	+0.06	-0.25	(2)	2.604	3	+7		(8)	A0 IB 7	(2)
124448	14 11.7	-46 2	317.65	14.19	9.99	-0.09	-0.80	(2)	2.46 :	4	-65		(6)	B3 P	(2)
124979	14 14.7	-51 15	316.40	9.09	8.535	+0.09	-0.84	(P)	2.572	6	-68	-14	(4)	O8.5	
125924	14 19.9	-8 1	338.15	48.28	9.68	-0.19	-0.85	(2)	2.615	4	+252	-1:	(7)	B2 IV	(2)
-69°2055	14 25.1	-69 54	311.16	-8.83	10.08	+0.085	-0.78		2.555	6	-130	-21		B2 III	
-74°1182	14 25.6	-74 32	309.44	-13.15	10.24	-0.01	-0.58		2.642	6	-17:	+4:		B5 V	
127493	14 29.4	-22 26	331.44	34.57					2.57 :	3	-30:			B0 V	
-72°1542	14 30.2	-73 19	310.21	-12.14	10.165	-0.02	-0.915		2.611	5	-11	+2		B1 III	
128585	14 35.9	-50 56	319.65	8.17	9.275	+0.065	-0.485	(P)	2.636	4	+26	-12		B3 V	
-74°1221	14 37.4	-74 39	310.13	-13.57	10.17	+0.055	-0.32		2.685:	6					
129929	14 43.2	-37 0	327.02	20.21	8.09	-0.16	-0.87	(2)	2.618	4	+66	-8:	(7)	B3 V	(2)
-44°6953	14 43.6	-45 1	323.36	13.01	10.14	+0.06	-0.54	(2)			-18:	-9:	(7)	B6 V E	(2)
-42°6798	14 43.8	-42 41	324.45	15.09	10.26	+0.05	-0.62	(2)	2.61 :	6	-74:	-25	(7)	B2III-II	(2)
132041	14 55.1	-35 52	329.80	20.11	7.80	-0.07	-0.38	(2)	2.719	4				B5 III	(2)
132907	15 1.2	-70 55	313.47	-11.06	7.675	-0.055	-0.42		2.698	3	+4	-16	(8)	B5 III	
132960	15 0.0	-41 4	327.99	15.09	7.39	-0.16	-0.94	(8)	2.605	4	V	-12	(8)	B1 IV	(8)
134411	15 7.9	-39 41	330.06	15.54	9.56	-0.18	-0.82	(2)	2.621	4				B2 V N	(2)
134591	15 8.7	-34 35	333.07	19.78	8.37	+0.06	-0.35	(2)	2.699	4				B5 III	(2)
135485	15 12.9	-14 29	347.31	35.46	8.17	-0.08	-0.54	(2)	2.703	4	-1	+2	(7)	B5 II P	(2)
137179	15 28.9	-83 4	307.80	-22.01	8.75	-0.08	-0.69	(2)	2.613	4	-43	-14	(7)	B2 III	(2)
137518	15 24.7	-44 57	329.80	9.40	7.82:	+0.11:	-0.68:	(P)							
137595	15 24.8	-33 21	336.73	18.87	7.49	+0.03	-0.74	(2)	2.604	4	+131	-12	(7)	B3 V N	(2)
-75°1197	15 2[illegible].9	-75 30	312.63	-15.97	9.52	-0.065	-0.80		2.597	6	-19	-28		B1 V N	
138503	15 30.3	-24 50	343.35	24.87	9.1 :	-0.03	-0.73	(2)						B5 V N	(2)
139431	15 36.3	-42 35	332.92	10.10	7.48:	+0.01:	-0.72:	(P)						E	
139432	15 36.3	-43 26	332.41	9.42	7.59	+0.06	-0.385	(P)	2.685	5	-20:	-4:	(8)	B6 III	(8)
140205	15 41.7	-64 45	320.15	-8.04	9.135	0.00	-0.245	(P)	2.796	1					
140249	15 41.9	-65 2	319.99	-8.28	9.945	+0.02	-0.32	(P)	2.737	1					
140277	15 42.1	-64 57	320.06	-8.23	9.875	-0.04	-0.43	(P)	2.632	1					
140543	15 41.9	-21 39	347.90	25.54	8.92	+0.01	-0.89	(9)	2.546	4	-11:		(8)	B0.5 III	(6)

Table 8 (cont.)

HD/CPD	ALPHA	DELTA	L	B	V	B-V	U-B	REF	BETA	N	VEL	CAII	REF	MK TYPE	REF
	h m	° ′	°	°	m	m	m				km/s	km/s			
142754	15 54.4	-40 51	336.69	9.33	8.595	+0.175	-0.67	(P)	2.603	4	-47	-11		B1 V	
143104	15 57.9	-66 24	320.39	-10.41	9.31	-0.105	-0.725	(P)	2.637	6	-62	-6:	(4)	B2 V	(4)
143156	15 58.0	-63 44	322.18	-8.41	8.115	-0.085	-0.535	(P)	2.697	4					
143414	15 59.3	-62 32	323.09	-7.60	10.04:	-0.065	-0.71	(P)						WN 6	(6)
143495	16 1.0	-72 33	316.34	-15.15	9.48	+0.07	-0.36	(2)	2.649	4	V	-5	(7)	B8 V	(2)
143549	16 0.8	-68 17	319.31	-11.98					2.675	4	-8	-16		B5 III	
143756	16 1.4	-62 16	323.44	-7.58	9.235	-0.03	-0.505	(P)	2.651	4					
143888	16 2.1	-61 56	323.73	-7.38	9.305	+0.005	-0.405	(P)	2.674	4					
144887	16 7.4	-64 29	322.43	-9.66	9.08	-0.08	-0.45	(P)	2.740	4					
144965	16 6.7	-40 0	339.04	8.42	7.045	+0.15	-0.52							E	
145537	16 9.5	-34 31	343.29	11.99	10.41	+0.10	-0.79	(2)	2.567	4	+61:	-4	(7)	B0.5 V	(2)
146332	16 13.8	-29 38	347.50	14.83	7.62	+0.185	-0.365		2.646	5	-14	-11		B5 III	
146755	16 17.8	-69 13	319.76	-13.74	9.485	-0.005	-0.545	(P)							
-59°6723	16 20.7	-59 57	326.77	-7.49	9.74	+0.30	-0.22		2.48 :	6	-6	-14		B5 P SH?	
148546	16 27.0	-37 52	343.37	7.14	7.71	+0.285	-0.715	(P)	2.546	6	-52	-21:		O9.5 I	
148614	16 28.3	-58 58	328.15	-7.52	10.24:	-0.025	-0.725	(P)	2.662	4	-22	-16		B2 V	
148740	16 29.7	-65 54	323.07	-12.32	7.345	-0.09	-0.535		2.703	6	-2	+1	(3)	B5 III	(3)
149273	16 31.8	-36 16	346.70	8.85	9.26:	0.00:	-0.835	(P)	2.589	3	+17	-3		B0.5 V	
149363	16 31.7	-6 1	9.84	26.69	7.81	+0.05	-0.80	(9)	2.564	3	+146	-26:	(5)	B0.5 III	(5)
149382	16 31.7	-3 53	11.83	27.89					2.611	3	+13		(8)		
-67°3184	16 35.7	-67 46	322.01	-13.97	10.75	-0.135	-0.85			V	+14	-5		B5 III	
149770	16 36.1	-62 26	326.19	-10.56	8.025	-0.105	-0.605	(P)	2.635	4	-29	-9		B5 V N	
150323	16 38.3	-32 42	348.81	8.87	7.60	-0.055	-0.295	(P)	2.729	4					
-74°1569	16 44.5	-74 27	317.02	-18.68	10.15	-0.17	-1.01		2.58 :	6	-123	-8		O9.5 V	
151310	16 44.5	-22 5	358.06	14.62	9.375	+0.015	-0.62		2.648	5	-31:	-1		B3 V N	
152179	16 49.8	-31 20	351.44	7.88	8.885	+0.225	-0.57	(P)	2.63 :	4					
152286	16 50.4	-28 19	353.91	9.66	9.665	+0.005	-0.675	(P)	2.585	4	+13	-10		B2 III	
152516	16 51.6	-21 47	359.34	13.47	8.025	+0.065	-0.565	(P)	2.605	4	-19		(8)		
152640	16 53.4	-55 46	332.82	-8.02	8.225	0.00	-0.455	(P)	2.709	4					
153084	16 55.3	-29 19	353.78	8.21	8.54	-0.065	-0.78	(P)	2.624:	4	+18	+3		B2 V	
153977	17 0.6	-24 44	358.19	10.04	9.475	+0.035	-0.45	(P)							
-69°2698	17 7.0	-70 2	321.87	-17.57	9.375	-0.085	-0.88		2.606	6	-63	-15		B2 IIIHE	
155409	17 10.3	-55 56	334.12	-10.01	7.98:	-0.06	-0.655	(P)	2.651	4	+17	-1		B3 V	
155418	17 10.1	-52 2	337.33	-7.75	9.56	+0.035	-0.615	(P)	2.655	4	-27	+5		B2 V	
-59°6926	17 11.9	-59 26	331.31	-12.16	10.75:	-0.02	-0.89			V	+44	+17		B3 E	
156359	17 16.5	-62 51	328.67	-14.52	9.67	-0.14	-0.98	(2)	2.541	6	-02	-10	(7)	O9 III	
156779	17 17.2	-18 45	5.43	10.33	9.275	+0.175	-0.535	(P)	2.577	4	+3	-7		B3 III	
157857	17 23.4	-10 57	12.95	13.31	7.775	+0.175	-0.785	(P)			+57	+7:	(3)	O7 F	(6)
158111	17 26.2	-54 11	336.88	-10.94	7.77	-0.015	-0.43	(P)	2.707	4	-26	-3	(8)	B6 III	(8)
158243	17 26.9	-53 25	337.60	-10.63	8.15	0.00	-0.82	(2)	2.578	6	-64	-11	(7)	B1 IAB	(2)

Table 8 (cont.)

HD/CPD	ALPHA	DELTA	L	B	V	B-V	U-B	REF	BETA	N	VEL	CAII	REF	MK TYPE	REF
	h m	° '	°	°	m	m	m				km/s	km/s			
158659	17 28.1	-11 7	13.42	12.24	10.255	+0.225	-0.705	(P)	2.597	4	+64	-5		B0 V	
158661	17 28.2	-17 4	8.30	9.06	8.20	+0.205	-0.735	(P)	2.565	4	-1	-12		B0 I	
-79°923	17 29.4	-79 19	313.95	-23.34	10.38	+0.33	+0.26		2.78 :	5	-9			B8 V	
159489	17 33.5	-45 6	345.29	-7.10	8.25	-0.02	-0.61		2.626	4	+9	-11		B3 V N	
159792	17 35.0	-46 16	344.44	-7.94	9.44	+0.145	-0.615	(P)	2.615:	6	V	-12		B2 III	
159864	17 34.6	-17 47	8.52	7.39	8.555	+0.245	-0.705	(P)	2.582	4	+21	-5		B0 III	
160207	17 37.1	-44 55	345.79	-7.54	8.40	-0.015	-0.42		2.686	4	+17	-17		B8 III	
160397	17 38.2	-48 48	342.54	-9.72	9.775	-0.005	-0.43	(P)	2.646	4					
160878	17 40.7	-44 11	346.77	-7.71	8.66	-0.05	-0.69	(P)	2.653	4	-45	-22		B2 IV	
160993	17 41.5	-45 36	345.60	-8.57	7.73	+0.02	-0.82	(2)	2.561	6	-11	-6	(7)	B1 I	(2)
160995	17 41.6	-48 17	343.27	-9.95	10.38	-0.05	-0.57	(2)	V		V	-2	(7)	B5 V	(2)
161306	17 42.4	-9 46	16.44	9.92	8.17	+0.595	-0.435	(P)			+18:	+2:	(5)	B0 NE	(5)
161633	17 45.1	-46 55	344.78	-9.77	9.82	-0.12	-0.95	(2)	2.614	6	+19:	-7:	(7)	B0 V	(2)
161961	17 45.9	-2 9	23.65	12.91	7.775	+0.22	-0.72	(P)	2.574	4	+3	-12		B0.5 III	
161972	17 47.0	-46 12	345.57	-9.69	8.34	-0.11	-0.57		2.696	3	-3	-9		B5 III	
162089	17 47.9	-47 48	344.24	-10.59	9.265	-0.08	-0.645		2.645:	4	-54:	-21		B5 III	
163254	17 53.6	-41 58	349.90	-8.63	6.72	-0.075	-0.655		2.663	4	-51:	-5	(3)	B5 NK SB	(3)
163522	17 54.9	-42 27	349.58	-9.08	8.43	-0.01	-0.86	(2)	2.558	6	+33	+1	(7)	B1 IP	(2)
164073	17 58.0	-48 47	344.17	-12.57	8.03	+0.035	-0.51		2.673	5					
164340	17 58.9	-40 4	352.06	-8.59	9.285	-0.14	-0.96		2.585	4	0:	-3		B0 III	
164806	18 2.0	-58 33	335.34	-17.37	6.83	-0.10	-0.53	(2)	2.663	4	-9	-8	(7)	B5 III	(2)
165955	18 6.5	-34 52	357.41	-7.43	9.19	-0.05	-0.82		2.613	5	-170V	-21		B3 V N	
-761313	19 7.1	-76 43	317.98	-27.65	10.265	-0.135	-0.815		2.622	6	+1	-2		B2 V	
165938	18 7.7	-61 14	333.06	-19.09	8.21	-0.09	-0.46	(2)	2.693	3	-21	-17	(7)	B5 III	(2)
166832	18 10.6	-36 52	356.01	-9.10	8.39	-0.065	-0.50		2.634	3	-27	-16		B8 III	
167003	18 11.3	-33 8	359.41	-7.48	8.47	-0.13	-0.955	(P)	2.602	6	-31	-12		B0.5 III	
167321	18 12.9	-38 56	354.35	-10.44	8.93	-0.04	-0.31		2.746	4					
168476	18 18.8	-56 39	338.12	-18.70	9.30	-0.01	-0.69	(2)	2.499	4	-170	+3		B5 P	
168785	18 19.5	-30 9	2.91	-7.65	8.47	+0.045	-0.735	(P)	2.604	4					
170385	18 27.5	-43 45	351.10	-14.99	7.90	-0.14	-0.63	(2)	2.691	4	-5	-10	(7)	B3 V	(2)
170638	18 28.5	-30 5	3.85	-9.35	8.61	-0.015	-0.525								
171141	18 31.5	-45 58	349.28	-16.51	8.38	-0.22	-0.96	(2)	2.597	4	+2	+8	(7)	B1 III	(2)
171757	18 34.4	-28 2	6.30	-9.61	8.93:	+0.125	-0.805	(P)							
172094	18 36.6	-41 57	353.49	-15.80	8.28	-0.15	-0.88	(2)	2.583	3	+44	+14	(7)	B2 III	(2)
172127	18 36.7	-39 46	355.58	-14.96	10.48	-0.12	-0.765		2.672	3	-71:	+8		B5 V	(2)
172140	18 36.5	-29 22	5.27	-10.60	9.96	-0.06	-0.90	(2)	2.58 :	4	+39:	-4:	(7)	B0.5 III	(2)
172533	18 38.6	-27 29	7.20	-10.21	8.305	-0.02	-0.495		2.628	4	-23	-7		B5 III :	
173502	18 43.6	-30 1	5.34	-12.27	9.725	-0.095	-0.92	(P)	2.564	4	+64	+5		B0.5 V	
173994	18 46.9	-47 49	348.46	-19.62	7.07	-0.15	-0.71	(2)	2.665	4	-8:	+5:	(7)	B2 V	(2)
174524	18 48.7	-27 12	8.45	-12.11	9.78	+0.025	-0.495	(P)	2.691	4					

Table 8 (cont.)

HD/CPD	ALPHA	DELTA	L	B	V	B-V	U-B	REF	BETA	N	VEL	CAII	REF	MK TYPE	REF
	h m	° '	°	°	m	m	m				km/s	km/s			
175141	18 51.8	-19 54	15.46	-9.63	9.235	+0.03	-0.315		2.741	4	+6:		(8)		
175754	18 54.5	-19 12	16.39	-9.91	7.00	-0.085	-0.96	(P)			-15:		(8)	O8 F	(6)
175876	18 55.2	-20 28	15.30	-10.59	6.92	-0.105	-1.00	(P)	2.565	5	-16	-3		O7	
177014	19 0.5	-19 29	16.76	-11.31	9.265	+0.195	-0.025	(P)	2.777	3	+2		(8)		
177015	19 0.6	-20 11	16.11	-11.61	7.80	-0.04	-0.44	(9)			+16		(8)	B5 E	(8)
177559	19 2.9	-19 33	16.94	-11.85	8.10:	+0.005	-0.67	(P)	2.633	4	V	-10		B6 V	
177566	19 3.5	-41 47	355.55	-20.42	10.20	-0.20	-1.00	(2)	2.544	2	-131	+11	(7)	B1 III	(2)
177989	19 4.6	-18 47	17.81	-11.89	9.33	-0.055	-0.895	(P)	2.584	4	+9	-7		B0 III	
178370	19 6.3	-32 0	5.46	-17.52	9.51	-0.12	-0.69	(2)	2.592	3	-148	-148:	(7)	B3 III	(2)
178487	19 6.4	-10 16	25.79	-8.55	8.66	+0.16	-0.78	(P)	2.565	4	-55	-6		B0 I	
178861	19 7.8	-12 32	23.89	-9.87	8.48	+0.135	-0.505		2.649	4	+5	-6		B3 III :	
179007	19 8.9	-36 1	1.70	-19.48	10.00	-0.13	-0.68	(2)	2.69 :	3	+5:	-1	(7)	B3 III	(2)
179202	19 9.4	-23 6	14.26	-14.70	8.35	0.00	-0.44	(2)	2.702	4	+6	+4	(7)	B5 V	(2)
179407	19 10.0	-12 39	24.03	-10.40	9.415	+0.085	-0.805	(P)	2.547	4	-117	+4		B0.5 I :	
180629	19 14.9	-17 1	20.52	-13.34	8.12	-0.055	-0.50		2.695	4	+19	-3		B3 V	
182975	19 24.7	-2 6	35.25	-8.92	8.375	+0.12	-0.505	(P)	2.661	6	+9		(8)		
183129	19 25.4	-1 11	36.15	-8.65	8.135	+0.10	-0.29		2.678	4	+8		(8)		
183570	19 27.9	-16 16	22.57	-15.85					2.682	4	+3		(8)		
183899	19 29.6	-26 15	13.07	-20.13	9.80	-0.08	-0.79	(2)	2.611	4	-45	-20:	(7)	B2 III	(2)
185534	19 37.3	-21 24	18.55	-19.95					2.711	6	-2		(8)		
185842	19 38.5	-2 25	36.58	-12.12					2.671	4	-8	-10		B3 V	
186610	19 42.8	-3 16	36.32	-13.47	9.64	+0.015	-0.755	(P)	2.581	5	+28	+5	(5)	B1 III	(2)
187311	19 47.5	-41 9	358.71	-28.17	10.25	-0.17	-0.67	(2)	2.660:	4	-13:	-4:	(7)	B3 V	(2)
187350	19 46.9	-1 13	38.67	-13.42	8.115	+0.12	-0.70	(P)			+15		(8)	B0 E K	(8)
187536	19 48.3	-28 19	12.52	-24.75	9.46	-0.08	-0.86	(2)	2.581	2	+16	-4:	(7)	B2 III	(2)
188618	19 53.7	-18 2	23.48	-22.21					2.611	4	-4		(8)		
195455	20 29.2	-24 13	20.27	-32.13	9.20	-0.18	-0.90	(2)	2.589:	4	+12	+1	(7)	B0.5III:	(2)
204076	21 23.9	-32 8	13.90	-45.68	8.79	-0.15	-0.84	(2)	2.583	4	-11	-11	(7)	B1 V	(2)
206144	21 37.8	-17 49	34.83	-45.12					2.534	4	+106:	-15		B3 V	
208213	21 52.4	-30 16	17.88	-51.48	8.42	-0.13	-0.57	(2)	2.649	4	-67	-1:	(7)	B3 V	(2)
214080	22 33.4	-16 39	44.80	-56.91	6.80	-0.14	-0.92	(2)	2.583	2	+8	0		B1 III	
214539	22 37.2	-67 55	319.77	-44.94	7.22	+0.02		(9)	2.589	4	+333	+331	(3)	B9 V	(3)
220172	23 19.1	-10 1	68.10	-62.64	7.68	-0.21	-0.83	(2)	2.608	4	+27	-9		B2 V	
220787	23 24.2	-11 18	67.78	-64.39	8.30	-0.15	-0.63	(2)	2.633	4	+26	+15		B3 V	
-45°7545	15 36.8	-45 37	331.20	7.60	10.74	-0.01		(1)			-71	-21	(5)	B0 III	(3)
-44°7577	15 42.2	-44 20	332.70	8.10	10.86	+0.05		(1)			+11	-15	(5)	B1.5 V	(3)
-50°9971	17 14.8	-50 29	339.00	-7.40	10.55	+0.01		(1)			-1:	-11	(5)	B0.5 III	(3)

Table 9 contains the following data:

(1)	HD or CPD number as in column (1) of Table 8.
(2), (3)	Proper motion in R.A. and declination in arc seconds/annum.
(4)	Proper motion references. A list of references follows the table.
(5)	Colour excess $E_{B-V} = (B-V) - (B-V)_o$ where (B-V) is from Table 8 and $(B-V)_o$ is derived as described in II.6.
(6)	Total extinction in the V-magnitude caused by interstellar matter and computed from $A_V = 3.2\ E_{B-V}$.
(7)	Absolute magnitude, $M_V(S)$, corresponding to the MK type. The calibration by Blaauw (1963) was used.
(8)	Distance modulus, mod = $V-A_V - M_V(S)$.
(9)	Stellar distance r, in parsecs, calculated from $5 \log r = V-A_V - M_V(S) + 5$.
(10) to (12)	As column s (7) to (9) but with $M_V(\beta)$, the absolute magnitude derived from the β-index, instead of $M_V(S)$.

Table 9

Proper motions, reddening corrections and distance determinations

HD/CPD	MU(A)	MU(D)	R	E(B-V)	AV	M(S)	MOD(S)	DIST(S)	M(β)	MOD(β)	DIST(β)
	″	″		m	m	m		pc	m		pc
87782	-0.030	-0.016	S	0.06	0.19	-2.2	10.17	1085	-0.1	8.07	412
88799	-0.006	00.000	C	0.18	0.58	-1.0	9.68	864	-0.5	9.18	686
89403	-0.009	+0.013	S	0.17	0.54	-2.5	9.65	853	-3.0	10.15	1074
91323						-2.2					
93840	0.000	-0.003	S	0.21	0.67	-6.2	13.32	4630			
95029						-2.5			-4.4		
97185				0.12	0.38	-1.3	8.40	479	-3.7	10.80	1449
97991	+0.022	+0.022	S	0.04	0.13	-3.6	10.88	1501	-3.5	10.78	1433
97895	-0.026	-0.017	S	0.07	0.22	-2.2	10.74	1409	-0.9	9.44	774
99205									-4.6		
102657	-0.016	-0.017	S	0.15	0.48	-1.7	8.95	616	-3.2	10.45	1230
103715	+0.006	-0.006	M								
-72°1184	+0.002	-0.006	N	0.23	0.74	-5.0	14.94	9745	-5.4	15.34	11716
105071	-0.015	-0.007	M	0.24	0.77	-7.1	12.65	3391	-5.8	11.35	1863
105139	-0.024	-0.022	M	0.22	0.70	-2.9	9.74	889	-2.3	9.14	674
107788	-0.007	+0.016	S	0.17	0.54	-2.5	10.66	1358	-4.9	13.06	4103
108230	-0.038	-0.028	M	0.02	0.06	-4.4	13.67	5435	-3.2	12.47	3127
108769	-0.040	-0.020	M	0.08	0.26	-1.7	10.49	1255	-2.2	10.99	1580
109399	0.000	-0.006	N	0.18	0.58	-4.7	11.73	2222	-5.9	12.93	3861
109885	-0.013	-0.023	M	0.41	1.31	-1.7	9.38	754	-3.4	11.08	1650
111079	-0.003	-0.023	M	0.23	0.74				-0.4	8.10	417
111290	+0.002	-0.008	Y	0.27	0.86	-4.4	11.29	1816	-4.4	11.29	1816
111822	+0.002	00.000	S	0.27	0.86	-4.7	11.69	2183	-4.7	11.69	2183
112192				0.07	0.22	-1.0	7.59	330	-1.5	8.09	416
112481	+0.005	-0.003	M	0.19	0.61	-5.7	13.45	4902	-3.7	11.45	1951
112491	+0.030	-0.027	S	0.28	0.90	-2.5	11.21	1749	-2.4	11.11	1670
112510	-0.057	-0.026	S	0.16	0.51				-2.1	10.91	1526
-69°1743	-0.033	-0.004	M	0.31	0.99	-3.6	12.03	2556	-5.9	14.33	7372
112843	-0.014	+0.007	Y	0.36	1.15	-3.6	11.97	2486	-6.2	14.57	8233
113134	-0.005	-0.015	S	0.17	0.54				-1.2	9.77	901
114200	+0.063	-0.048	M								
114441	-0.004	-0.015	S								
114444				0.26	0.83	-3.6	13.08	4145	-7.0	16.48	19842
116455	-0.007	-0.007	S	0.24	0.77	-1.7	11.27	1796			
116538	-0.049	+0.025	S	0.22	0.70	-3.3	10.51	1268			
116852						-5.7			-6.7		
117170	-0.008	-0.023	S	0.22	0.70	-2.5	9.42	767	-2.8	9.72	881
119069	+0.007	-0.005	M	0.09	0.29	-4.4	12.54	3224	-5.2	13.41	4819
119109	+0.004	+0.001	M	0.17	0.54	-0.4	7.31	290	-0.9	7.81	365
119608	-0.014	+0.004	S			-5.7			-6.8		

Table 9 (cont.)

HD/CPD	MU(A)	MU(D)	R	E(B-V)	AV	M(S)	MOD(S)	DIST(S)	M(β)	MOD(β)	DIST(β)
	"	"		m	m	m		pc	m		pc
119644	-0.015	+0.004	M	0.07	0.22	-2.5	10.37	1189	-2.4	10.27	1135
120086	-0.007	-0.012	S	0.04	0.13	-2.9	10.66	1356	-2.2	9.96	982
120377	-0.025	-0.011	M	0.19	0.61				-0.1	8.62	530
120958	+0.001	-0.007	M								
121483	-0.013	-0.001	M			-2.5			-1.8		
121968				0.07	0.22				-6.4	16.48	19824
121983	+0.019	-0.019	M	0.14	0.45	-2.9	10.55	1289	-4.6	12.25	2820
122180	-0.016	-0.081	S	0.11	0.35				-0.9	8.65	539
122449	-0.021	-0.009	M	0.06	0.19	-2.2	10.12	1060	-0.9	8.82	582
-70°1704	-0.007	-0.025	M	0.21	0.67				-1.3	10.14	1070
123884	-0.016	-0.010	S	0.06	0.19	-5.2	14.36	7474	-4.0	13.16	4301
124979	-0.015	+0.006	S	0.40	1.28	-5.0	12.25	2818	-5.2	12.45	3090
125924	+0.027	-0.036	S	0.06	0.19	-3.3	12.78	3610	-3.5	12.98	3959
-69°2055	-0.002	-0.006	N	0.37	1.18	-3.6	12.49	3156	-6.7	15.59	13158
-74°1182	-0.004	+0.004	N	0.18	0.58	-1.0	10.66	1357	-2.4	12.06	2587
127493	-0.015	-0.004	S			-4.4			-5.7		
-72°1542	-0.006	-0.011	N	0.29	0.90	-4.4	13.63	5325	-3.7	12.93	3858
128585	-0.001	-0.015	S	0.24	0.77	-1.7	10.20	1097	-2.6	11.10	1661
-74°1221	+0.001	+0.030	M	0.18	0.58				-1.3	10.89	1509
129929	-0.005	-0.020	M	0.08	0.26	-1.7	9.53	806	-3.3	11.13	1685
-42°6798				0.27	0.86	-4.2	13.59	5238	-3.7	13.09	4161
132041	+0.001	-0.026	M	0.05	0.16	-2.2	9.84	928	-0.6	8.24	444
132907	-0.012	-0.036	M	0.09	0.29	-2.2	9.58	824	-1.0	8.38	474
132960				0.13	0.42	-4.1	11.07	1639	-3.9	10.87	1495
134411	+0.007	+0.020	M	0.06	0.19	-2.5	11.86	2363	-3.2	12.56	3262
134591	-0.021	-0.005	M	0.20	0.64	-2.2	9.93	968	-1.0	8.73	557
135485	+0.006	-0.042	S	0.03	0.10	-4.4	12.47	3124	-0.9	8.97	623
137179	-0.024	+0.006	M	0.14	0.45	-3.6	11.90	2401	-3.6	11.90	2401
137518	+0.014	-0.017	M								
137595	-0.026	-0.026	M	0.29	0.93	-1.7	8.26	449	-4.0	10.56	1295
-75°1197	-0.015	+0.012	N	0.20	0.64	-3.6	12.48	3133	-4.3	13.18	4325
138503	-0.003	+0.007	S	0.22	0.70	-1.0	9.39	757			
139431	+0.006	-0.011	M								
139432	+0.005	-0.017	M	0.21	0.67	-1.9	8.81	580	-1.3	8.21	440
140205	-0.005	+0.019	C	0.09	0.29				0.5	8.34	466
140249	-0.011	+0.014	C	0.14	0.45				-0.3	9.79	908
140277				0.10	0.32				-2.8	12.35	2951
140543	-0.019	-0.012	S	0.32	1.02	-4.7	12.59	3305	-7.4	15.29	11460
142754	+0.003	-0.005	M	0.45	1.44	-3.6	10.75	1412	-4.0	11.15	1698
143104	-0.014	-0.024	C	0.12	0.38	-2.5	11.42	1928	-2.6	11.52	2019

Table 9 (cont.)

HD/CPD	MU(A)	MU(D)	R	E(B-V)	AV	M(S)	MOD(S)	DIST(S)	M(β)	MOD(β)	DIST(β)
	″	″		m	m	m		pc	m		pc
143156	-0.001	0.000	S	0.08	0.26				-1.0	8.85	589
143414	+0.021	+0.038	S								
143495				0.22	0.70	0.1	8.67	543	-2.2	10.97	1567
143549	+0.001	-0.010	S			-2.2			-1.5		
143756	+0.013	+0.031	S	0.14	0.45				-2.1	10.88	1501
143888	-0.037	-0.018	S	0.15	0.48				-1.5	10.40	1202
144887	+0.005	+0.001	C	0.06	0.19				-0.2	9.08	657
144965	-0.001	-0.016	M								
145537				0.30	0.96	-4.0	13.45	4897	-5.9	15.35	11748
146332	+0.011	-0.020	S	0.35	1.12	-2.2	8.70	549	-2.3	8.80	575
146755	+0.049	0.000	M	0.18	0.58						
-59°6723	+0.005	+0.002	S								
148546	+0.003	-0.009	M	0.60	1.92	-6.2	11.99	2500	-7.8	13.59	5223
148614				0.22	0.70	-2.5	12.03	2553	-1.8	11.33	1850
148740	+0.016	-0.044	S	0.07	0.22	-2.2	9.31	729	-0.9	8.01	401
149273	+0.009	+0.006	Y	0.28	0.90	-4.0	12.36	2970	-4.7	13.06	4100
149363	+0.007	+0.002	S	0.33	1.06	-4.7	11.45	1953	-6.1	12.85	3722
149382	-0.025	-0.010	S						-3.7		
-67°3184	+0.009	-0.014	C	0.12	0.38	-2.2	12.56	3259			
149770	+0.009	-0.013	S	0.08	0.26	-1.0	8.76	565	-2.7	10.46	1238
150323	-0.002	-0.016	M	0.04	0.13				-0.4	7.87	375
-74°1569	+0.010	-0.018	M	0.14	0.45	-4.6	14.30	7251	-5.2	14.90	9558
151310	-0.011	-0.013	S	0.23	0.74	-1.7	10.33	1166	-2.2	10.83	1468
152179	-0.025	+0.009	M	0.47	1.50				-2.9	10.27	1135
152286	+0.004	+0.022	S	0.23	0.74	-3.6	12.52	3197	-4.9	13.82	5818
152516	-0.012	-0.012	S	0.36	1.15				-3.9	10.76	1424
152640	+0.011	-0.031	S	0.16	0.51				-0.8	8.50	503
153084	+0.025	-0.007	S	0.19	0.61	-2.5	10.43	1220	-3.1	11.03	1608
153977	+0.011	-0.005	S	0.19	0.61						
-69°2698	+0.008	-0.029	N	0.20	0.64	-3.6	12.33	2924	-3.9	12.63	3357
155409	-0.024	0.000	S	0.15	0.48	-1.7	9.20	691	-2.1	9.60	831
155418	+0.017	-0.008	S	0.25	0.80	-2.5	11.26	1786	-2.0	10.76	1419
-59°6926	+0.013	+0.010	S								
156359	+0.020	0.000	S	0.16	0.51	-5.7	14.85	9366	-7.8	16.95	24637
156779	-0.003	-0.001	S	0.39	1.25	-2.9	10.92	1528	-5.3	13.32	4617
157857	-0.013	+0.022	S	0.49	1.57						
158111	-0.040	-0.016	S	0.14	0.45	-1.9	9.22	698	-0.8	8.12	421
158243	+0.004	-0.020	S	0.17	0.54	-6.2	13.80	5770	-5.3	12.90	3812
158659				0.52	1.66	-4.4	12.98	3955	-4.3	12.88	3777
158661	-0.004	+0.010	S	0.41	1.31	-6.2	13.08	4145	-6.1	12.98	3959

Table 9 (cont.)

HD/CPD	MU(A)	MU(D)	R	E(B-V)	AV	M(S)	MOD(S)	DIST(S)	M(β)	MOD(β)	DIST(β)
	"	"		m	m	m		pc.	m		pc
-79°923	-0.009	-0.001	N	0.33	1.06	0.1	9.22	699	0.3	9.02	637
159489	-0.003	-0.015	M	0.18	0.58	-1.7	9.37	749	-3.0	10.67	1363
159792	+0.011	0.000	M	0.38	1.22	-3.6	11.82	2316	-3.5	11.72	2212
159864	-0.001	+0.009	S	0.54	1.73	-5.0	11.82	2314	-5.0	11.82	2314
160207	-0.003	+0.001	M	0.14	0.45	-1.0	8.95	617	-1.3	9.25	708
160397	+0.002	-0.006	M	0.15	0.48				-2.3	11.59	2079
160878	+0.013	+0.004	M	0.18	0.58	-3.3	11.38	1891	-2.1	10.18	1086
160993	-0.001	-0.004	M	0.20	0.64	-6.2	13.29	4549	-6.3	13.39	4764
160995				0.13	0.42	-1.0	10.96	1558			
161306	+0.006	-0.021	S								
161633	+0.002	-0.002	M	0.18	0.58	-4.4	13.64	5355	-3.5	12.74	3538
161961	+0.025	+0.005	S	0.52	1.66	-4.7	10.80	1449	-5.5	11.60	2095
161972	+0.004	-0.014	M	0.06	0.19	-2.2	10.34	1173	-1.1	9.24	707
162089	+0.001	-0.009	M	0.12	0.38	-2.2	11.07	1641	-2.3	11.17	1718
163522	+0.006	+0.012	M	0.18	0.58	-6.2	14.05	6468	-6.5	14.35	7426
164073	+0.008	-0.011	M	0.21	0.67				-1.6	8.95	618
164340	+0.010	+0.003	M	0.15	0.48	-5.0	13.80	5754	-4.9	13.70	5495
164806	+0.011	-0.012	S	0.06	0.19	-2.2	8.83	585	-1.8	8.43	487
165955	+0.015	+0.002	M	0.22	0.70	-1.7	10.18	1089	-3.6	12.08	2613
-76°1313	+0.022	-0.028	N	0.12	0.38	-2.5	12.37	2986	-3.2	13.07	4122
165938	+0.020	-0.008	S	0.05	0.16	-2.2	10.25	1122	-1.1	9.15	676
166832	+0.012	-0.010	M	0.10	0.32	-1.0	9.07	651	-2.7	10.77	1425
167003	-0.002	+0.027	M	0.16	0.51	-4.7	12.65	3400	-4.0	11.95	2463
167321	+0.003	-0.001	M	0.06	0.19				-0.1	8.83	585
168476	-0.003	+0.008	S								
168785	+0.022	+0.026	M	0.29	0.93				-4.0	11.54	2034
170385	+0.008	-0.005	M	0.04	0.13	-1.7	9.47	784	-1.2	8.97	622
170638	-0.002	-0.018	M	0.17	0.54						
171141	+0.002	+0.005	M	0.05	0.16	-4.4	12.62	3341	-4.3	12.52	3191
171757	-0.003	+0.058	S	0.43	1.38						
172094	+0.017	-0.006	M	0.10	0.32	-3.6	11.56	2051	-5.0	12.96	3908
172127				0.12	0.38	-1.0	11.09	1656	-1.6	11.69	2183
172140	+0.024	+0.007	S	0.23	0.74	-4.7	13.92	6092	-5.2	14.42	7670
172533	-0.001	-0.056	S	0.14	0.45	-2.2	10.05	1024	-2.9	10.75	1413
173502	-0.024	+0.013	M	0.21	0.67	-4.0	13.04	4070	-6.1	15.14	10705
173994	-0.016	+0.009	S	0.06	0.19	-2.5	9.37	750	-1.8	8.67	544
174524	+0.003	-0.023	S	0.19	0.61				-1.2	10.37	1186
175141				0.15	0.48				-0.2	8.95	616
175754				0.23	0.74						
175876	+0.020	0.000	S	0.22	0.70	-5.4	11.61	2104	-6.1	12.31	2905

Table 9 (cont.)

HD/CPD	MU(A)	MU(D)	R	E(B-V)	AV	M(S)	MOD(S)	DIST(S)	M(β)	MOD(β)	DIST(β)
	"	"		m	m	m		pc	m		pc
177014				0.26	0.83				0.3	8.12	422
177015				0.11	0.35						
177559	+0.042	+0.013	S	0.23	0.74	-0.7	8.06	410	-2.8	10.16	1078
177566				0.09	0.29	-4.4	14.31	7284	-7.6	17.51	31798
177989				0.24	0.77	-5.0	13.56	5157	-4.9	13.46	4924
178370	-0.007	-0.023	M	0.08	0.26	-2.9	12.15	2696	-4.5	13.75	5633
178487	-0.012	-0.011	S	0.38	1.22	-6.2	13.64	5355	-6.1	13.54	5114
178861	-0.012	+0.027	S	0.33	1.06	-2.9	10.32	1160	-2.2	9.62	841
179007	-0.011	0.000	M	0.07	0.22	-2.9	12.67	3429	-1.2	10.97	1567
179202	-0.003	-0.037	S	0.14	0.45	-1.0	8.90	603	-0.9	8.80	575
179407	-0.025	+0.037	S	0.28	0.90	-6.2	14.71	8765	-7.3	15.81	14547
180629	-0.046	-0.019	S	0.11	0.35	-1.7	9.46	782	-1.1	8.86	593
182975	-0.004	-0.008	S	0.32	1.02				-1.9	9.24	706
183129	-0.016	-0.003	S	0.23	0.74				-1.4	8.79	573
183570	+0.014	+0.004	S						-1.4		
183899	+0.017	-0.006	S	0.17	0.54	-3.6	12.85	3725	-3.7	12.95	3901
185534	+0.011	-0.012	S						-0.8		
185842	+0.004	+0.009	S			-1.7			-1.6		
186610	+0.003	-0.001	S	0.27	0.86	-4.4	13.17	4317	-5.1	13.87	5959
187311	-0.005	-0.012	M	0.02	0.06	-1.7	11.88	2383	-1.9	12.08	2613
187350	+0.004	+0.009	S	0.39	1.25						
187536	+0.012	+0.059	S	0.19	0.61	-3.6	12.45	3093	-5.1	13.95	6171
188618	-0.010	+0.012	S						-3.7		
195455	+0.026	+0.011	S	0.08	0.26	-4.7	13.64	5355	-4.7	13.64	5355
204076	+0.026	-0.009	M	0.10	0.32	-3.6	12.07	2594	-5.0	13.47	4943
206144	-0.011	-0.013	S			-1.7					
208213	+0.020	+0.001	M	0.05	0.16	-1.7	9.96	981	-2.2	10.46	1235
214080	-0.004	-0.012	S	0.14	0.45	-4.4	10.75	1413	-5.0	11.35	1863
214539	-0.015	-0.032	S	0.02	0.06	0.6	6.55	204	-4.7	11.85	2350
220172	-0.026	-0.012	S	0.03	0.10	-2.5	10.08	1039	-3.8	11.38	1891
220787	+0.007	+0.050	S	0.01	0.03	-1.7	9.96	985	-2.8	11.06	1635
-45°7545							15.3	11480			
-44°7577							13.0	3980			
-50°9971							14.6	8320			

References to Tables 8 and 9

Photometry, radial velocities and MK types.

(1) Feast, Stoy, Thackeray and Wesselink (1961)
(2) Hill (1970)
(3) Feast, Thackeray and Wesselink (1955)
(4) Feast, Thackeray and Wesselink (1957)
(5) Feast, Thackeray (1963)
(6) Jaschek, Conde and de Sierra (1964)
(7) Hill (1971)
(8) Thackeray, Tritton and Walker (1973)
(9) Blanco, Demers, Douglass and FitzGerald (1968)
(10) Bidelman (private communication)

(B) Abt and Biggs (1972); N.B. Neubauer (1943) stars corrected by +10 km/s.

Proper motions

C Stoy (1966)
S Smithsonian Star Catalogue (1966)
Y Hoffleit (1967, 1968)
Hoffleit, Eckert, Lü and Paranya (1970)
Lü (1971)
M Mean of S and Y data
N Mean of C and Y data

CHAPTER VI

STELLAR DISTRIBUTION AND GALACTIC STRUCTURE

1. Apparent distribution of programme stars

The distribution of the programme stars in galactic co-ordinates is illustrated in fig. 18. In some areas of the sky, the stars appear grouped together as if physically associated. As an example, ten stars near $l = 345^{\circ}$, $b = -10^{\circ}$ are listed in Table 10 with distances determined by absolute magnitudes from both MK types and β-indices, and radial velocities. From this data the stars would appear to be unrelated; similar results were obtained for other apparent groupings, although a few pairs of apparently close stars may be remotely related. Table 11 gives data for two such pairs. HD 88799 and 89403 show good agreement in spectroscopic distance but not in the photometric determination. No radial velocity was available for HD 88799. If these stars were both at a distance of 850 pc, their linear separation would be about 5 pc. The second pair of stars, HD 220172 and 220787, located at rather high latitudes, have similar distances and radial velocities. They were classified B2V and B3V respectively, from 1971 spectra, but Hill (1971) give B3V and B3III. The proper motions of the two stars are dissimilar but errors in OB star proper motions are usually quite large. On the assumption that these stars are at the same distance from the sun, their separation will be of the order of 30 to 50 pc, implying that they are unlikely to be connected now, although they may have had a common origin.

The programme star distribution was compared with that of clusters and associations in the "Atlas of open star clusters" (Alter and Ruprecht, 1963). Only one star, HD 175141, had line-of-sight coincidence with a cluster, the star being apparently within the boundary of NGC 6716.

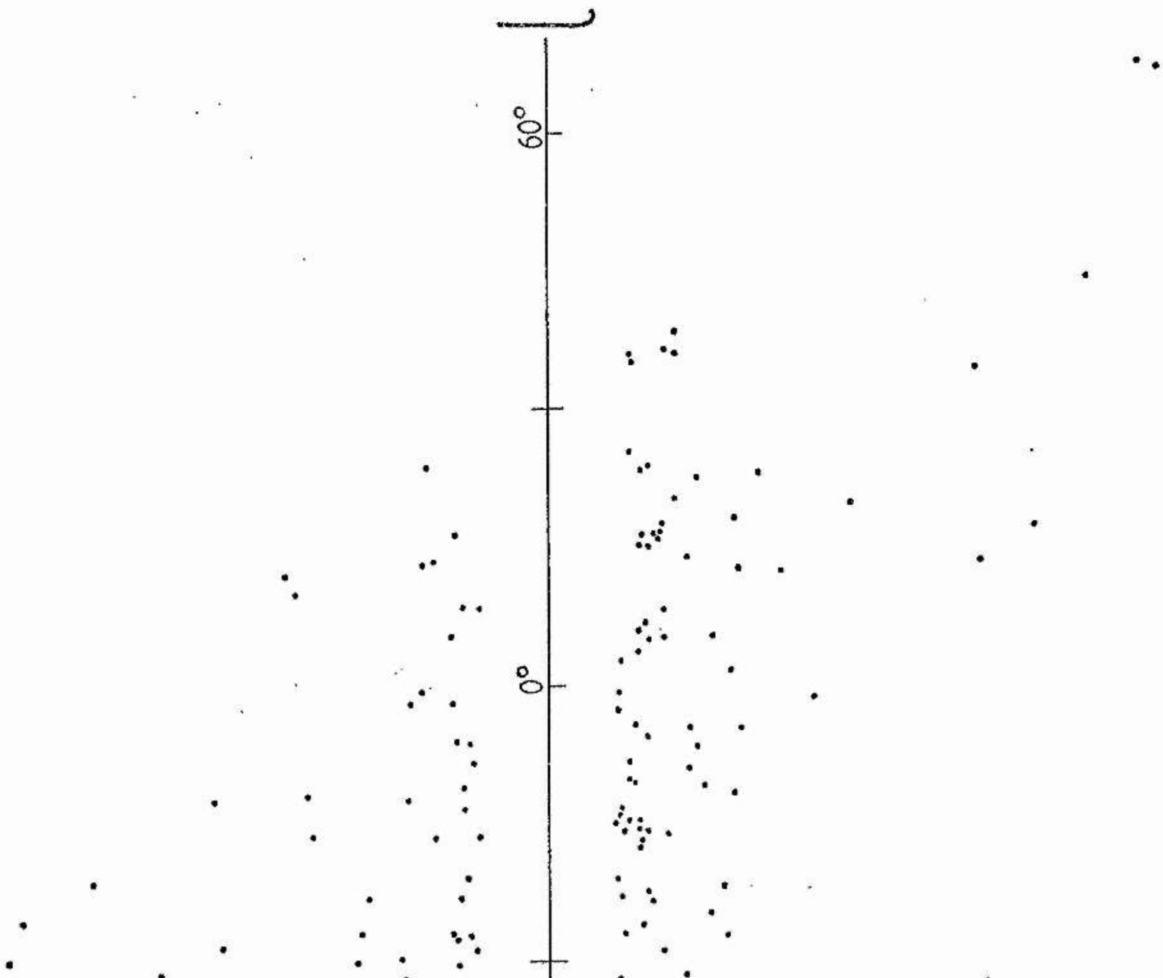

Fig. 18 Distribution of programme stars in galactic co-ordinates

Table 10

Stars near l = 345°, b = −10°

Star (HD)	l	b	dist (s)	dist (ß)	Rad. vel.
159489	345°.3	−7°.1	0.75 kpc	1.36 kpc	+9 km/s
159792	344 .4	−7 .9	2.32	2.21	Var.
160207	345 .8	−7 .5	0.62	0.71	+17
160397	342 .5	−9 .7	–	2.08	–
160878	346 .8	−7 .7	1.89	1.09	−45
160993	345 .6	−8 .6	4.55	4.76	−11
160995	343 .3	−9 .9	1.56	–	Var.
161633	344 .8	−9 .8	5.36	3.54	+19
161972	345 .6	−9 .7	1.17	0.71	−3
162089	344 .2	−10 .6	1.64	1.72	−54

Table 11

Possibly related stars

Star (HD)	l	b	dist (s)	dist (ß)	Rad. vel.
88799	295°.3	−18°.4	0.86 kpc	0.69 kpc	–
89403	295 .6	−18 .4	0.85	1.07	+10 km/s
220172	68 .1	−62 .6	1.89	1.04	+27
220787	67 .8	−64 .4	1.64	0.99	+26

Alter, Balázs and Ruprecht (1970) list several values for the distance of NGC 6716, the most recent and numerically smallest determination was 760 pc. The distance of HD 175141 from the UBVβ photometry is 620 ± 50 pc, so it seems likely that the star is a foreground star between the cluster NGC 6716 and the sun.

2. Galactic spiral structure

Before investigating the programme star distribution, it will be useful to outline the spiral arms by considering the distribution of objects generally thought to be good spiral arm tracers. Figure 19 shows various young objects plotted in projection on the plane of the Galaxy. Seventy per cent of them are nearer the galactic plane than 100 pc and 90% are nearer than 200 pc. Many of the very distant objects are Wolf-Rayet stars and consequently these stars have a greater proportion of their number at large distances from the plane than other objects. The galactocentric distance of the sun is assumed to be 10 kpc.

The OB-associations were taken from the list by Ruprecht (1964); O-B2 clusters and H II regions were mostly from publications by Becker and Fenkart (1963) and Becker (1964). Also included are six clusters at $l = 291^{\circ}$ with distances between 1.2 and 3.9 kpc determined by Schmidt and Santanilla (1964), and a group of early-type stars in Norma, at $l = 327^{\circ}$ and a distance of 2.5 kpc (Bok, Bok and Graham, 1964). McCuskey (1970) has reported work by Westerlund on groups of stars in Ara-Norma at $l = 332^{\circ}$ and 337° with distances of 3.9 and 3.5 kpc respectively. Wolf-Rayet stars were taken from a list by Smith (1968) and bright Cepheids were selected from a publication of Kraft and Schmidt (1963). Finally, a few distant OB stars from the lists of Morgan, Whitford and Code (1953) and Beer (1964) were plotted; absolute magnitudes in the latter source being determined from equivalent widths of Hγ.

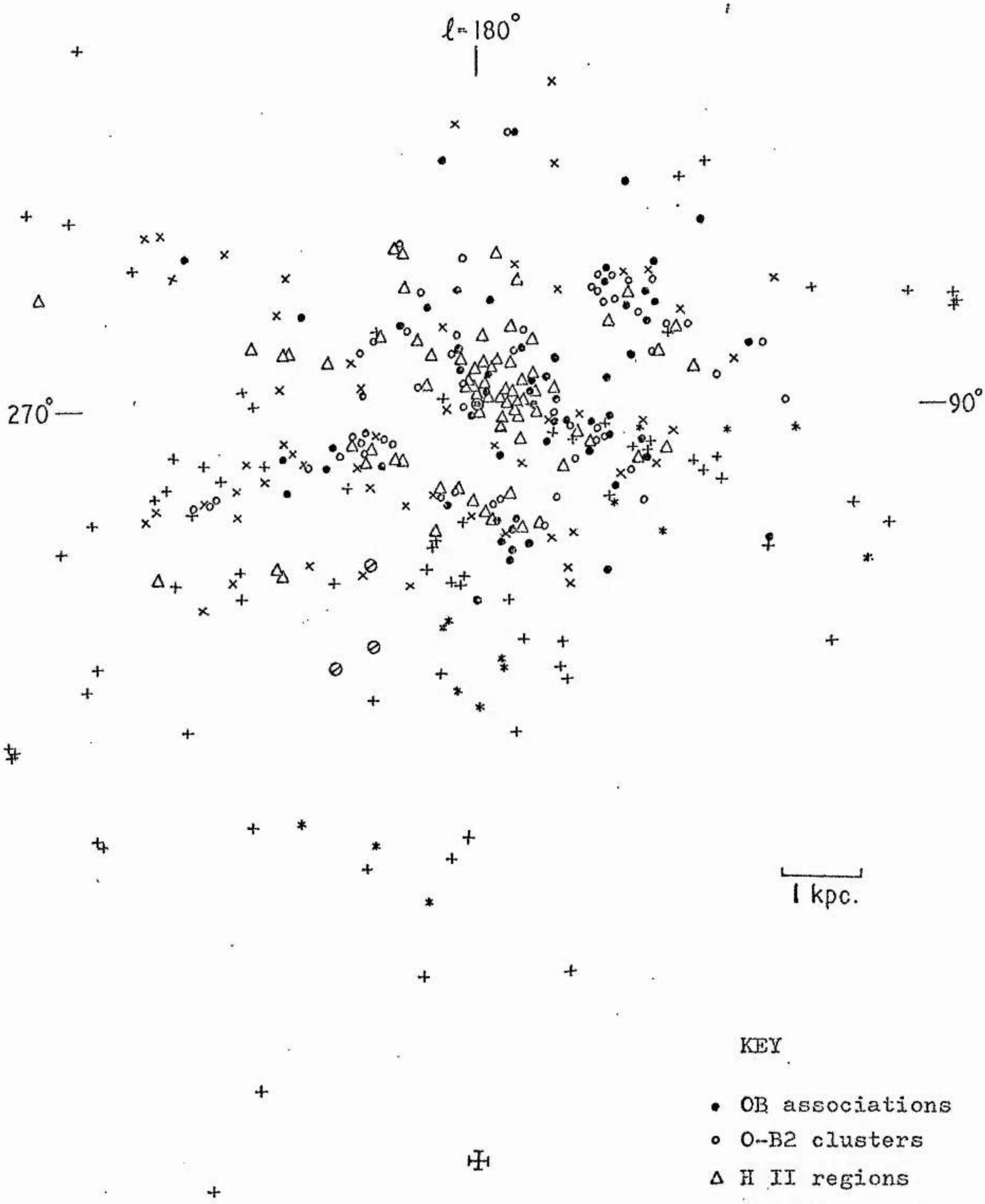

Fig. 19 Optical spiral arm tracers

Rohlfs (1967) in a statistical study of the relative value of various spiral arm tracers, concluded that OB-associations, O-B2 clusters, H II regions and Bpe stars of types BO-1 (III-V) were the best tracers. Bpe stars are not included in fig. 19; they exhibit a similar distribution to the other early-type objects (Schmidt-Kaler, 1964a, b). Rohlfs (1967) excludes Cepheids and Wolf-Rayet stars as spiral arm tracers but indicates that bright Cepheids may be suitable. The Cepheids in fig. 19 are all brighter than $M_v = -4.3$, following Kraft and Schmidt (1963), and with the Wolf-Rayet stars, show substantial agreement with the distribution of other spiral arm tracers. Schmidt-Kaler (1971) has recently shown Wolf-Rayet stars to be better for tracing spiral arms than was suggested by Rohlfs' analysis.

In fig. 19 the local feature is clear, extending for 3 kpc towards $l = 50^\circ$ to 60° and about 2 kpc towards $l = 200^\circ$. There may be an extension to the local feature out to 6 kpc from the sun at $l = 240^\circ$. The Perseus or +I spiral arm is evident at 2 to 3 kpc, between $l = 90^\circ$ and an apparent cut-off at $l = 140^\circ$. A +II feature is sparsely defined in the range $110^\circ < l < 180^\circ$ at about 4 kpc from the sun.

The Carina spiral feature extends along the line of sight at $l = 290^\circ$, between 1 and 6 kpc from the sun. This feature probably extends much further, according to Bok, Hine and Miller (1970). The Carina region and the Sagittarius arm at 1.5 kpc in the direction of the galactic centre, are considered to form the -I arm (e.g. Becker and Fenkart, 1970). There is some evidence of a -II arm, although Westerlund's groups of stars in Ara and Norma (see McCuskey, 1970), supposed to define the -II or Norma arm, lie beyond this feature in fig. 19 and may represent part of a -III arm. The picture is far from clear beyond the Sagittarius-Carina features.

Spiral arm tracers are represented schematically in fig. 20 together with the relevant parts of a diagram of neutral hydrogen distribution from the Hat Creek survey (Weaver, 1970). Hatched areas in fig. 20 indicate the reasonably well defined regions of fig. 19, whilst the broken lines are more tentative features. The solid lines represent the neutral hydrogen. Contrary to the discussion by Weaver (1970), there does not appear to be particularly good correspondence between the radio and optical spiral structure; there is no evidence from optical tracers to suggest that the local and Sagittarius features are linked. When fig. 19 is compared with the neutral hydrogen distribution described by Kerr (1970), the correlation between radio and optical data is also poor.

Evaluation of the spiral structure from radio observations has a weakness in that it is dependent upon some kind of galactic model for the distance determination of the hydrogen. The use of models of galactic rotation is especially restricted in the general direction of the galactic centre where differential effects on radial velocities are small. Further, Piddington (1973) has suggested that the neutral hydrogen may not be concentrated in spiral arms but could be more randomly distributed. He notes that where spiral structure is observed in other galaxies, it is "provided by the spiral tracers, comprising young stars and the gas ionized by those stars". Finally, Becker and Fenkart (1970) have shown that the local spiral structure, inferred from the distribution of HII regions and O-B2 clusters, is comparable with part of the structure of an external galaxy, NGC 1232.

3. Galactic distribution of programme stars

The programme star distribution is illustrated in fig. 21 which is drawn to double the scale of fig. 20. Distances are all projected on to the plane of the Galaxy and were determined from ß-index absolute magnitudes where possible. Three stars had no Hß measurements and

Fig. 20 Optical spiral structure compared with neutral hydrogen distribution. Shaded areas and broken lines represent objects from fig.19 ; solid lines represent neutral hydrogen (Weaver,1970). Circled dot and barred cross indicate positions of Sun and galactic centre respectively.

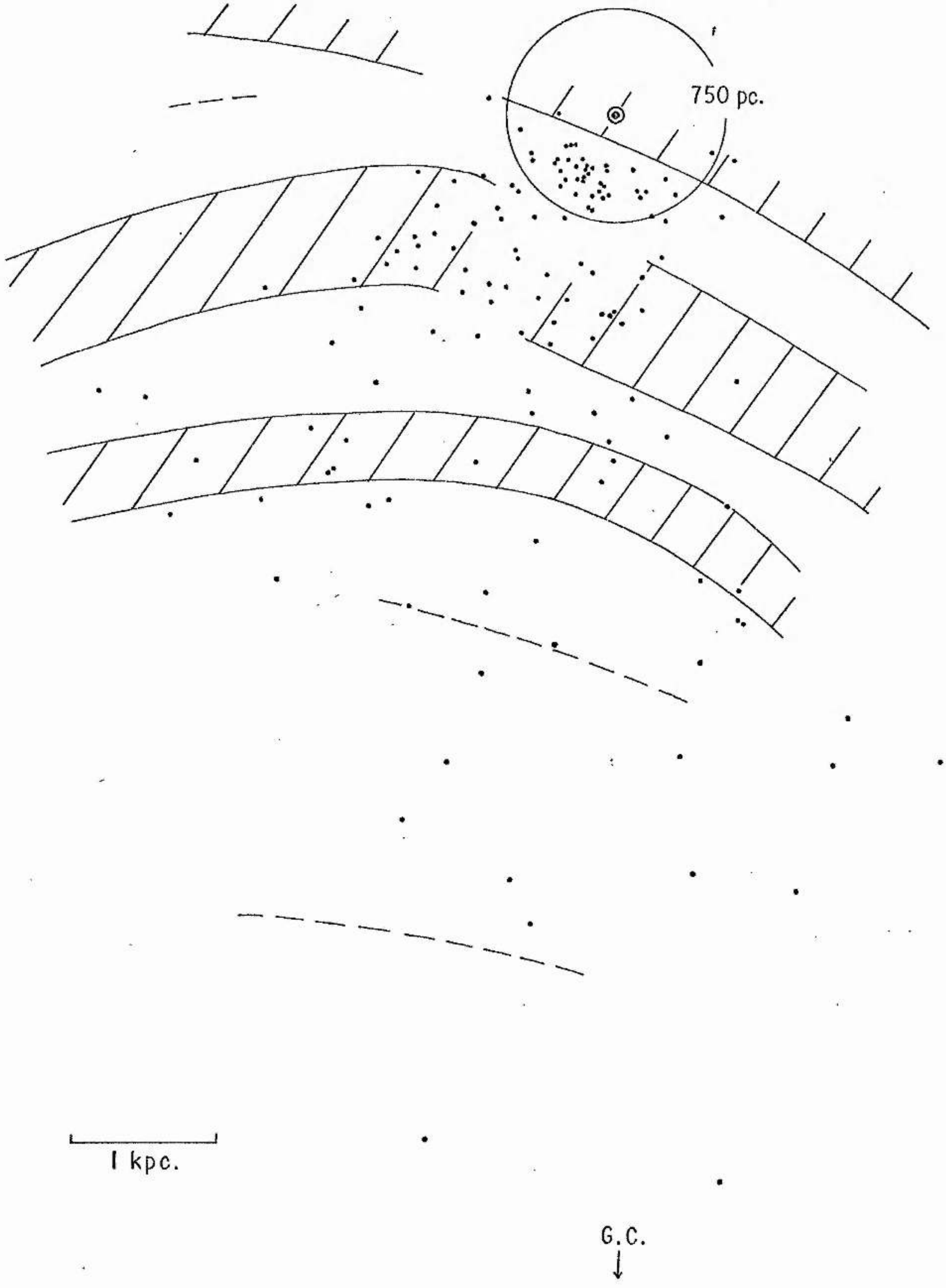

Fig. 21 Distribution of programme stars projected on to plane of Galaxy. Schematic spiral arms are from fig.20 and the scale is doubled.

MK-type absolute magnitudes were used instead. Spiral features are shaded areas or broken lines extracted from fig. 20. A few apparently very distant stars are not plotted and will be discussed in a later section.

There is a conspicuous group of stars in the region $300^\circ < l < 360^\circ$, between 400 and 700 parsecs from the sun. The longitude boundaries may reflect the survey limits and the 400 pc limit is almost certainly due to the magnitude and spectral type range of the survey. It was thought probable that this group of stars was an observationally selected sample from a fairly uniform galactic distribution of later B stars. Some 60% of the group has been classified in the range B5-6 (III-V), 20% are B3V or III and the remainder are mostly late B stars. With appropriate absolute magnitudes (Blaauw, 1963), approximate values for the apparent magnitude limit of the survey, and typical reddening corrections, the B5(III-V) and B3V stars should be observed from 400 pc to over 1 kpc from the sun, if the distribution is really uniform. However the observed density of B3-B5 stars appears to decrease sharply beyond 700 pc, although a few B5III and several B3 stars are observed near the -I spiral arm. It may be a result of selection effects or it may be that the distribution of later B stars is "patchy" but unrelated to the very young object distribution, in either case it would be unwise to regard these nearby stars as spiral tracers.

Beyond the nearer stars, a moderate number of stars are superimposed on the Carina-Sagittarius (-I) arm, but at greater distances the distribution seems to be fairly random. Schmidt-Kaler (1971) has suggested that objects used as spiral arm tracers should be very young because a spiral feature composed of objects with random motions of 10 to 15 km/s will be completely smeared out in 50 million years. Combining data on the masses of early-type stars (e.g. Schmidt-Kaler, 1965) with theoretical evolutionary tracks (Iben, 1967) we find that

B3V and B1.5V stars should have main sequence lifetimes of 4×10^7 and 2×10^7 years respectively. Hence the distribution of stars later than about B2 should not be expected to show galactic spiral structure. This agrees with the work of Becker and Fenkart (1970) who have shown that the distribution of O-B2 clusters coincides with that of the HII regions, whereas the open clusters with earliest spectral type B3-F8 have a uniform distribution. Figure 22 shows the O-B2 programme stars, including two Radcliffe intermediate latitude stars from Table 8 and excluding eight stars with variable radial velocity which may be binary or multiple systems. A definite gap can be seen between the local and -I arms although the local arm is hardly represented due to the survey limits; there is now more indication of a -II arm and four or five stars are at a comparable distance to the tentatively identified feature at 4 kpc.

Figure 23 illustrates the vertical distribution of the O-B2 stars, that is the distribution of stars projected on to the XZ plane, perpendicular to the galactic plane and passing through the sun and galactic centre. The barred lines at z = o indicate a cross section of the spiral arms at $l = o^{\circ}$; distant arms are very uncertain. Vertical structure is not apparent due to the projection of arcs into straight lines.

4. <u>Distant stars</u>

The stars listed in Table 12 are apparently more distant than 5 kpc, as derived from either MK-type or ß-index absolute magnitude. Up to roughly 6 kpc from the sun there does not appear to be any systematic difference between the two sources of distance determination; beyond 6 kpc the ß-indices give greater distances. It is a direct result of the divergence from a 45° relation seen in fig. 16 for high luminosities. For extremely distant stars, ß-index distances are often

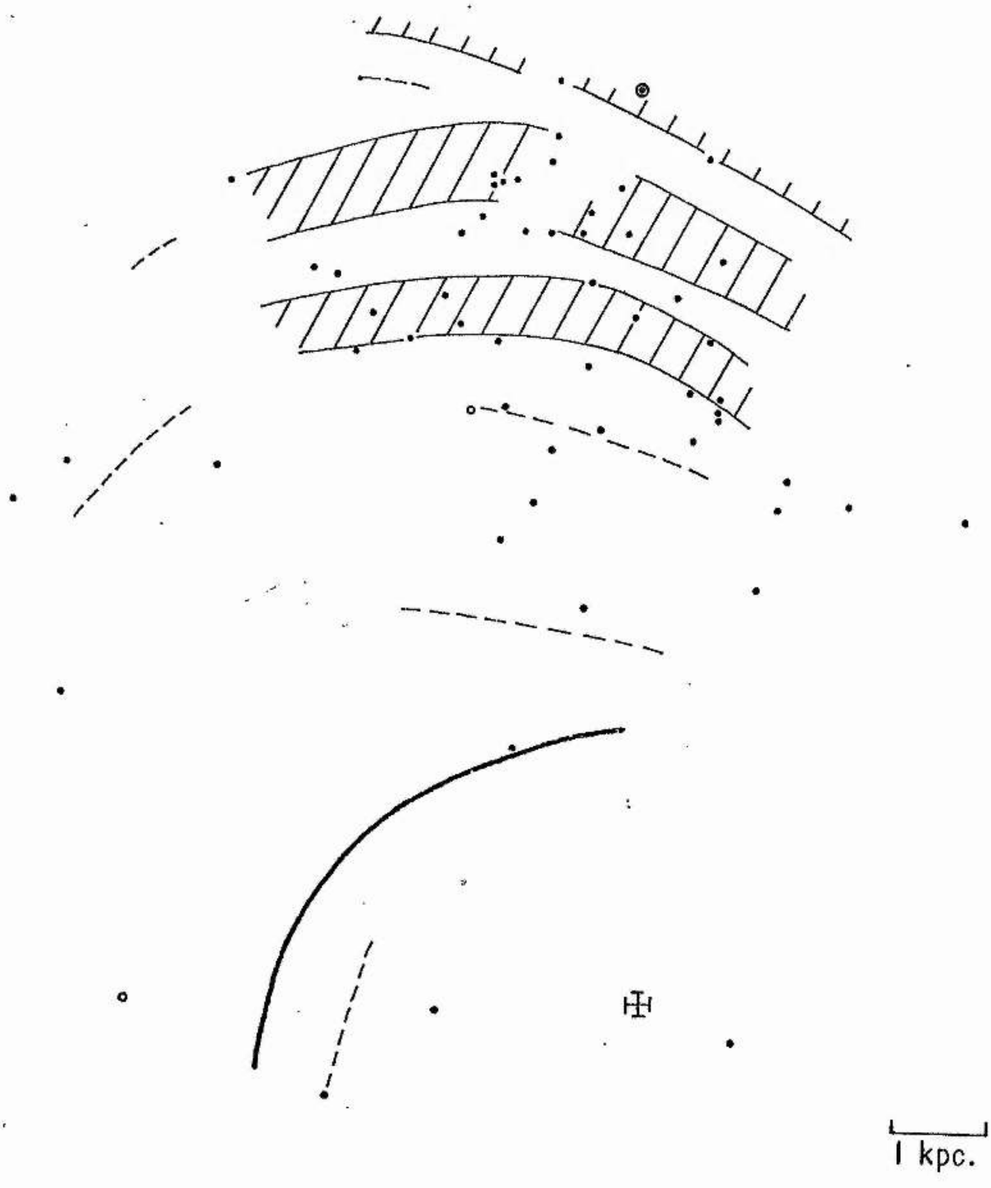

Fig. 22 O -B2 programme stars projected on to plane of the Galaxy. Schematic spiral arms are from fig.20 . The circled dot and barred cross indicate positions of the Sun and galactic centre respectively. Open circles represent distances from MK type absolute magnitudes; filled circles represent distances from β -index absolute magnitudes.

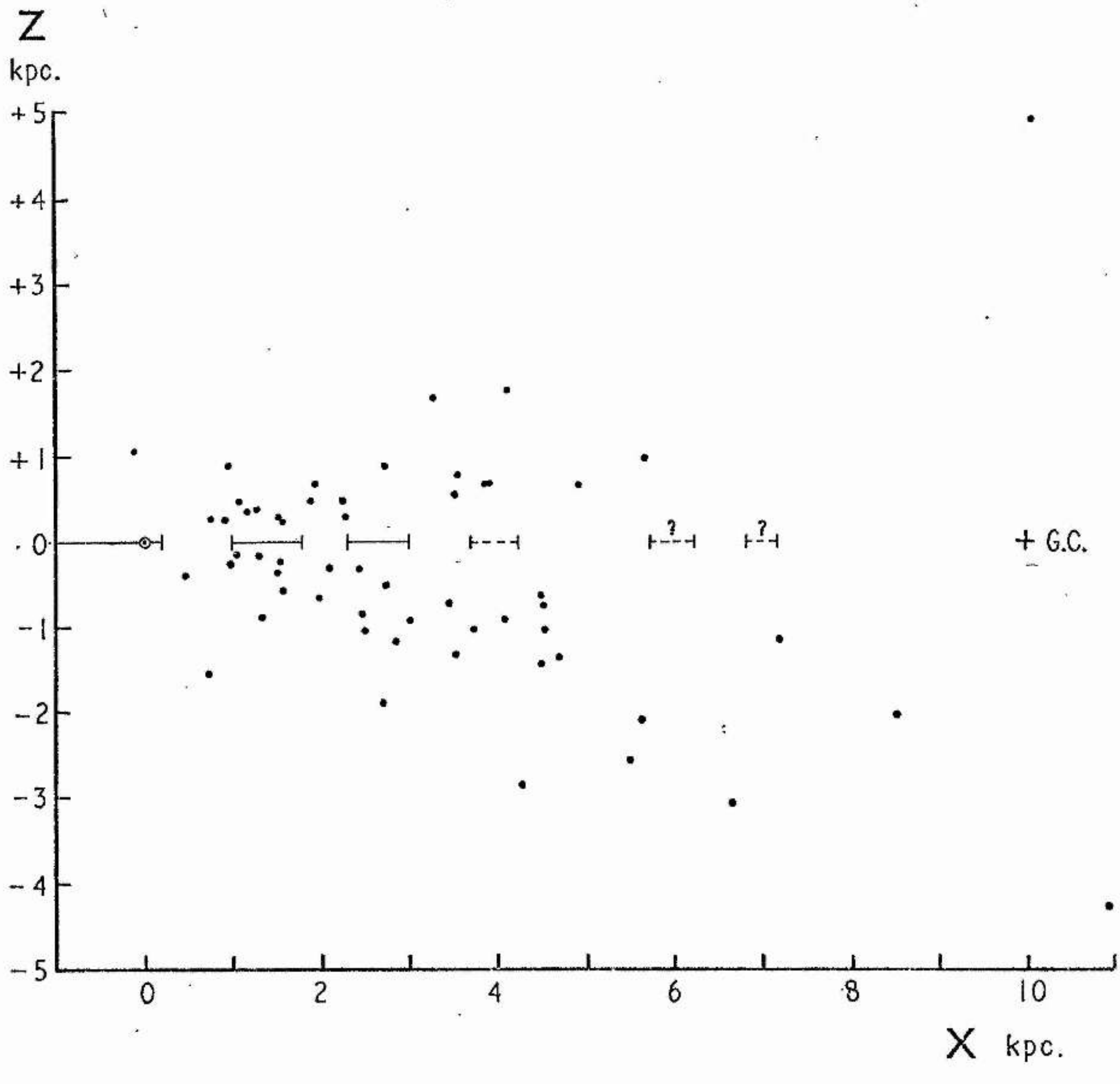

Fig. 23 Distribution of programme stars perpendicular to the galactic plane. Barred lines indicate cross sections of spiral arms at $\ell = 0^{\circ}$, as sketched in fig.20 .

Table 12

Apparently very distant stars

Star (HD/CPD)	Dist (s)	Dist (β)	Comments
$-72^\circ 1184$	9.75 kpc	11.72 kpc	Very high radial velocity
108230	5.44	3.13	
$-69^\circ 1743$	2.56	7.37	
112843	2.49	8.23	
114444	4.15	19.84	Velocity variable
119069	3.22	4.82	High radial velocity
121968	–	19.83:	β uncertain
123884	7.47	–	
$-69^\circ 2055$	3.16	13.16	High radial velocity
$-72^\circ 1542$	5.33	3.86	
$-42^\circ 6798$	5.24	4.16	Velocity variable
140543	3.31	11.46	Velocity variable
145537	4.90	11.75	Velocity variable
148546	2.50	5.22	
$-74^\circ 1569$	7.25	9.56:	β uncertain; high radial velocity
152286	3.20	5.82	
156359	9.37	24.64	
158243	5.77	3.81	
161633	5.36	3.54	Velocity variable
163522	6.47	7.34	
164340	5.75	5.50	Velocity variable
172140	6.09	7.67	Velocity variable
173502	4.07	10.71	
177566	7.28	31.80	High radial velocity
177989	5.16	4.92	
178370	2.70	5.63	High radial velocity
178487	5.36	5.11	
179407	8.77	14.55	High radial velocity
186610	4.32	5.96	
187536	3.09	6.17	
195455	5.36	5.36	
$-45^\circ 7545$	11.48	–	Radcliffe star
$-50^\circ 9971$	8.32	–	Radcliffe star; variable velocity

unreliable because most of these stars are amongst the faintest observed in this programme and, as fig. 13 shows, the average standard deviation of the ß-index increases for fainter stars. As a result of this and the shape of the β/M_V calibration curve, the high luminosity, apparently faint stars will have the most uncertain distances.

Several of the apparently distant stars have variable radial velocity and are probably unresolved binary or multiple systems for which the present distance determinations can have little meaning. Seven of the stars in Table 12, plus a few others, have very large radial velocities which appear to be non-variable from 1971 plates and which in many cases cannot be accounted for by the effect of differential galactic rotation. These stars will be discussed in the next chapter. Figure 24 shows the distribution of stars in Table 12. The apparent distances of HD 114444, 156359 and 177566 are almost certainly over-estimated although the distances of the last two are great whichever value is used for the absolute magnitude (i.e. MK-type or ß-index). There is considerable overlap between figs. 22 and 24.

5. Evolutionary and dynamical ages

Figure 22 suggests that the spiral structure in the galactic plane is followed by O-B2 stars even though these may be as much as 1 to 2 kiloparsecs from the plane. The evidence is not conclusive as the results are rather limited by the accuracy of the Hß photometry. For example, at 3 kpc, $\sigma(\beta) = \pm\ 0.013$, as determined in III.5, will give an uncertainty in stellar distances of ± 0.3 kpc. The majority of Hß measurements in this programme were made from chart recorder output and it is probable that the use of current integration, or pulse counting techniques for faint stars, would improve the accuracy of the ß-indices. In addition, the small number of stars observed to be more than two or three kiloparsecs from the sun restricts the picture to the

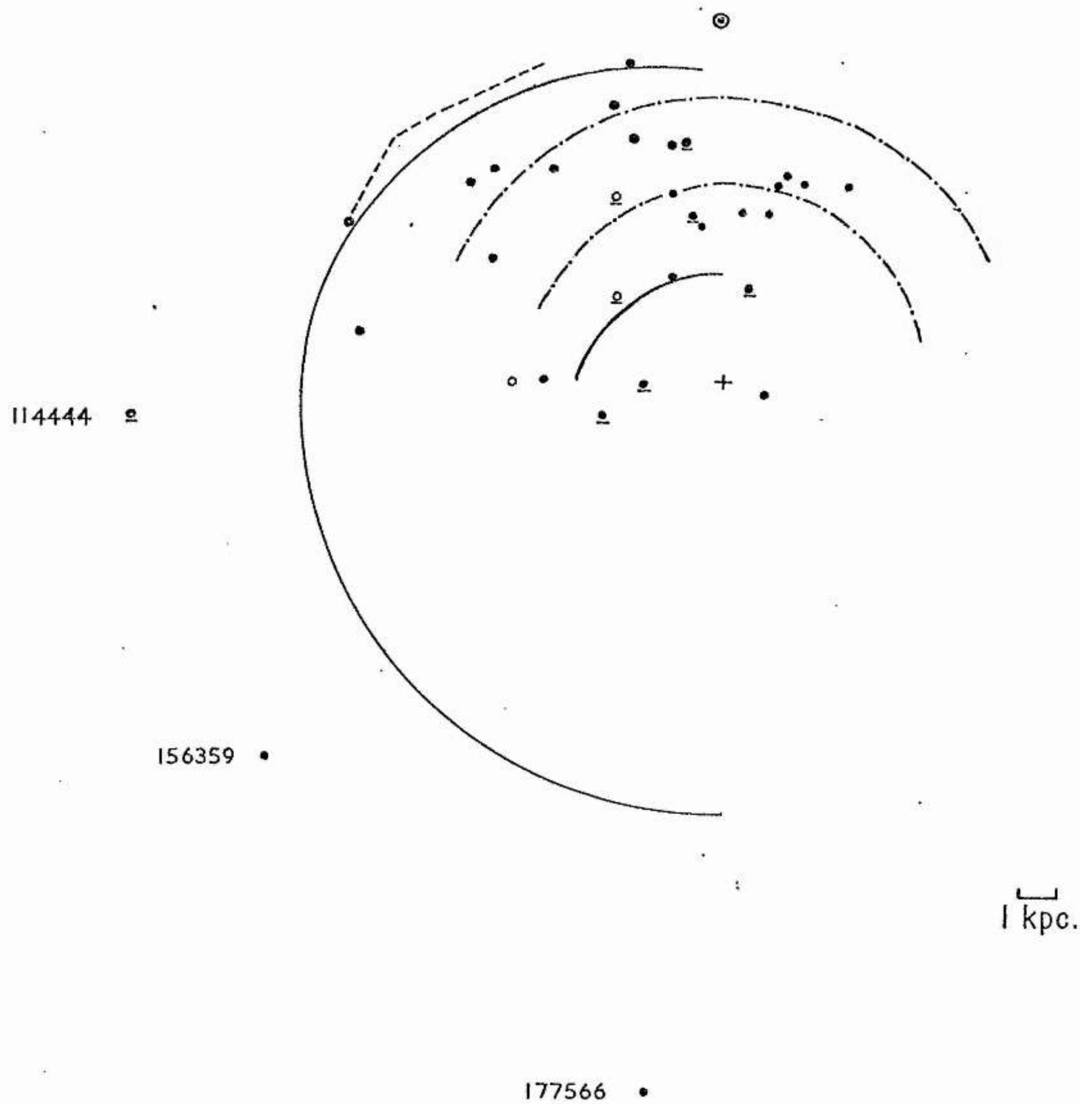

• programme stars, β-index distances
o programme stars, MK type distances
—— H I (Weaver, 1970)
—·— H I (Kerr, 1970)
--- Carina spiral feature (Bok et al., 1970)

• } velocity variables (the • and o symbols are printed underlined)
o }
⊙ Sun
\+ Galactic centre

Fig. 24 Distant stars

-I and -II spiral features. Future observational programmes concentrating on rather fainter stars, say $V > 10^m$, and spectral types earlier than B3 could greatly improve and extend the material in fig. 22. Observations of very distant stars in this programme indicate that interstellar extinction should not be a problem at intermediate latitudes.

An interesting speculation arises from fig. 23, the distribution of O-B2 stars perpendicular to the galactic plane. Early-type stars exist in quantity up to 1 kpc from the plane and a small percentage are observed at greater distances than this, if stars of the present programme can be considered at all representative. It is generally thought that early-type stars are formed close to the galactic plane and if this is the case, then stars distant from the plane should be able to achieve their present positions in a time compatible with their evolutionary lifetimes. Otherwise, it is necessary to consider that blue stars can be formed well away from the galactic plane or that a significant proportion of the programme stars are subluminous. As to the latter possibility, particular stars have been discussed in some detail by other authors. Hill (1968) considered the space motion of high latitude HD 125924 to be unlikely for a normal B star, in particular the large motion towards the plane suggested the star was a subdwarf. Conversely, Berger, Fringant and Rebeirot (1970) have shown that despite the distance of BD + 6° 2461 from the plane (5.5 kpc), it could be a runaway B star which has achieved this height by virtue of very high velocity. They also consider HD 125924 to be similar in nature and probable origin to BD + 6° 2461. In general, it might be expected that the programme stars have rather bright apparent magnitudes to include many subluminous stars. Greenstein (1971) investigated 170 blue stars between 9th and 16th magnitude and found "the brighter stars are largely uninteresting, in that they seem normal". Most of the subdwarf or hot horizontal branch stars of Greenstein's survey were fainter than 11th magnitude. However, the survey was concentrated in the galactic polar regions and the possibility that some of the programme stars are subluminous cannot be ruled out.

From the stars in Table 8 were selected all those more than 500 pc from the galactic plane, as calculated from both ß-index and MK-type distances. Stars with $z(\beta) > 500$ pc and $z(s) > 500$ pc totalled 56, later reduced to 41 by elimination of two helium-rich stars and several possible or probable velocity variable stars. For each star an estimate is required of "dynamical time" or time taken to reach the observed z-distance and some estimate of the age is necessary for comparison with t_{dyn}.

Calculation of stellar ages is heavily reliant on theoretical models of stellar evolution. In a recent review paper, Iben (1972) gave the approximate formula

$$t_{ms} \sim 3.4 \times 10^{7} \left[\frac{7M_{\odot}}{M} \right]^{1.9}$$

for the duration of the main-sequence, hydrogen-burning phase of a population I star of mass M. The formula is valid for massive stars with $M > 3M_{\odot}$, where $M_{\odot}$ represents the solar mass. Estimates of the masses of early-type stars have been given by several authors; in this case masses were taken from a review by Schmidt-Kaler (1965) and are listed in Table 13 with the corresponding main sequence lifetimes. These results for t_{ms} are really upper limits for ages of main sequence stars, since theoretical studies of the evolution of massive stars indicate that when core hydrogen burning ends and shell hydrogen burning takes over, the stars move rapidly towards the red giant phase, leaving the OB star region of the H-R diagram in a time which is small compared with t_{ms}.

Table 13

Masses and main sequence lifetimes of early-type stars

Spectral type	Mass	$\sim t_{ms}$
O5	35 $M_\odot$	2×10^6 years
O6	32	2×10^6
O8	23	4×10^6
B0	15.5	8×10^6
B1.5	10.5	2×10^7
B3	7.6	3×10^7
B5	5.5	6×10^7

Giant and supergiant stars present something of a problem because their masses are not well-known and because they are almost certainly evolved to an extent. Comparison of some of these stars with colour-magnitude diagrams of young open clusters (Hagen, 1970) indicated their ages to be about five to ten million years. Since the age of a cluster can be determined by fitting its colour-magnitude diagram to theoretical curves of equal time in the H-R diagram, it seemed reasonable to suppose that crude estimates of ages of stars could be similarly obtained, provided the stars were young and luminous. Barbaro, Dallaporta and Fabris (1969) derived a set of isochronous curves in the M_V, $(B-V)_o$ diagram for comparison with cluster colour-magnitude arrays. They used theoretical evolutionary tracks by Iben for stars with masses between 2 and 15 solar masses, and by Stothers for a 30 solar mass star (see Barbaro et al. for references). Figure 25 reproduces part of fig. 2 from Barbaro et al., showing some of the isochronous curves. It can be seen that if a star is brighter than $M_V = -4$, or well-evolved, a reasonable estimate of the age should be possible. No programme star is redder than $(B-V)_o = 0.0$ but most of the giants and supergiants are more luminous than $M_V = -4$. Approximate ages t_{evol} were derived and where overlap occurs, these ages are in fair agreement with hydrogen

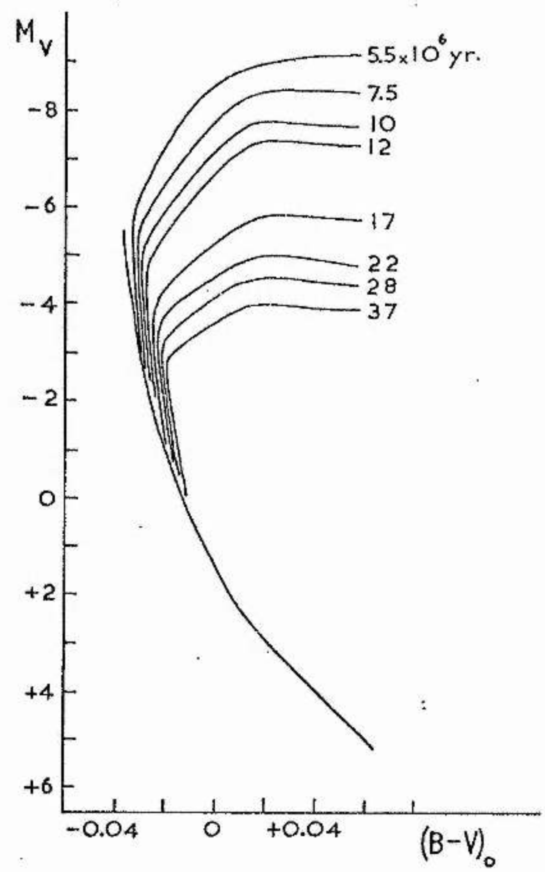

Fig. 25 Isochronous curves. Reproduction of part of a diagram by Barbaro, Dallaporta and Fabris (1969).

burning lifetimes, t_{ms}.

Dynamical ages of stars are difficult to determine with any accuracy; the force field perpendicular to the plane is not well determined for the local region and can only be approximated for more distant regions by using galactic mass models. A method described by Searle, Sargent and Jugaku (1963) and used by them to find t_{dyn} for high latitude supergiants 89 Herculis (F2Ia) and HD 161796 (F3Ib) is outlined here. They approximated the acceleration perpendicular to the plane at a height z for "any plausible trajectory" by

$$K(z) = K(z_o)(^z/z_o)^n$$

where $o < n < 1$ and z_o is the height of the star at the peak of its trajectory. They found that

$$t_{dyn} = \alpha \left(\frac{z_o}{K(z_o)} \right)^{\frac{1}{2}}$$

the constant of proportionality is "not critically dependent on the assumed trajectory" and is a function of n. Searle et al. adopted $\alpha = 1.5$. To estimate the acceleration $K(z_o)$ at the peak of the trajectory, they multiplied the value of K(z) at 1 kpc above the sun (Oort, 1960) by the ratio

$$\frac{K(z_o,\ R)}{K(z = 1\ \text{kpc},\ R = R_\odot)}$$

from the relation between z and K(z) given by Schmidt's (1956) galactic model. Searle et al. followed Schmidt in assuming the galactocentric distance of the sun to be 8.2 kpc. However, if the model is used with $R_\odot = 10$ kpc, then the values of K(z) in the solar region agree more closely with Oort's (1960) determination of K(z), at least for $z < 2$ kpc. As a rough test, t_{dyn} was re-computed for the two F-type supergiants with $R_\odot = 10$ kpc. In Table 14, results are compared with the original results for $R_\odot = 8.2$ kpc.

Table 14

Dynamical and evolutionary ages of 89 Her and HD 161796

Star	z_0	t (evol.) $\times 10^6$ yr	$t_{dyn} \times 10^6$ yr ($R_\odot = 8.2$)	$t_{dyn} \times 10^6$ yr ($R_\odot = 10$)
89 Her	1 kpc	14 ± 6	24	15
HD 161796	1.7	20 ± 10	33	22

The first four columns are from Searle et al. (1963) and it should be noted that their t (evol.) is not determined in exactly the same manner as the t_{evol} of the present work; they used evolutionary calculations by Hoyle (1960). The final column of Table 14 is the re-computed values of t_{dyn} which seem to be in good agreement with t(evol.) if the stars were ejected from the plane very soon after formation. With z_0 in parsecs and $K(z_0)$ in units of 10^{-9} cm/sec^2, the equation for t_{dyn} becomes:

$$t_{dyn} = 2.65 \times 10^6 \left(\frac{z_0}{K(z_0)} \right)^{\frac{1}{2}} \quad \text{years}$$

which was applied to the stars with $z > 500$ pc. The assumption was made that stars are at the peak of their trajectories, in other words the velocity perpendicular to the plane is zero at z_0. This is a reasonable approximation for most of the programme stars provided the W components of the space velocity are determined from radial velocities alone. When proper motions are included, the space motions of many programme stars become extremely large, an effect which is almost certainly more dependent on errors in the proper motions than on real velocities.

Of the 41 stars with $z > 500$ pc, 19 were found to have $t_{dyn} < t_{ms}$ or t_{evol}, 10 had $t_{dyn} > t_{ms}$ or t_{evol} by a marginal amount and twelve had $t_{dyn} > t_{ms}$ or t_{evol} by an amount which may be significant. The latter group of stars is listed in Table 15. The first column gives the star number and MK-type, the second lists distance from the plane computed from β-index distance and MK-type distance. The next two columns give W-velocities for four cases; for the star at distances given by β-index and MK-type, both with and without proper motion components. The W components of the space velocities were computed as described in appendix II. An asterisk following a velocity indicates that the proper motion components are both greater than twice the standard deviation of the measurements. Where no asterisk follows a velocity, either the proper motion components are small compared with the standard deviation or two sources give widely differing values. In either case the proper motion is unreliable. The last three columns of Table 15 list t_{dyn}, t_{ms} and t_{evol} in units of millions of years; t_{dyn} has been calculated for $z(\beta)$ and $z(s)$. Where t_{evol} is given as a range of values, this represents the range covered by the difference between $M_v(\beta)$ and $M_v(s)$ when applied to the $M_v/(B-V)_o$ diagram of isochronous curves. The stars in Table 15 will be discussed in some detail.

HD 149363 has $W > 60$ km/s and so the "true" t_{dyn} must be regarded as smaller than the quoted result, derived on the assumption that $W = 0$. Proper motion components from the Smithsonian Star Catalogue (1966) are very small, considerably less than the standard deviations. HD 97991 has annual proper motion components

$$\mu_\alpha = +0''.022 \pm 0''.009 \qquad \mu_\delta = +0''.022 \pm 0''.008$$

which give the star a considerable velocity in the z-direction, $W = +150$ km/s. For HD 97991 and 149363 t_{dyn} is about 50% greater than t_{evol} but the dynamical time is over-estimated as both stars have appreciable velocities away from the plane.

With proper motions taken into account HD 156359, 195455, 204076

Table 15

<u>Stars with dynamical age > evolutionary or main sequence lifetime</u>

Star	z(β) z(s)	W(β) W(s)	W(β) W(s) +p.m.	t_{dyn} (β) (s)	t_{ms}	t_{evol}
				(millions of years)		
93840						
B1 I	+0.89 kpc	-3 km/s	+31 km/s	27		8
97991	+1.12	+14	+150 *	30	20	15-20
B1 V	+1.18	+22	+160 *	31		
$-72^{o}1184$	-2.22	+47	-150	42		7
B0 III	-1.84	+42	-110	33		
119069	+1.78	-18	-220	20		8-12
B1 III	+0.89	-24	-130	18		
149363	+1.67	+64	-1	18		7-12
B0.5 III	+0.88	+68	+34	18		
$-74^{o}1569$	-3.06	+20	-760	26	8	6
09.5 V	-2.32	+18	-590	22		
156359	-6.17:	+33	-1900:	100:		5-7
09 III	-2.35	-3	-700	17		
179407	-2.63	+28	+2600	22		5-8
B0.5 I:	-1.59	+37	+1600	11:		
195455	-2.85	+13	-470	22		13
B0.5 III	-2.85:	+13	-470	22:		
204076	-3.54	+19	-440	27	20	12-17
B1 V	-1.86	+12	-230	24		
214080	-1.56	-2	-17	27		10-12
B1 III	-1.18	-4	-15	26		
220172	-1.68	-22	+20	30	20	17
B2 V	-0.92	-23	-1	28		

and CPD $-72^{\circ}1184$ and $-74^{\circ}1569$ all have high velocities in the right direction to drastically reduce t_{dyn}. W components are very uncertain for these stars, but would need to be only a fraction of the computed values to give the stars sufficient energy to reach observed distances from the plane in times comparable with evolutionary lifetimes. It follows that the proper motions could be too small to be observed at present and yet equivalent to quite large W-velocities.

For HD 93840, 119069 and 214080, the anomalous results for t_{evol} and t_{dyn} can only be reconciled with the proposition that all early-type stars originate near the plane by invoking large uncertainties in the computations. In the case of HD 214080, values of W for the possibilities considered are small and yet the dynamical age is two or three times the estimated age of the star. The computed values of W for HD 119069 have opposite sign to the z-distance, implying motion towards the plane, although if radial velocity is considered alone, the effect is small. The B1 supergiant, HD 93840, has $t_{dyn} > 3\ t_{evol}$. It is worth noting at this point that if HD 93840 was misclassified and is really, for example, a B1 giant, then it will be nearer the sun and nearer the galactic plane than the present estimate, consequently t_{dyn} will be smaller. Also, if the star is less luminous than supposed, its lifetime t_{evol} might be longer than estimated. In other words, apart from the possibility of errors in the methods of calculating lifetimes, there may be errors in the data which would affect the final results. It is hoped that the use of Hß photometry minimises errors in absolute magnitudes and that errors in $(B-V)_o$ are small, so that "input" errors will not be comparable to uncertainties in the methods.

Of the stars in Table 15, HD 179407 has the largest annual proper motion:

$$\mu_{\alpha} = -0''.025 \pm 0''.017 \qquad \mu_{\delta} = +0''.037 \pm 0''.018$$

If these are accepted and the absolute magnitude is not greatly in error, then the resultant space motions are extremely large. HD 179407 was classified BO.5 I: from one c spectrum, based mainly on the presence of O II blends at 4317–20 and 4415–17 Å and the comparatively strong N II 3995 line. The Si IV line at 4089 Å is approximately equal to Si III 4552. The MK-type implies an absolute visual magnitude of −6.2 according to the calibration by Blaauw (1963). Four measurements of the β-index gave $\beta = 2.547 \pm 0.010$ (s.e.) equivalent to $M_V = -7.3 \pm 0.8$. The radial velocity of HD 179407 relative to the sun is − 117 ± 4 km/s from only 2 plates. If the stellar velocity is not variable, it is rather unusual, being large and of opposite sign to that expected from a star at $l = 24^{\circ}$ involved in differential galactic rotation.

Taking $M_V = -6.2$ gives HD 179407 a distance of 8.8 kpc. With proper motions included, the components of the space motion are

$U = -380$ km/s $\quad V = +1060$ km/s $\quad W = +1600$ km/s

which seem unreasonably large. Could the star be subluminous? The interstellar Ca II K-line in the spectrum of HD 179407 is strong and sharper than the stellar lines. The K-line velocity, + 17 km/s, when corrected for the solar motion relative to the local standard of rest, is consistent with absorption by material within one or two kiloparsecs of the sun, involved in differential galactic rotation. HD 178487 is less than 3° from 179407 and was classified BO I on this programme. The former star has a distance estimated at 5.4 kpc and reddening $E_{B-V} = 0^{m}.38$. HD 179407 is slightly less reddened, $E_{B-V} = 0^{m}.28$, but is 2° further from the plane and could still be more distant than HD 178487 provided most of the reddening occurs within about 200 pc of the plane. From the evidence of reddening and the interstellar calcium line, it appears improbable that HD 179407 is subluminous. Could the star be less luminous than supposed? It is conceivable that the MK-type is B1 III instead of B0.5 I. In this case, the absolute magnitude would be -4.4 and components of the space motion are still extremely large:

$U = -200$ km/s $\qquad$ $V = +390$ km/s $\qquad$ $W = +710$ km/s

There seem to be two possibilities; either the proper motion components are in error or HD 179407 really is a very high velocity star. In the latter case, the stellar motion is not compatible with formation near the galactic plane.

To summarise; of the small sample of 41 stars with $z > 500$ pc, twelve appear to have lifetimes too short to enable them to reach their present distances from the plane. For the most part, the dynamical and evolutionary lifetimes can only be reconciled with star formation near the plane of the Galaxy by assuming the very uncertain proper motions to be correct or by assuming large systematic errors in the computed lifetimes. The latter assumption seems more justifiable than the former, since inclusion of proper motions leads to improbably large space motions in many instances. In the case of HD 179407 it does not seem likely that it could have originated in the galactic plane unless it is subluminous.

6. Star formation

For stars with $z > 500$ pc and $t_{dyn} \lesssim t_{evol}$, the differences $\Delta t = t_{evol} - t_{dyn}$ were calculated and the mean Δt found to be

$$\overline{\Delta t} = 0.2 \pm 3 \qquad (27 \text{ stars})$$

which is effectively zero and implies that if these stars were ejected from the plane, then this occurred shortly after formation. This result is reasonable, for if early-type stars are formed in expanding stellar associations then stars which reach appreciable distances from the plane could represent the high velocity "tail" of the velocity distribution. Along similar lines, can the stars in Table 15 be related to "run-away" stars? Blaauw (1961) supposed run-away stars to be secondary components of proto-double stars, the primary of which underwent rapid and violent mass loss, releasing the secondary as a result of the suddenly diminishing gravitational attraction. Three of Blaauw's stars were in the present programme or previous high-latitude studies (Hill, 1970, 1971), HD 97991, 149363 and 157857; the first two are in Table 15. Blaauw was unable to link any of the three with known associations because of the uncertain proper motions. Similarly, other stars of this programme are generally too distant or have proper motions too indeterminate to permit connection with associations.

It has been shown that most of the intermediate and high latitude early-type stars can be considered to have formed in or near the galactic plane and been ejected shortly after formation, probably by motions originating in expanding stellar associations, possibly by more violent phenomena such as explosion of the primary of a binary system. The formation of young stars is usually connected with OB-associations, open clusters and the concentrations of gas and dust in the plane of the Galaxy but the possibility of star formation away from the plane should be considered. In the northern hemisphere, Kepner (1970) has shown that the neutral hydrogen appears to extend vertically from the plane for up to 2 kpc. Isserstedt (1968a) has described stellar rings, apparently elliptical aggregates of young stars, presumed to be projections on to the celestial sphere of star groups in the form of ellipsoidal or spheroidal shells. According to Isserstedt (1968a, b), stellar rings exist in numbers to more than 1 kpc from the plane and for $z < 1$ kpc are useful spiral tracers. Schmidt-Kaler (1968a) investigated the reality of rings and found that up to 25% may be chance configurations but the majority are probably real. He considers them to originate in shock fronts produced by H II regions around high-luminosity stars such as P Cygni or Wolf-Rayet stars; the latter have been observed at more than 1 kpc from the plane in distant regions (Smith, 1968). It is difficult to imagine how a spheroidally distributed group of stars could remain recognisable for very long; Isserstedt (1968a) gives 5×10^5 to 2×10^6 years for ring lifetimes, hence the disintegration of stellar rings could be a mechanism for producing early-type stars at appreciable distances from the plane. Very early spectral types do occur in stellar rings, for example the O-ring in Centaurus (Schmidt-Kaler, 1968b), but until rings at higher latitudes are observed in detail, direct comparisons are not in order. Furthermore, it should be noted that some doubt has been cast upon the reality of stellar rings, for example, Crampton and Byl (1971) have demonstrated that stars of the Orion ring are indistinguishable from field stars in the region, and have shown the Aquila ring to be the effect of a chance projection of stars. Thus the possibility that rings are a source of early-type stars must, for the present, be considered a rather speculative hypothesis.

CHAPTER VII

KINEMATICS AND HIGH VELOCITY STARS

1. Radial velocities

Radial velocities of programme stars are plotted in fig. 26 after correction for the solar motion relative to the local standard of rest and multiplication by cos b to give the component of the radial velocity parallel to the Galactic plane. The solar motion used was that determined by Feast and Shuttleworth (1965). Excluded from fig. 26 are stars with "probable" velocity variation; possible variables are included but denoted by open circles. Some of the stars may be subluminous, for example, Hill (1968) has suggested HD 125924 is a hot subdwarf. Curves are theoretical determinations of the effect of differential galactic rotation on radial velocities of stars situated 2 and 5 kpc from the sun.

It would appear that the velocities of many of the stars in fig. 26 are at least partly a result of differential rotation of the Galaxy. There is undoubtedly considerable scatter in the diagram due to peculiar motions, as might be expected if the stars are supposed to originate near the plane. Between latitudes 320° and 360° and particularly around $l = 350^{\circ}$, an appreciable number of stars have positive radial velocities where negative velocities are expected. The effect is not apparent for $l > 0^{\circ}$. Admittedly the survey is not complete but there is a reasonable sample of stars in the range $0^{\circ} < l < 25^{\circ}$ and very few have unusual velocities.

In fig. 27 are plotted the radial velocities from fig. 26 corrected for differential galactic rotation. Stellar distances for the correction were determined from β-index absolute magnitudes where

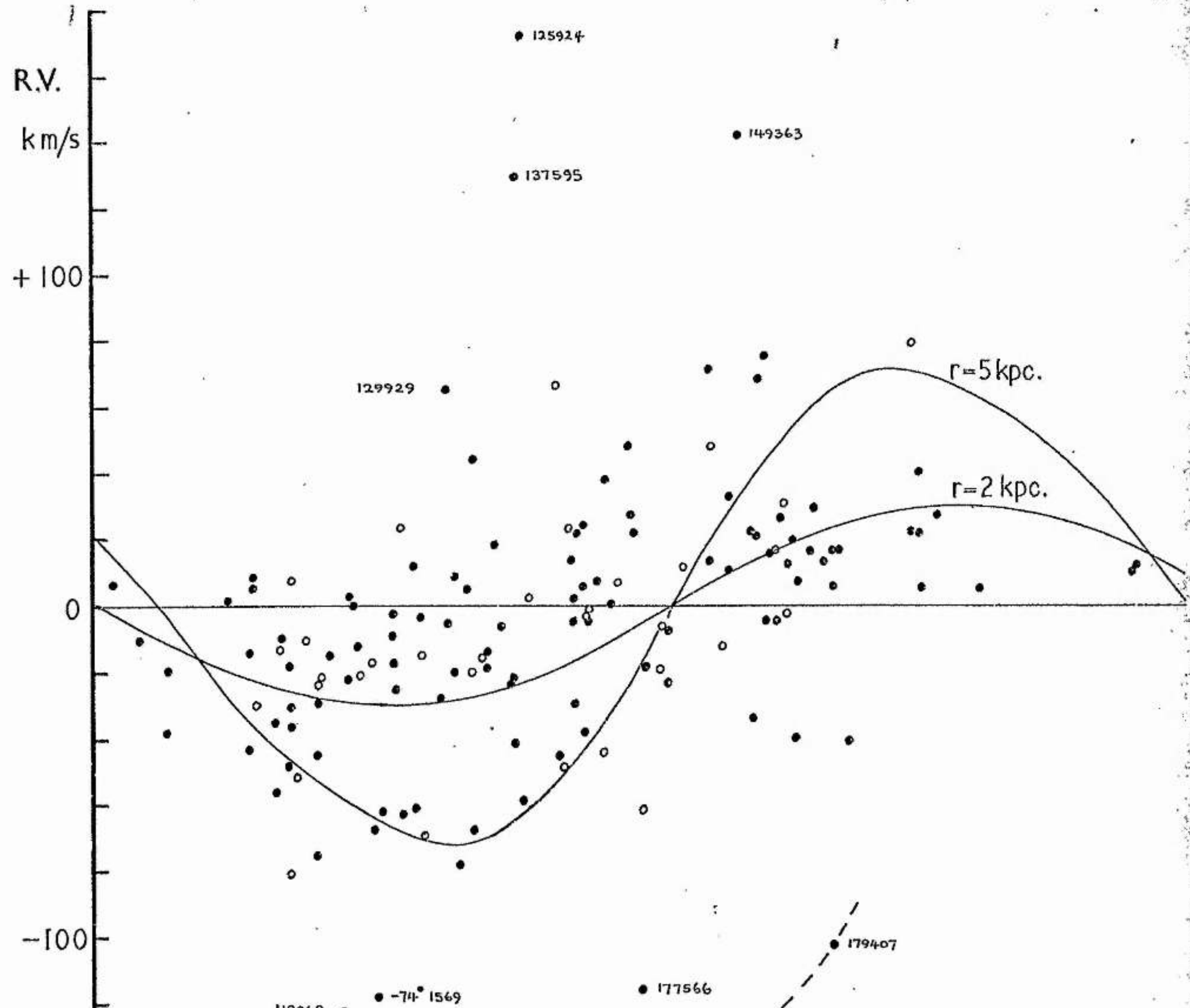

Fig. 26 Radial velocities of programme stars relative to the local standard of rest. Open circles indicate possible velocity variables. Solid curves represent the expected effect of differential galactic rotation on velocities of stars at 2 and 5 kiloparsecs from the Sun. Star numbers are from the HD and CPD catalogues.

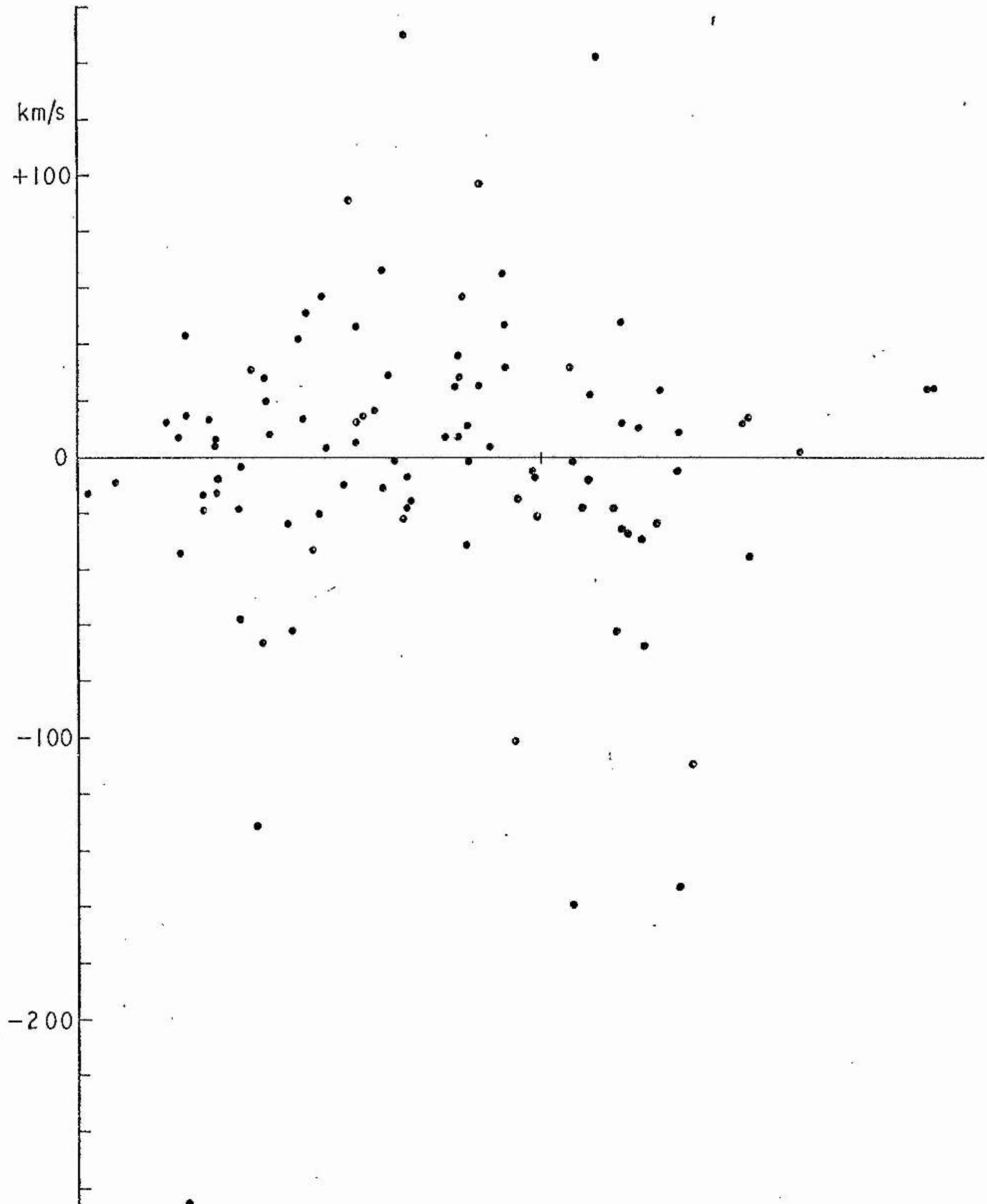

Fig. 27 Radial velocities of programme stars corrected for the effect of differential galactic rotation. Possible velocity variables are excluded and half filled circles indicate stars for which the correction is uncertain.

available and only constant velocity stars are included. Half filled circles represent stars for which the correction is uncertain. For HD 156359 and 177566 absolute magnitudes were taken from MK types rather than β-indices because the latter result in somewhat improbable distance determinations (fig. 24). Helium star HD 168476 was excluded because of the uncertainty of its absolute magnitude. Most of the stars represented in fig. 27 have corrected radial velocities smaller than 40 km/s; for these the mean corrected velocity is $+ 1 \pm 19$ km/s. High velocity stars may be considered to be those in the range $60 < |\text{velocity}| < 160$ km/s, though there are a few stars with very high velocities outside this range. Considering the available spectra, almost all high velocity stars show constant radial velocity, consistent with the low percentage of binaries observed by Blaauw (1961) in his analysis of run-away stars and attributed to the origin of these stars in disrupted binary systems.

Returning to a point made above, in both fig. 26 and 27 can be seen a tendency for stars between $l = 340^\circ$ and 360° to have positive radial velocities. This effect may be related to similar observations by various authors investigating the radial velocities of interstellar Ca II and H II emission regions and has been ascribed to deviations from circular motion in the -I or Sagitarrius arm. Courtès (1967) has summarised the data. Only about half the programme stars in the range $340^\circ < l < 360^\circ$ have estimated distances such that they can be reasonably related to the -I arm so the effect, if real, may be more widespread. Radial velocities of interstellar Ca II lines will be discussed in the next chapter.

2. Space motions

The method used to determine space motions of stars has been described in detail in Appendix II. UVW components of the space motion were computed for all stars which had not been found to have variable radial velocity. Initially, space motions were calculated from radial velocities alone, because for most distant early-type stars proper motions are not significantly different from zero. Then space motions, including proper motions, were calculated for stars which had at least one component of the proper motion significant at the 2σ level, that is either $\mu_\alpha \geqslant 2\sigma_\alpha$ or $\mu_\delta \geqslant 2\sigma_\delta$ or both, where σ is the standard deviation of the measurement in question. The results are presented graphically in fig. 28. U and V are components of the space motion towards the galactic centre and in the direction of galactic rotation respectively. The solid circle centred on the local standard of rest has a radius of 65 km/s and the broken arc has a radius of 365 km/s. These are reproduced from early work by Oort (1928); no stars had been located outside the arc and it was thought that this represented the velocity of escape from the Galaxy, in the solar neighbourhood. The circular velocity at the sun's galactocentric distance of 10 kpc is generally accepted to be about 250 km/s, implying an escape velocity in the direction of rotation of 315 km/s. At the present time it is considered that stars with velocities of this order move out as far as a "boundary" of the Galaxy at roughly 24 kpc from the centre (Schmidt, 1965) but do not escape. Schmidt calculates the escape velocity near the sun to be about 380 km/s and this limit will be adopted in following discussions on high velocity stars. In fig. 28, filled circles represent space motions computed from radial velocities alone; filled squares, motions computed from radial velocities plus proper motions. The cross at U = + 10 km/s, V = + 13 km/s represents the solar motion relative to the local standard of rest. In each case, U, V motions were calculated with β-index absolute magnitudes where possible. Connected to many of the high velocity star points in

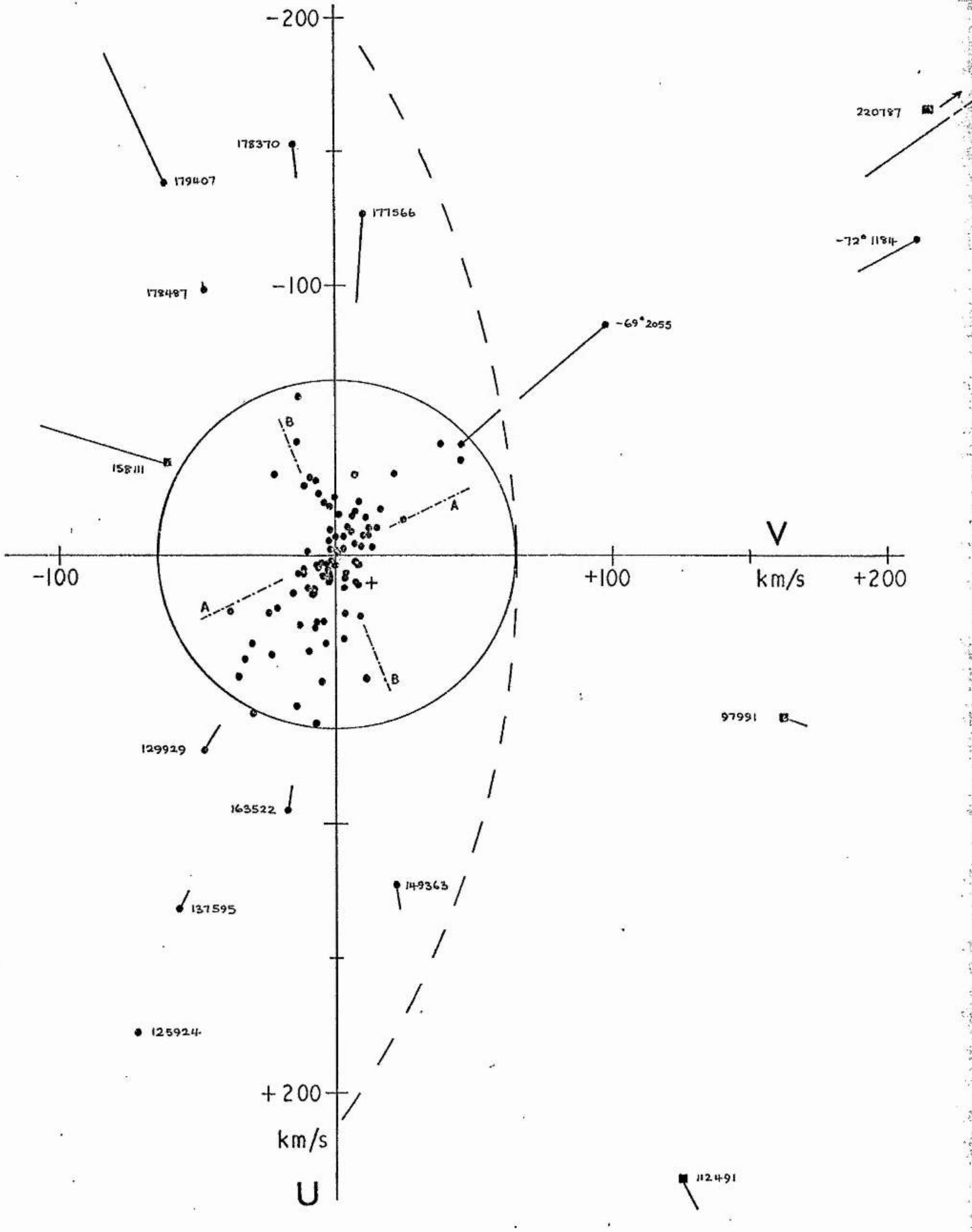

Fig. 28 Programme stars in the U,V plane. See text for discussion.

fig. 28 are straight lines which indicate the difference in results when absolute magnitudes are taken from the Blaauw (1963) calibration of MK-types. Many of the stars with significant proper motions had U, V components too large to fit into fig. 28 and are included in Table 16 which lists stars with velocities greater than $(U^2 + V^2)^{\frac{1}{2}} = 65$ km/s. References in Table 16 are to Smithsonian and Yale catalogues, as in Table 9.

For the majority of programme stars, only radial velocities were considered, hence the distribution in the U, V plane is dependent on galactic longitude. Line AA in fig. 28 corresponds to stars with $l \simeq 300^\circ$ and line BB is equivalent to $l \simeq 25^\circ$. Nearly all programme stars were within these longitude limits and cannot, therefore, be considered to be a representative sample for the purposes of statistical kinematics. It would, for example, be meaningless to fit a velocity ellipsoid to the data.

3. High velocity stars

For convenience of discussion, high velocity stars can be divided into three groups; stars with high radial velocity and relatively large proper motion, stars with high radial velocity but insignificant proper motion and stars with significant proper motion and low radial velocity. Because the programme stars are mostly distant early-type stars, it might be expected that they would have very small proper motions although the corresponding tangential velocities could be quite large. A list of high velocity programme stars was compiled and included the eleven proper motion stars of Table 16, four of which have large radial velocities, and fourteen stars with radial velocities greater than 60 km/s after correction for differential galactic rotation (see fig. 27). A selection of the more interesting of these stars will be considered in some detail after a few general notes.

Table 16

High space velocities from proper motions and radial velocities

Star	μ_α (0".001)	μ_δ (0".001)	Ref.	(M_V from β-index) U	V (km/s)	W	(M_V from MK-type) U	V (km/s)	W
97991	+22 ± 9	+22 ± 8	S	+62	+163	+156	+65	+170	+162
108769	−55 ± 21	−19 ± 21	S						
	−25	−20	Y						
Mean	−40	−20		−199	−168	−175	−162	−126	−144
112491	+30 ± 14	−27 ± 14	S	+230	+125	−220	+245	+130	−230
116538	−49 ± 15	+25 ± 11	S				−255	−85	+170
125924	+27 ± 12	−36 ± 12	S	+806	−217	−365	+748	−205	−315
137595	−28 ± 14	−33 ± 11	S						
	−24	−19	Y						
Mean	−26	−26		+55	−265	+11	+96	−127	+33
158111	−40 ± 7	−16 ± 17	S	−35	−62	+54	−44	−107	+86
172533	−1 ± 18	−56 ± 18	S	−2	−348	−152	−5	−254	−109
179407	−25 ± 17	+37 ± 18	S	−498	+1920	+2640	−385	+1060	+1600
187536	+12 ± 20	+59 ± 17	S	−319	+1760	+200	−140	+870	+95
220787	+7 ± 15	+50 ± 17	S	−238	+315	+70	−141	+194	+32

High velocity objects of the present study show a fairly strong concentration towards the galactic plane, typical of early-type stars. Eighteen out of twenty-six lie between $|b| = 7^{\circ}$, the lower limit of the survey, and $|b| = 21^{\circ}$. Apart from this concentration towards the plane, the sky distribution seems to be random.

Figure 29 is the two-colour diagram for high velocity stars. The intrinsic colour line for class V unreddened stars is included, together with approximate reddening lines for B0 and B1 main sequence stars. By colour, the stars are mainly B0-B1 spectral types with 0.07 to 0.45 magnitudes of extinction in (B-V), plus a few later types with $E_{B-V} < 0^{m}.2$. Comparing colours with spectral types, it is found that the stars are systematically bluer than the spectral types suggest. In other words, if spectral type S_Q (Johnson and Morgan, 1953) is derived from the colours, then for 22 class III - V stars, S_Q is systematically earlier than the visually determined spectral type by one subdivision. This effect was discussed in III.6 and is not restricted to high velocity stars.

(a) Stars with large radial velocity and proper motion

Four stars fall into this category; HD 214539, a subluminous B9p star, according to Thackeray (1962); HD 125924, suggested by Hill (1968) to be a possible subdwarf; HD 137595 and 179407. The first two stars have been discussed by other authors; HD 137595 has a radial velocity of +131 km/s but this may be variable (Hill, 1971).

HD 179407 was considered in VI.5 where it was concluded that the star was unlikely to be greatly underluminous because of the strong interstellar Ca II line and the fact that the star is reddened by $0^{m}.3$ in (B-V). The proper motion components convert into extremely large space motions if the absolute magnitudes suggested by β-index and MK-type are correct. In addition, the radial velocity, -115 km/s,

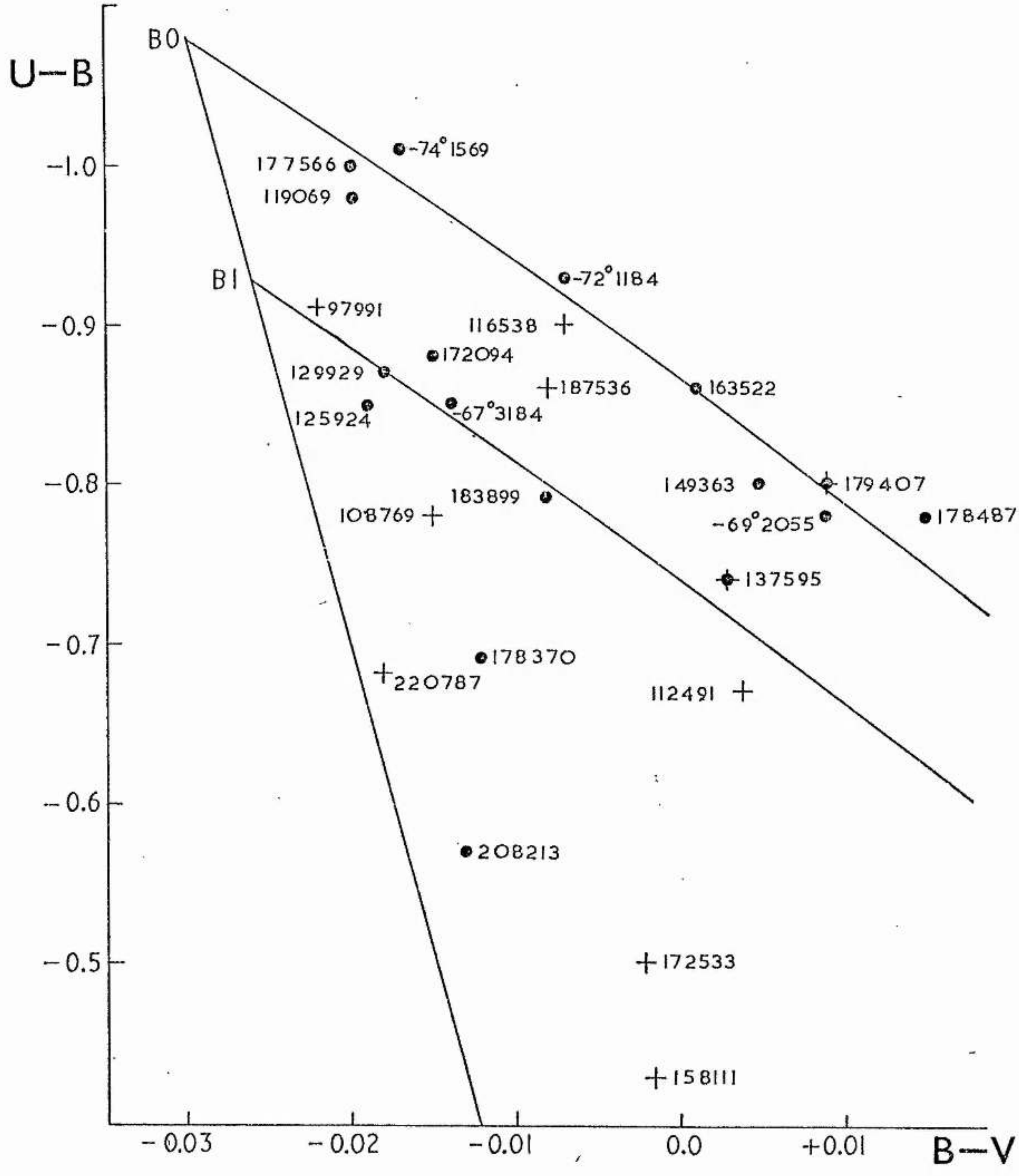

Fig. 29 Two-colour diagram for high velocity stars. The intrinsic colour line for class V stars and approximate reddening lines for B0 V and B1 V stars are sketched. Filled circles denote stars with high radial velocity; crosses indicate large proper motion stars.

is unusual for a normal population I star at $l = 24^{\circ}$. An ultra violet spectrum showing the confluence of the Balmer series in this star would be useful and might determine whether or not it is subluminous.

(b) High radial velocity stars

CPD -72° 1184 is, in terms of kinematic properties, one of the most interesting stars observed. Classified BO III from 1971 spectra, the star has a radial velocity of -217 ± 5 km/s from four plates with 86 Å/mm at Hγ. The proper motion is not significant and the β-index is equivalent to $M_V = -5.4 \pm 0.6$, in moderately good agreement with the MK-type which gives $M_V = -5.0$. These values of absolute magnitude yield distances of 11.7 and 9.75 kpc respectively. Projected on to the galactic plane this locates the star near the Carina spiral feature (Bok et al., 1970) but with a latitude $b = -10^{\circ}.9$, CPD -72° 1184 will be approximately 2 kpc from the plane.

HD 109399 and CPD -72° 1184 have an angular separation of less than 2°. The former has an MK-type of Bl Ib (Morgan, Code and Whitford, 1955), an estimated distance of 3.7 kpc and hence is 0.6 kpc from the galactic plane. The colour excess of HD 109399, $E_{B-V} = 0^{m}.18$, compared with $0^{m}.23$ for CPD -72° 1184, suggests that the latter star is more distant, particularly since it has a higher latitude. It is therefore unlikely that CPD -72° 1184 is greatly underluminous.

Space motion components U, V and W were computed from the radial velocity of CPD -72° 1184 for a range of absolute magnitudes $-5.4 \leq M_V \leq +3$. Cases plotted in fig. 28 are $M_V = -5.4$ and -5.0, however, in no instance was the component V, in the direction of galactic rotation, less than +160 km/s, a velocity which is improbable for a subdwarf. Combining this with a circular velocity of 250 km/s at the sun's distance from the galactic centre gives CPD -72° 1184 a velocity $V' = 410$ km/s in a frame of reference at rest relative to the galactic centre. V′ is greater than the estimated velocity of escape from the Galaxy in the solar neighbourhood, 380 km/s (Schmidt, 1965). The computation may seem unrealistic since CPD -72° 1184 is apparently very far away from the sun, but at a galactic longitude $l = 299^{\circ}$, the star cannot be nearer the galactic centre than 8.7 kpc whatever value is assumed for the absolute magnitude, and at 9.75 kpc, CPD -72° 1184 would have a galactocentric distance of 9.9 kpc. Hence the above discussion is reasonable provided there are no significant deviations from symmetry about the axis of rotation of the Galaxy.

In summary, the reddening and high positive velocity in the direction of galactic rotation suggest that CPD -72° 1184 is a luminous star rather than a subdwarf. It is a star which may have sufficient kinetic energy to escape from the Galaxy.

HD 119069 and CPD -69° 2055 have certain similarities and are discussed together. Some relevant data are reproduced below:

	l	b	MK type	Rad. velocity
CPD $- 69^{\circ}$ 2055	$311^{\circ}.16$	$-8^{\circ}.83$	B2 III	-130 km/s
HD 119069	$312^{\circ}.06$	$+16^{\circ}.12$	B1 III	-126 km/s

The proper motions are small but both stars must have appreciable tangential velocities to have reached their present locations. Velocity and MK-type of HD 119069 are by Hill (1971), the same data for CPD $- 69^{\circ}$ 2055 are from two 1971 spectra. Neither star appears to have variable velocity or variable UBVβ; both stars are included in the U, V diagram (fig 28). The similarities in longitude, radial velocity and spectral type are striking. Distances were computed with the following results:

	β	n	Dist (β)	Dist (s)
CPD $- 69^{\circ}$ 2055	2.555 ± 0.011 (s.e.)	6	14 ± 5 kpc	3.2 kpc
HD 119069	2.579 ± 0.010 (s.e.)	4	4.8 ± 1.4	3.2

n is the number of separate measurements in each mean ß-index. A spectral type error of one subdivision either way will lead to errors in the absolute magnitudes of about $\pm 0^m.5$, equivalent to approximately ±0.8 kpc in distance. Thus the MK-type distances are identical and it may be that CPD -69° 2055 and HD 119069 are related, possibly originating in the same stellar aggregate and deriving their velocities from some event ten to twenty million years ago.

CPD -74° 1569, classified O 9.5 V and with a radial velocity of −123 km/s from four 1971 plates (89 Å/mm), has a galactic latitude of $-18^\circ.68$. Spectroscopic and photometric distances are 7.2 and 9.6 kpc respectively, implying a distance from the galactic plane of 2.3 to 3 kpc. Differential galactic rotation will account for about half the observed radial velocity. In VI.5 it was found that the distance of CPD -74° 1569 from the plane was not compatible with the short lifetime of an O 9.5 V star unless the star had an appreciable W-velocity. Using estimated distances for CPD -74° 1569, it can be shown that very small proper motion components are equivalent to large space velocities. For example, the Yale data (Lu, 1971)

$$\mu_\alpha = +0''.006 \qquad \mu_\delta = -0''.008$$

combined with distances of 7 − 9 kpc give values of W in excess of −200 km/s.

The extinction in (B−V) is only $0^m.14$ which is rather small for a distant star; the interstellar K-line is present but not particularly strong. The possibility that CPD -74° 1569 is subluminous cannot be ruled out but in any case the star would appear to be worth further study.

HD 177566 has been classified B 1 III and has a radial velocity of −131 km/s (Hill, 1971). The ß-index, based on only two measurements, gives an extremely large estimate for the distance which is almost certainly incorrect. Adopting the MK-type gives a spectroscopic distance of 7.4 kpc, locating the star 2.6 kpc from the galactic plane in the region of the 3 kpc "expanding" arm. No proper motion determination was found in the literature, probably because the star is faint ($V = 10^m.2$). The galactic longitude is $l = 355^\circ.6$ so that galactic rotation can account for only a small part of the observed velocity of HD 177566.

HD 178487 at galactic longitude $25^\circ.8$, has a velocity -55 ± 2 km/s, equal and opposite to that expected from the effect of differential galactic rotation at the estimated distance of the star. HD 178487 was classified B0.5 I from three plates at 49 Å/mm. This is rather high dispersion for classification purposes but absolute magnitudes from MK-type and β-index agree quite well. Spectroscopic and photometric distance estimates are 5.36 and 5.11 kpc respectively, putting HD 178487 about 800 parsecs from the plane. The extinction in (B-V) is $0^m.38$ and there is no reason to suppose that the star is subluminous; it appears to be an early-type run-away star.

(c) Large proper motion stars

HD 97991 is a high latitude star included in the list of run-away stars published by Blaauw (1961), who computed a total space velocity of -156 km/s for the star. A higher value, -230 km/s, was obtained in the present analysis due to use of a slightly different absolute magnitude. Hill (1970) classified HD 97991 as B 1 V, equivalent to an absolute magnitude of -3.6, in good agreement with the Hβ result, $M_V = -3.5 \pm 0.2$. The latter result gives a distance of 1.4 kpc from the sun and 1.1 kpc from the galactic plane. From the Smithsonain Star Catalogue, the proper motions are:

$$\mu_\alpha = +0''.022 \pm 0''.009 \qquad \mu_\delta = +0''.022 \pm 0''.008$$

which seem quite significant. Plaskett and Pearce (1931) found the radial velocity to be -23.5 ± 0.6 km/s. Combining the various results, the space motions were found to be:

$U = +62$ km/s $\qquad V = +163$ km/s $\qquad W = +156$ km/s

A large, positive W-component is necessary if HD 97991 is supposed to have originated near the plane of the Galaxy. Referring back to the discussion of CPD -72° 1184, it can be seen that HD 97991 has a similar V-component and so should be regarded as a potential "escape velocity" star. At latitude $262^{\circ}.3$ and an estimated distance of 1.4 kpc, HD 97991 will be approximately 10 kpc from the galactic centre.

HD 112491 has a velocity -27 ± 3 km/s from two plates at 49 Å/mm and one at 86 Å/mm. It was classified B 2 V, equivalent to an absolute magnitude of -2.5, and the ß-index gives $M_V = -2.4 \pm 0.2$. Both are equivalent to a distance of approximately 1.7 kpc. Smithsonian proper motions are

$\mu_{\alpha} = +0''.030 \pm 0.014 \qquad \mu_{\delta} = -0''.027 \pm 0''.014$

which give

$U = +230$ km/s $\qquad V = +125$ km/s $\qquad W = -220$ km/s

and a total space motion of 350 km/s. The large W-component is motion towards the plane, as HD 112491 has a positive galactic latitude. The star may have originated in one of two clusters in the region sketched in fig. 30. Tracing the probable path of HD 112491 and assuming it to have had a constant velocity, it would have taken approximately half a million years to reach its present position from cluster Ruprecht 106 and about two million years from NGC 3680. The "Catalogue of star clusters and associations" (Alter et al., 1970) gives no information for the distance of Ru 106. Stars in this cluster are reported to be fainter than 15^{m}, so if Ru 106 were at comparable distance to HD 112491, the cluster stars would be about F0 and later. Several distance estimates are available for NGC 3680, the maximum being

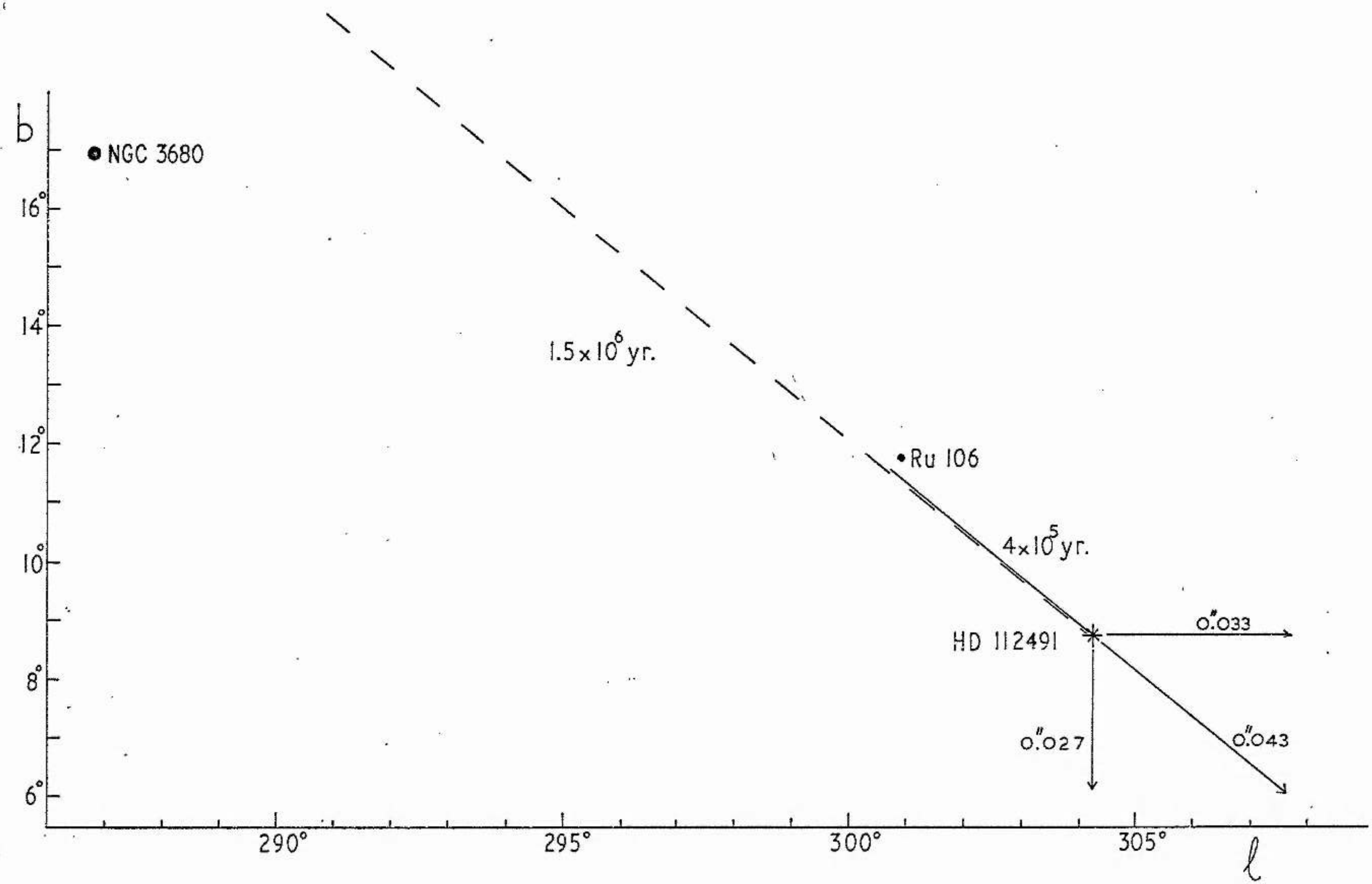

Fig. 30 The proper motion of HD 112491. Approximate kinematical ages of the star relative to clusters NGC 3680 and Ru 106 are shown.

1.7 kpc, although a recent determination indicates a smaller value. No spectral information is available for NGC 3680 but the cluster stars are 10th to 14th magnitude, closer than Ru 106 to the apparent magnitude of HD 112491 ($V = 9^m.2$).

If HD 112491 did originate in one of these cluster, the cluster will have moved since the event which produced the run-away star. This cannot be taken into consideration without more data on the cluster, however, the effect of differential galactic rotation will be small compared with the uncertainty in the stellar proper motion.

HD 116538 was classified B2 IVn by Hill (1971) who also determined its radial velocity as -74 km/s. The Smithsonian Star Catalogue gives proper motions:

$$\mu_\alpha = -0''.049 \pm 0''.015 \qquad \mu_\delta = +0''.025 \pm 0''.011$$

At an estimated distance of 1.3 kpc, the correction for differential galactic rotation reduces the radial velocity to -58 km/s and the proper motion in R.A. to -0".046. Computed space motions are

$$U = -255 \text{ km/s} \qquad V = -85 \text{ km/s} \qquad W = +170 \text{ km/s}$$

Sketching a probable path of HD 116538 from the vicinity of the galactic plane indicates several possible clusters of origin but no particularly outstanding possibility.

HD 187536 has an absolute magnitude of -5.1 ± 0.6 from the Hβ measurements and was classified B2 III (Hill, 1971) equivalent to $M_V = -3.6$. Adopting the smaller of these values, the resulting distance of 3.1 kpc when combined with proper motion components

$$\mu_\alpha = +0''.012 \pm 0''.020 \qquad \mu_\delta = +0''.059 \pm 0''.017$$

gives

$$U = -140 \text{ km/s} \qquad V = +870 \text{ km/s} \qquad W = +95 \text{ km/s}$$

and a total space motion of almost 900 km/s. HD 187536 could be subluminous, but the fact that radial velocity and proper motion in

R.A. are normal for an early-type star may indicate that a sizeable error exists in μ_δ in this case.

HD 220787 was classified B3 V from 1971 spectra and B3 III by Hill (1971). The β-index is equivalent to an absolute magnitude of -2.8 ± 0.2 which agrees well with the latter classification. Proper motion components from the Smithsonian Star Catalogue are

$$\mu_\alpha = +0''.007 \pm 0''.015 \qquad \mu_\delta = +0''.050 \pm 0''.017$$

Assuming $M_V = -2.8$ we obtain a distance of 1.6 kpc and

$$U = -240 \text{ km/s} \qquad V = +315 \text{ km/s} \qquad W = +70 \text{ km/s}$$

The large, positive V-component may give HD 220787 sufficient energy to escape from the Galaxy if the proper motion is reliable. In this respect the star is similar to HD 187536; for both stars the space motion components are largely dependent upon μ_δ.

HD 220787 has a galactic latitude $b = -64^\circ.4$ and is estimated to be 1.4 kpc from the galactic plane. Kinematical and evolutionary lifetimes of the star, computed as in VI.5, are roughly equal and indicate ejection from the plane some 30 million years ago.

4. Helium stars

In a private communication to Dr. Hill, Bidelman described CPD -69° 2698 as having strong helium lines. The star had already been included in the intermediate latitude programme and three spectra were obtained. Balmer lines of hydrogen in the spectrum of CPD -69° 2698 are comparable with those of CPD -69° 2055, classified B2 III on the present programme. The helium lines are much stronger in the former star. Relative intensities of pairs of helium lines in the spectra of CPD -69° 2698 suggest luminosity class III or V. The β-index is equivalent to $M_V = -3.9$, in moderate agreement with MK-type B2 III although the uncertainty in the luminosity of a peculiar star such as this will be large. The mean radial velocity, -63 km/s, does not appear to be variable and, at an estimated distance of 3 kpc, two thirds of the velocity would be attributable to differential galactic rotation.

The helium star HD 168476, discovered by Thackeray (1954) and investigated in detail by Hill (1964, 1965a, b, 1969a), has no recorded hydrogen lines. Thackeray (1954) reported a radial velocity −165.0 ± 0.8 km/s from 21 plates and noted some relatively small variations in velocity which, if real, could not be attributable to a regular fluctuation with a period in excess of one day. Single plates of HD 168476 were taken in June and July, 1971. In August, one plate was obtained on the 3rd and one on the 5th; on the 4th, six spectra were taken, alternated with spectra of a radial velocity standard star HD 157457 (Evans et al., 1959). No systematic variation in radial velocity was established from these plates and it seems likely that any variation must be irregular. The total range of velocities was about 7 km/s for the August 4th plates. For all spectra obtained in 1971, the mean velocity of HD 168476 was calculated to be −170.1 ± 1.2 (s.e.) km/s from ten plates.

CHAPTER VIII

INTERSTELLAR MATTER

1. Ca II radial velocities

Radial velocities relative to the sun of interstellar Ca II lines from spectra of 127 intermediate and high latitude stars are plotted in fig. 31. This diagram contains the Ca II velocity data listed in Table 8 with the exception of spectra in which the K-line was judged to be stellar or greatly affected by stellar absorption lines. In a very few cases it was possible to measure the H-line, in helium stars and sharp-line supergiants for example, but the greater part of the results depend on K-line velocities alone.

Mean results for the Ca II velocities are illustrated in fig. 32. The velocities were averaged for 10° intervals and represented by a filled circle in the centre of each longitude interval. No attempt was made to average longitude but comparison with fig. 31 shows that taking the mid-point of each interval is a good approximation in nearly every case. Small circles are means of three data points or less. Error bars indicate the size of the standard error of the mean and absence of error bars implies representation of only one data point. Curves represent the computed effect of differential galactic rotation at 0.5 and 1 kpc; most of the mean Ca II points lie between these two curves. This result might be expected for, considering that the programme stars have $|b| > 7^{\circ}$ and assuming the Ca II gas to be concentrated towards the plane, the greater part of the absorption will occur within roughly 2 kpc of the sun, even for very distant stars. The Ca II velocities are then integrations of velocities between 0 and 2 kpc of the sun with a probable mean velocity somewhere under 1 kpc.

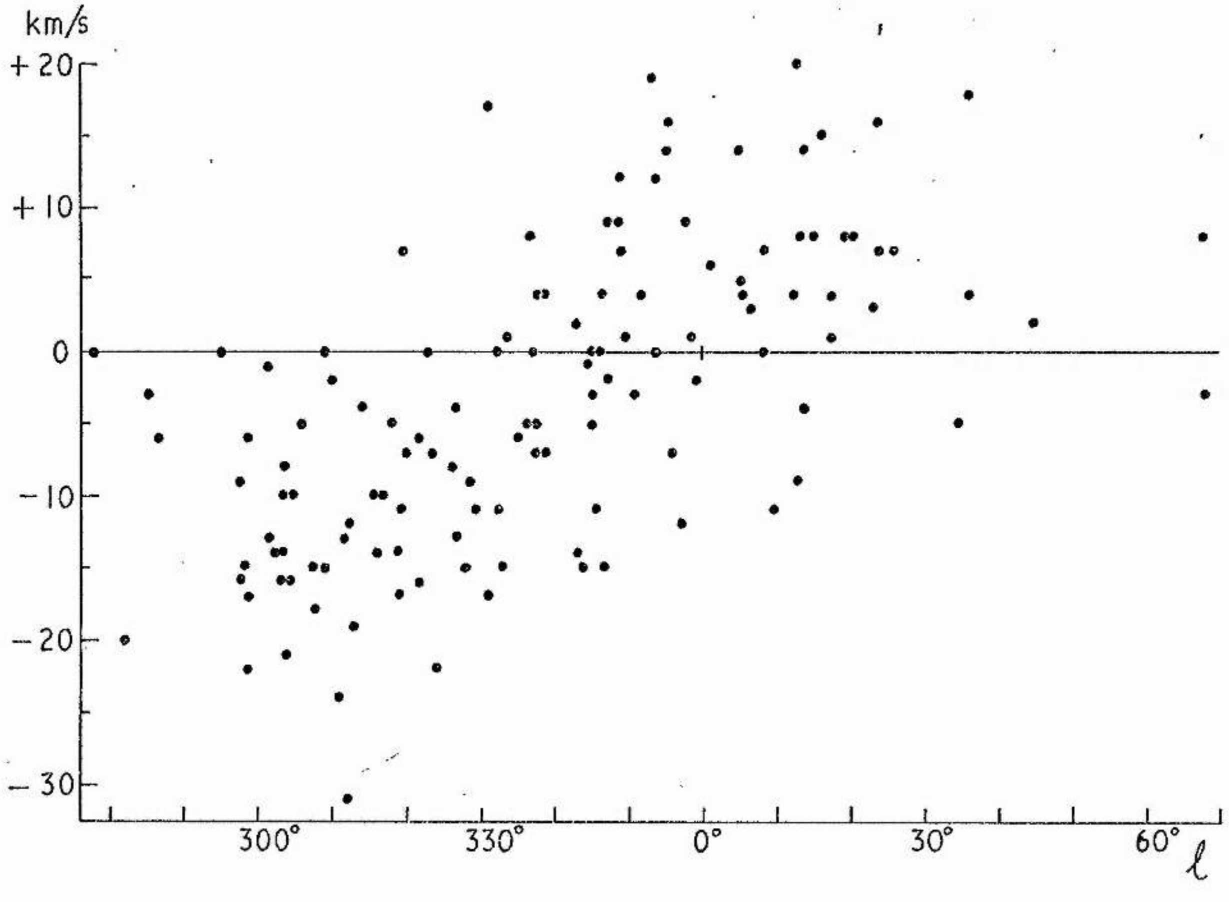

Fig. 31 Radial velocities of interstellar Ca II K-lines.

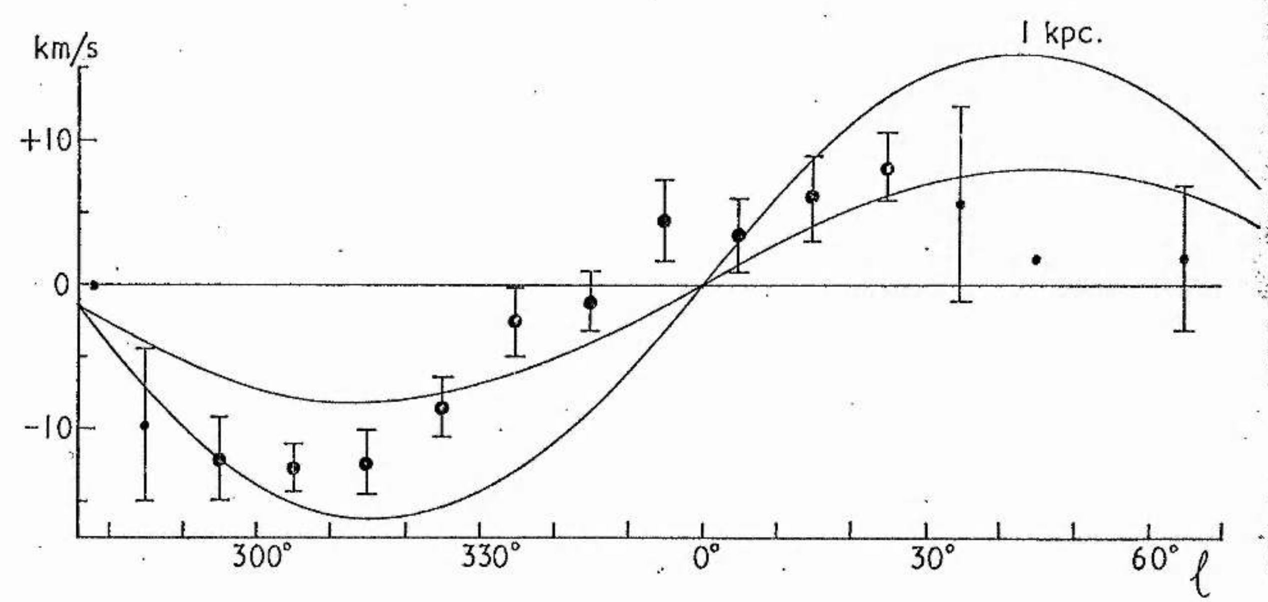

Fig. 32 Ca II velocities averaged over 10° intervals. Error bars indicate the size of standard errors.

Mean points between $l = 30^\circ$ and 70° are based on few spectra, mostly of high latitude stars, and are therefore of low weight.

Between $l = 330^\circ$ and 0° the mean points appear to be systematically more positive than expected, an effect which was also observed in the stellar velocities (VII.1) and in a study by Cruvellier (1967) of radial velocities of H II regions. Cruvellier suggests three possible causes of the anomalous velocities. First, that some of the H II regions do not have circular orbits around the galactic centre; the present work shows that if this is the case then a percentage of stars and the Ca II gas also have non-circular motions. The second hypothesis is that the local arm, including the sun, has a net movement away from the galactic centre. Against this, as Cruvellier points out, there is no equal and opposite effect observed for velocities of H II regions in the anticentre direction. Furthermore, velocities of Ca II between $l = 0^\circ$ and 30° are more or less as expected for local material involved in differential galactic rotation, whereas if the sun were moving away from the galactic centre, the systematic effect observed between $l = 330^\circ$ and 360° should also be present for $0^\circ < l < 30^\circ$. The third possibility is that part of the Sagittarius (-I) arm is moving towards the galactic centre. A comment was made in VII.1 to the effect that only half of the total number of programme stars with positive velocities and $330^\circ < l < 360^\circ$ could be related to the -I arm. However, nearly all these stars lie between the near edge of the -I arm and the distant edge of the -II arm, as sketched in fig. 20. If there were an inter-arm connection of some kind between the -I and -II arms with a velocity component towards the galactic centre, then this might explain the apparent superposition of "normal" and systematically positive velocities suggested by fig. 18 of Cruvellier (1967) and supported by fig. 31 of this dissertation.

The H II regions observed by Cruvellier are mostly very close to the galactic plane whereas the programme stars at 1 to 2 kpc from the Sun will be approximately 200 to 500 pc from the plane. Hence, in the region $330^{\circ} < l < 360^{\circ}$, it appears that abnormal velocities of planar objects, in this case H II regions, are reflected by velocities of stars with $z > 200$ pc and intermediate latitude Ca II velocities. Feast and Thackeray (1958) analysed early Radcliffe radial velocities, considering stars and Ca II lines divided into groups based on distance from the sun, r. The effect of systematically positive velocities is only suggested in one diagram, that for Ca II velocities in spectra of stars with $1 \leqslant r < 2$ kpc, but it is noticeable that in the Radcliffe analysis there tend to be few spectra of stars in the longitude range under discussion.

2. The cosecant equation of reddening

From the programme star photometry can be derived a measure of the vertical height of reddening material near the sun and the constant of proportionality in the cosecant representation of reddening. Abt and Golson (1962) approximate the density distribution of scattering material to that of a gas in hydrostatic equilibrium and obtain

$$E_{B-V} = \alpha \operatorname{cosec} b \left(1 - e^{-\frac{z}{h}} \right)$$

where b and z are galactic latitude and distance from the plane of a given star and h is the scale height of the scattering material. An estimate of h can be made in the following way. Consider stars at the same non-zero latitude but different distances from the sun. As distance increases, E_{B-V} will increase, rapidly at first but tending to flatten out as the density of material approaches that of inter-galactic space. A plot of E_{B-V} against distance should enable a crude estimate to be made of the thickness of the reddening layer. Colour excesses of programme stars were plotted against z-distances for various latitude ranges; fig. 33 illustrates the 8° to 9° range. All results are listed in Table 17 together with the number of stars in each range.

Table 17

Estimates of the height of the reddening layer

Latitude range	Height	n
$7^{\circ} \leq b < 8^{\circ}$	175 pc	14
$8^{\circ} \leq b < 9^{\circ}$	200	23
$9^{\circ} \leq b < 10^{\circ}$	250:	14
$10^{\circ} \leq b < 11^{\circ}$	190	16
$11^{\circ} \leq b < 13^{\circ}$	210	15
$13^{\circ} \leq b < 17^{\circ}$	200:	21

The unweighted mean of these results is 204 ± 10 (s.e.) parsecs which compares moderately well with h = 187 pc obtained by Abt and Golson (1962) for the scale height of the scattering layer. A value h = 200 pc was adopted for the cosecant equation. For each programme star, a determination of α can now be made since, for a given star, b is known, E_{B-V} has been derived and z can be computed from stellar distances. Initially, α was calculated for stars in latitude zones similar to those of Table 17. No latitude dependence was apparent so the analysis was repeated for all stars, segregated into northern and southern galactic hemispheres, with the following results:

$b > 0$	$\alpha = 0.062 \pm 0.005$ (s.e.)	53 stars
$b < 0$	$\alpha = 0.051 \pm 0.003$	97 stars

Hill and Hill (1966) obtained $\alpha = 0.049$ for faint blue stars at high negative latitudes and Abt and Golson (1962) derived $\alpha = 0.057$ using stars near the north celestial pole. These results, together with the present analysis, suggest there may be a difference between values of α in the two hemispheres. The constant α represents the colour excess at the galactic poles (cosec b = 1) and the difference could be

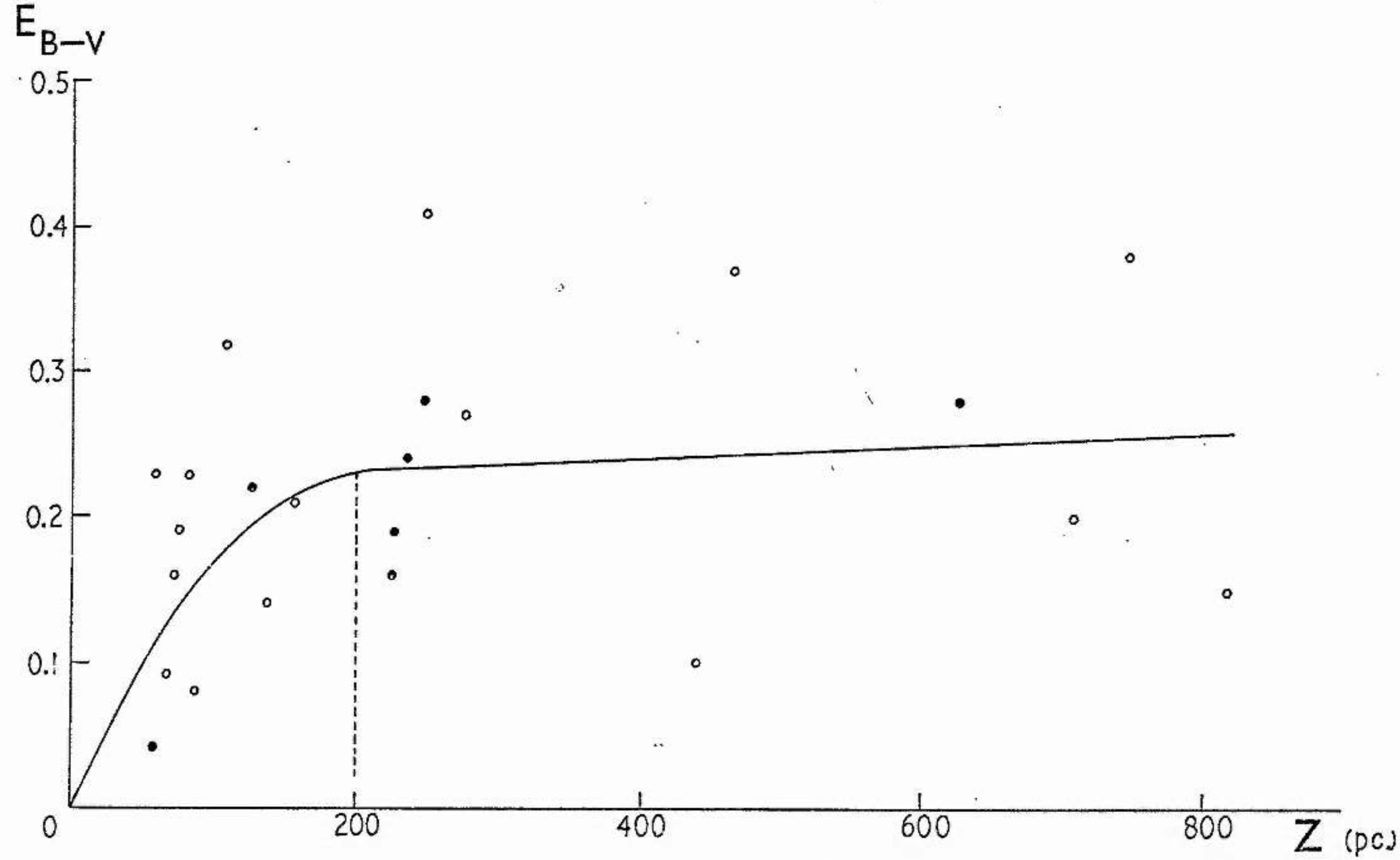

Fig. 33 Colour excess against distance from the galactic plane for stars with $7^\circ \leqslant b < 8^\circ$

Open circles represent negative latitude stars; filled circles, positive latitude stars.

explained by assuming the Sun to be slightly below the median plane of the scattering material. Gum, Kerr and Westerhout (1960) have determined the distance of the Sun from the plane of the Galaxy to be $z_0 = +4 \pm 12$ pc, which is small and in the opposite sense to that expected from the evidence of stellar reddening presented above. Gum et al. used the distribution of neutral hydrogen to derive z_0, so the hypothesis that an appreciable solar z-distance causes the observed difference in α for northern and southern galactic hemispheres must be discarded unless there is a systematic difference in the distribution of gas and dust.

A possible cause of the different results for α is that the interstellar medium does not have a smooth distribution. Examination of the E_{B-V}/z diagrams revealed that a few stars seemed to be more reddened than the general sample. There are nine programme stars with $E_{B-V} \geqslant 0^m.4$ and eight of them have positive latitudes, relatively high values of α and are earlier than type B1. Excluding these stars gives

$$b > o \qquad \alpha = 0.056 \pm 0.005 \text{ (s.e.)} \qquad 45 \text{ stars}$$

in better agreement with the result for $b < o$ and very close to the Abt and Golson determination. The eight stars are spread between $l = 316^\circ$ and $l = 24^\circ$ so that if irregularity in the interstellar medium is the cause of higher reddening, it is not likely to be a local effect. The Lundmark-Melotte survey of dark nebulae (Lundmark, 1926) shows more dark regions in northern intermediate latitudes than in southern, for $330^\circ < l < 20^\circ$. If the dust distribution reflects this asymmetry at all, then it is probably the cause of observed differences in α for northern and southern galactic hemispheres.

CHAPTER IX

SUMMARY AND SUGGESTIONS

Analysis of the distribution of early-type stars at intermediate and high latitudes has shown the earliest of these objects to be related to optically determined spiral structure in the plane of the Galaxy. Potentially the most important result of the distance estimates is that it has proved possible to observe very distant stars with medium and small telescopes, largely due to the relatively small loss of light by interstellar extinction.

In VI.5 consideration was given to the possibility that some of the early-type stars with appreciable z-distances may have been formed away from the galactic plane. Stellar rings were suggested as a possible source of such stars. Estimates were made of kinematical and evolutionary lifetimes of various stars but it was not possible to show conclusively that a significant proportion of stars were too young to have reached their present locations, assuming origin near the plane of the Galaxy. The principal obstacle to proof or disproof of the hypothesis is the poor quality of proper motions available for early-type stars, a problem which is not likely to be overcome in the near future.

Chapter VII concentrated on radial and space velocities of programme stars. The radial velocities were shown to be related to the general pattern of galactic rotation; high velocity stars, with a few very high velocity exceptions, were considered to have radial velocities of about 60 to 160 km/s relative to the standards of rest of their projected positions on the galactic plane. By this criterion, five to ten per cent of all stars considered had high velocities.

Detailed kinematic investigation of high velocity stars indicated that three may have sufficient kinetic energy to escape from the Galaxy, although in only one case, CPD -72° 1184, was the analysis independent of proper motion.

Logically, the next step would be to attempt to observe stars with fainter apparent magnitudes, perhaps extending the lower latitude limit to $|b| = 6^{\circ}$ or 5° in the hope of including more distant, albeit more reddened stars at roughly 1 to 2 kpc from the galactic plane. It is hoped to institute a programme based on objective prism surveys such as the catalogue "Luminous stars in the Southern Milky Way" (Stephenson and Sanduleak, 1971); similar projects in the northern hemisphere are at present being carried out by other St. Andrews observers. The northern hemisphere programme and extensions to the present work should greatly increase the data on early-type intermediate latitude stars. It is probable that more high velocity stars will be discovered amongst the fainter stars, although proper motions will still be a major difficulty.

A region of particular interest is the Carina spiral feature, extensively discussed by Bok, Hine and Miller (1970) and by Graham (1970) who finds a distortion of the galactic plane in the region $285^{\circ} < l < 300^{\circ}$. The OB stars are concentrated symmetrically about the galactic equator out to 4 kpc from the sun, but between 4 and 10 kpc appear to deviate by 2° to 3° towards negative latitudes. The high velocity star CPD -72° 1184 lies at $l = 299^{\circ}.2$, $b = -10^{\circ}.9$ and is approximately 10 kpc from the sun according to present estimates. It might prove interesting to search for faint blue stars in the Carina region between $b = -11^{\circ}$ and the upper limit of Graham's survey.

Time permitted only a brief discussion of interstellar matter. The velocities of interstellar Ca II absorption lines were shown to exhibit more or less the distribution expected from material within one or two kiloparsecs involved in differential galactic rotation. Determinations of constants in the cosecant equation of reddening were made, including an estimate of the height of the scattering layer. For the future, more accurate estimates of the scale height could be made using more stars and more distant stars. The northern hemisphere survey should provide comparison between positive and negative latitudes in the anticentre region, of the constant of proportionality in the cosecant equation. A rather more detailed examination of stellar and interstellar radial velocities in the region $325^{\circ} < l < 360^{\circ}$ might shed light on the anomalous velocities observed. Existing measures of stars in and near the plane could be used to investigate the extent of the phenomenon.

Finally, a project which could be carried out with spectroscopic and photometric results of the present programme is the determination of the dust to gas ratio at intermediate and high galactic latitudes. Equivalent widths of Ca II lines will give an estimate of the mean Ca II gas density along the lines of sight to a selection of stars. These densities might then be related to radio measurements of neutral hydrogen densities. UBV photometry yields the colour excess E_{B-V} which depends on the dust column density.

Appendix I

CURVATURE IN THE Hβ TRANSFORMATIONS

The presence of a small but significant curvature in the transformations from the two instrumental Hβ systems to the standard system of Crawford and Mander (1966) was discussed in III.4 where it was concluded that the difference in the intermediate filter bandwidths of the three systems was the probable cause of the curvature. The purpose of this appendix is to give details of the numerical calculations which support the conclusion.

Transmission curves for the Cape and Bochum (La Silla) filters were readily available. The filters used at the Cape were the property of St. Andrews University Observatory and had been supplied with spectrophotometer tracings of the transmission functions. Similar tracings existed for the Bochum filters and copies of these were made on La Silla. Astronomers at Kitt Peak National Observatory have used several sets of filters which were, in general, fairly closely matched. An enlargement was made of a set of transmission curves published by Crawford (1964). For each filter, measurements were made of the percentage transmission, expressed as a fraction of unity, at 1Å intervals from 4650 to 5149 Å, so that 500 evenly spaced data points represented the transmission of the filter. These "digitised" transmission functions were stored on punched cards for computer analysis. The next step was to find suitable spectrophotometer tracings of early-type stars, covering the same sort of wavelength range as the Hβ filters, and reduce the tracings to a digitised form, taking measurements at 1Å intervals of the intensity of a spectrum expressed as a fraction of the continuum intensity. Then a given spectrum could be combined with a given filter by multiplying each point of the spectrum by the corresponding point of the filter and summing the resultant products. For 500 points this would be exceptionally tedious to perform manually but with a computer such a convolution of filter and spectrum takes only a few seconds. From narrow and intermediate filter convolutions with a given spectrum, a simulated instrumental β-index can be computed by the usual formula. A short Fortran programme was written which performed the calculations described, computing from the input data, a numerical value of β. The programme also produced a graphical output of the simulated filter transmission functions and input spectrum.

To approximate the effect of He I 4922 on the β-index, data were extracted, in the form described above, from the spectrophotometric atlases by Wilson (1956) and Butler and Seddon (1958). These atlases cover a sufficient wavelength range for B1 and B2 main sequence and supergiant stars. Digitised spectra were combined with digitised transmission curves of the three filter sets and the resultant instrumental β-indices for the Cape and La Silla simulated filters were plotted against corresponding indices for the Kitt Peak simulated filters. Results are shown in fig. A1 where it can be seen that the La Silla transformation is linear and the Cape transformation nearly so; curvature in the latter case is not in the same sense as the observed curvature in the actual transformations. The range of spectral type covered is rather unsatisfactory due to the shortage of suitable data.

In the attempt to investigate the effect of variation of Hβ absorption on the intermediate band filters, it was decided to use theoretical line profiles as these were readily available for an adequate range of spectrum and luminosity types. Mihalas (1964) has

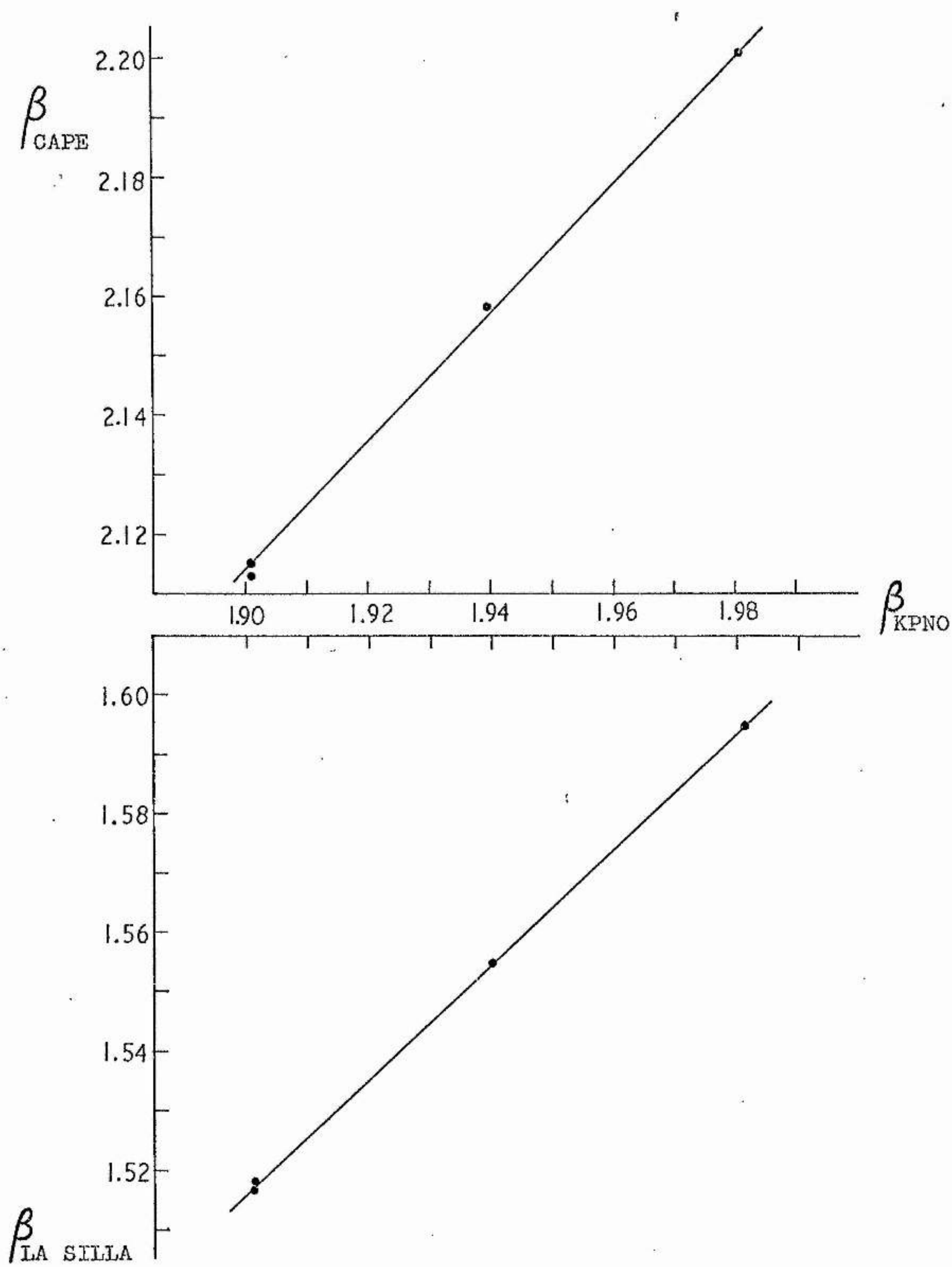

Fig. A1 Simulated transformations (a) effect of He I 4922 on intermediate filters published profiles of Hβ and Hγ, computed for various values of log g and θ_e (= $5040/T_e$). Log g and θ_e for different MK-types were obtained from "Astrophysical Quantities" (Allen, 1963) and, although the values of these quantities used by Mihalas did not always correspond exactly to a particular type of star, it was possible to match Mihalas' profiles fairly closely to MK-types for a good range of early-type stars. Profiles corresponding to types B9 V, III and I and spectral types B8, B5, B3, B2, B1 and B0 for luminosity classes III and V were available. In addition, profiles equivalent to types O9 and O5 were used, for which Mihalas had included blending with the overlapping line of the Pickering series of He II at 4859 Å. Equivalent widths of the line profiles varied from 19.6 to 1.7 Å.

Simulated β-indices were computed from convolutions of line profiles with Kitt Peak, Cape and Bochum (La Silla) filters and the last two sets of results were plotted against the first set as for fig. A1. The simulated transformations are illustrated in figures A2 and A3 where the curvature is apparent. Residuals were derived as for the actual transformations using $\Delta\beta$ = Standard - Standard (calculated). In this case 'Standard' is the simulated Kitt Peak β-index and the residual $\Delta\beta$ is the difference between plotted point and least squares solution, measured parallel to the abscissa, as before. Figure A4 shows the $\Delta\beta/\beta$ (instrumental) points compared with the observed transformation curvatures reproduced from figs. 8 and 9. Zero-points of the observed curves on the β' axes are arbitrary. It appears that it is possible to reproduce the observed curvatures moderately well with a rather crude model. the actual effect is larger than the simulated effect and the Cape curve might be partially cancelled by the smaller effect of the helium line at 4922 Å, but as far as the analysis goes, it indicates that the effect of Hβ absorption on the intermediate band

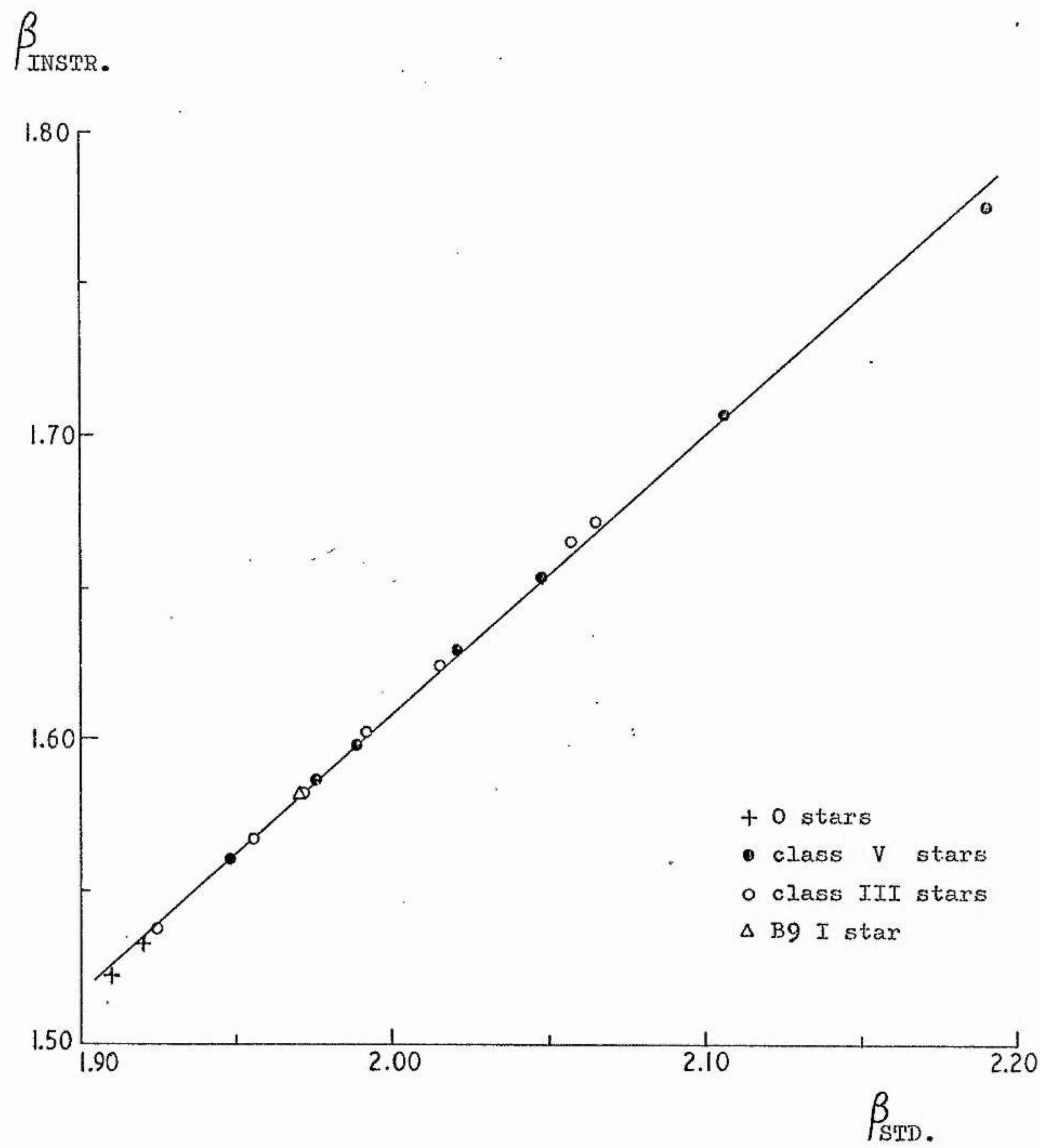

Fig. A2 Simulated transformation (b) effect of Hβ on La Silla intermediate band filter

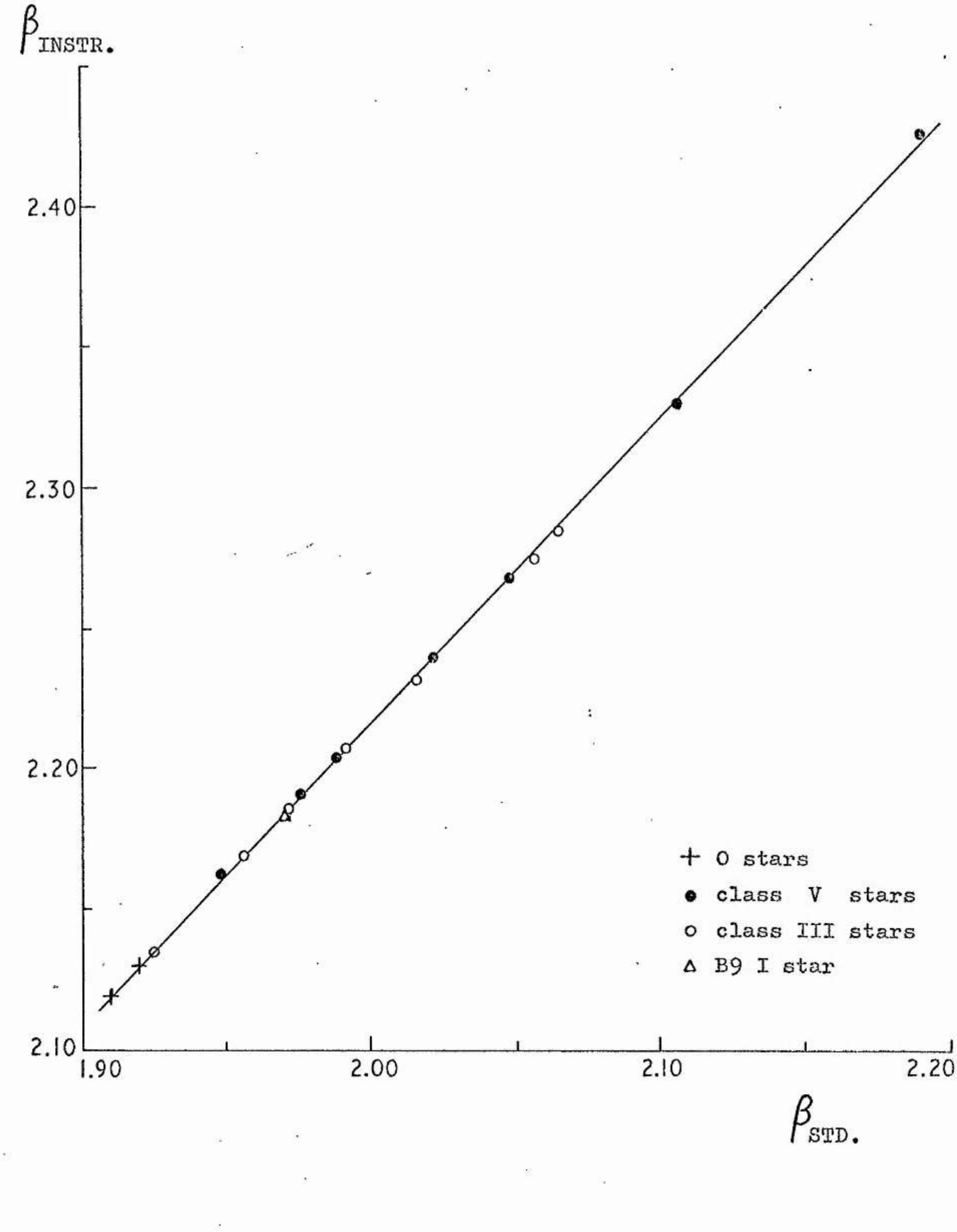

Fig. A3 Simulated transformation (c) effect of Hβ on Cape intermediate band filter

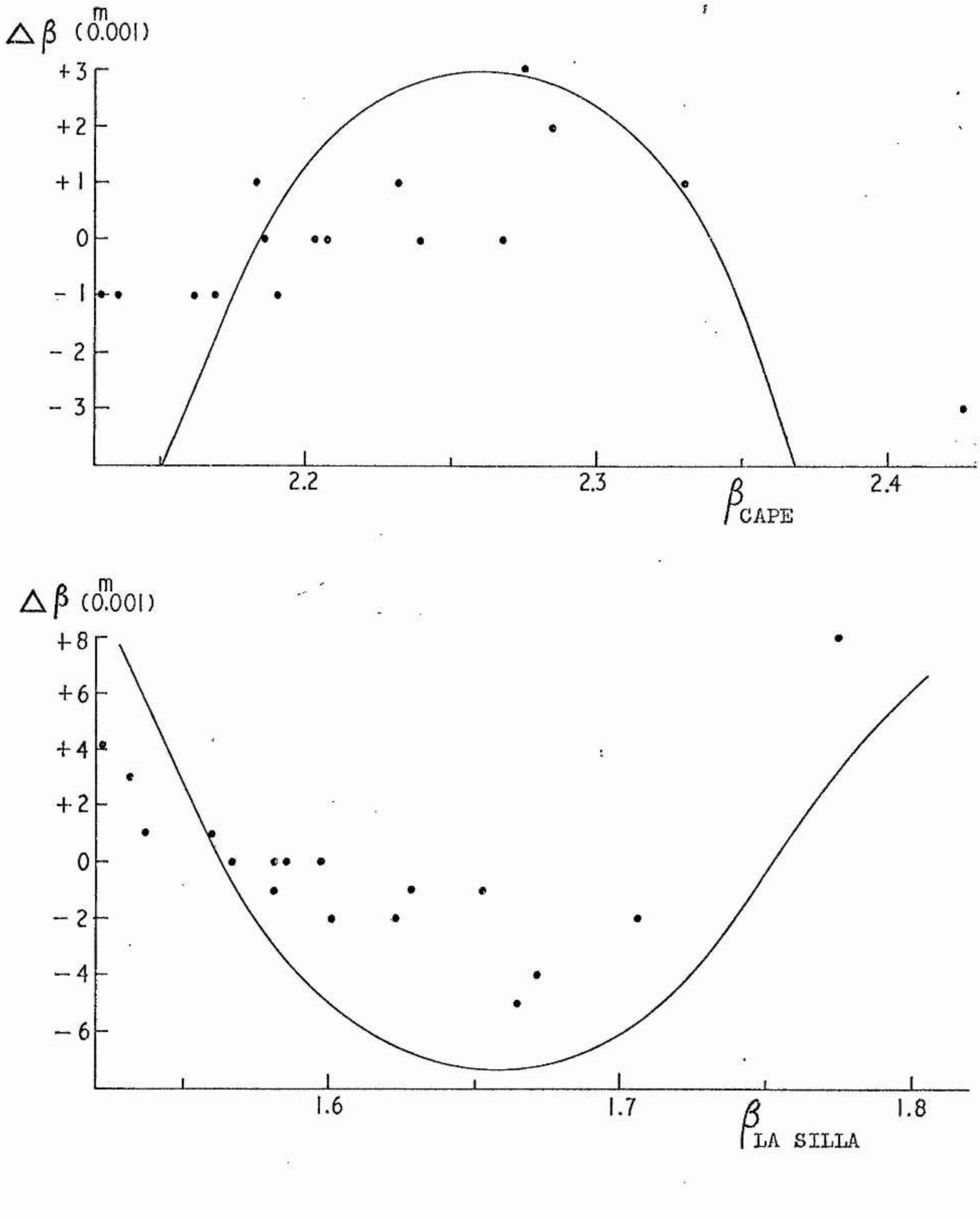

Fig. A4 Simulated curvature compared with observed curvature.

Filled circles are $\Delta\beta$ (standard - 'calculated standard') from simulated transformations in figures A2 & A3 . Solid lines are observed transformation curvatures from figures 8 & 9 .

filters is non-negligible and is likely to produce a substantial proportion of the observed transformation curvature.

Appendix II

SPACE VELOCITY COMPONENTS

The conversion of stellar tangential and radial velocities, t_α, t_δ and V_r into velocity components U, V and W in a translational galactic frame of reference has been reviewed by Hill (1969b) and will be briefly described in this appendix together with a Fortran programme to compute U, V and W with corrections for differential galactic rotation and the solar motion relative to the local standard of rest.

1. From observed to galactic velocity components

Observed components of stellar motion are radial velocity V_r and proper motions in equatorial co-ordinates, μ_α and μ_δ. The latter must be converted into velocities tangential to the celestial sphere. Usually μ_δ is given in seconds of arc per annum and μ_α in seconds of time per annum so that

$$\mu_\alpha \text{ (arcseconds)} = 15 \cos\delta \,.\, \mu_\alpha \text{ (seconds of time)}$$

When μ_α is used in this appendix it will be μ_α(arcseconds). Since stellar proper motions are always very small, tangential velocities can be written

$$t_\alpha = Kr\mu_\alpha \qquad\qquad t_\delta = Kr\mu_\delta$$

where r is stellar distance in parsecs and K = 4.738 is a conversion factor from parsec . arcseconds/annum to km/s. The velocity axes t_α, t_δ, V_r are dependent on the location of a star on the celestial sphere, so defining velocity axes $\dot{x}$, $\dot{y}$, $\dot{z}$, with $\dot{x}$ towards the vernal equinox, $\dot{y}$ towards $\alpha = 90^\circ$, $\delta = 0^\circ$ and $\dot{z}$ towards the north celestial pole, gives

$$\begin{aligned} \dot{x} &= -t_\alpha \sin\alpha - t_\delta \cos\alpha \sin\delta + V_r \cos\alpha \cos\delta \\ \dot{y} &= +t_\alpha \cos\alpha - t_\delta \sin\alpha \sin\delta + V_r \sin\alpha \cos\delta \qquad (A1) \\ \dot{z} &= t_\delta \cos\delta + V_r \sin\delta \end{aligned}$$

which are the equations (3.5) given by Trumpler and Weaver (1953, p. 265) and are equivalent to matrix equation (2) of Hill (1969b). Three rotations are required to convert $\dot{x}$, $\dot{y}$, $\dot{z}$ into U, V, W components and these are performed by Hill's equation (3)

$$\begin{bmatrix} U \\ V \\ W \end{bmatrix} = \begin{bmatrix} \cos l_0 & \sin l_0 & 0 \\ \sin l_0 & -\cos l_0 & 0 \\ 0 & 0 & 1 \end{bmatrix} \begin{bmatrix} 1 & 0 & 0 \\ 0 & \sin\delta_0 & -\cos\delta_0 \\ 0 & \cos\delta_0 & \sin\delta_0 \end{bmatrix} \begin{bmatrix} -\sin\alpha_0 & \cos\alpha_0 & 0 \\ \cos\alpha_0 & \sin\alpha_0 & 0 \\ 0 & 0 & 1 \end{bmatrix} \begin{bmatrix} \dot{x} \\ \dot{y} \\ \dot{z} \end{bmatrix} \qquad (A2)$$

where $\alpha_0 = 12^h\ 49^m$ and $\delta_0 = +27^\circ.4$ are the 1950.0 co-ordinates of the north galactic pole, and $l_0 = 33^\circ$ is the galactic longitude of the ascending node of the galactic plane on the celestial equator. Substituting, (A2) reduces to

$$\begin{bmatrix} U \\ V \\ W \end{bmatrix} = \begin{bmatrix} -0.066989 & -0.872756 & -0.483539 \\ +0.492729 & -0.450347 & +0.744585 \\ -0.867601 & -0.188375 & +0.460200 \end{bmatrix} \begin{bmatrix} \dot{x} \\ \dot{y} \\ \dot{z} \end{bmatrix} \qquad (A3)$$

Using (A1) and (A3) we can convert from t_α, t_δ, V_r to U, V, W velocity axes where U is directed towards the galactic centre, V is in the direction of galactic rotation and W is directed towards the north galactic pole.

2. The solar motion

In theory, correction for the solar motion relative to the local standard of rest is simple. If the solar motion is represented by components $U_\odot$, $V_\odot$, $W_\odot$ then the radial velocity of a star relative to the local standard of rest is given by

$$V_* = V_{obs} + U_\odot \cos l \cos b + V_\odot \sin l \cos b + W_\odot \sin b$$

where V_{obs} is the radial velocity of a star relative to the sun and l, b are the star's galactic co-ordinates. For the solar motion, weighted mean results of Feast and Shuttleworth (1965) have been used in all calculations. These are

$$U_{\odot} = +10 \pm 0.5 \text{ km/s} \qquad V_{\odot} = +13 \pm 0.5 \text{ km/s} \qquad W_{\odot} = +6 \text{ km/s}$$

and have the advantage of being determined from early-type stars. Errors introduced into stellar velocities by errors in the solar motion will be small compared with errors from other sources such as proper motion data or distance determination errors which will affect corrections for differential galactic rotation.

3. Correction of radial velocities for differential galactic rotation

Represented in fig. A5 are the local standard of rest, A, with a galactocentric distance R_o and circular velocity Θ_o, and a distant standard of rest, B, with galactocentric distance R and circular velocity Θ; 1 is the galactic longitude of B.

Fig. A5

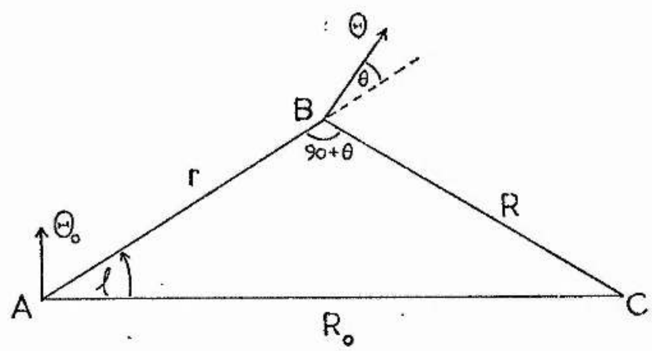

The radial velocity of B relative to A is the observed velocity due to differential galactic rotation and is given by

$$V_{BA} = \Theta \cos\theta - \Theta_o \sin 1$$

The sine formula in ABC gives

$$\cos\theta = \frac{R_o}{R} \sin 1$$

$$\therefore \quad V_{BA} = \Theta \frac{R_o}{R} \sin 1 - \Theta_o \sin 1$$

$$\therefore \quad V_{BA} = R_o \left(\Theta/_R - \Theta_o/_{R_o} \right) \sin 1$$

$$\therefore \quad V_{BA} = R_o \left[\omega(R) - \omega(R_o)\right] \sin 1$$

where $\omega(R_o)$ and $\omega(R)$ are the angular velocities about C of A and B respectively. The only assumption made is that A and B have circular orbits and for this reason the result is preferable to the Oort (1927) approximation formula which requires $^r/R_o$ to be small and is therefore restricted to within 1 or 2 kpc of the sun. For stars away from the galactic plane we have

$$V_{BA} = R_o \left[\omega(R) - \omega(R_o)\right] \sin l \cos b \qquad (A4)$$

In this case $\omega(R)$ should really be $\omega(R, z)$, a function of galactocentric distance and height above or below the galactic plane. However, $\omega(R, z)$ is not well known and use of $\omega(R)$ should not lead to great errors in most cases as the majority of programme stars have $z < 500$ pc.

To implement (A4), the function $\omega(R) - \omega(R_o)$ must be known. A determination of the function for B stars was made by Feast and Shuttleworth (1965) and compared with observations of the 21 cm. line of neutral hydrogen. Schmidt-Kaler (1967) revised the analysis using a slightly different value for the ratio of total to selective extinction, $A_V / E_{B-V} = 3.2$. Figure A6 is taken from Schmidt-Kaler's fig. 3 and is a comparison of the amended B star rotation curve and the Leiden 21 cm. curve (Kwee, Muller and Westerhout, 1954). The agreement appears to be good and it was decided to adopt this curve for the $\omega(R) - \omega(R_o)$ function. For Fortran programming, the curve must be in equation form and this was achieved by fitting five straight lines to the curve as illustrated in fig. A7. Originally, this was intended as a first approximation for trial purposes but the maximum difference between curve and straight lines is only about 0.5 km/s which compares favourably with errors in the B star mean points and is negligible when other sources of error in the correction for differential galactic rotation are considered. The straight line approximations were retained and are as follows:

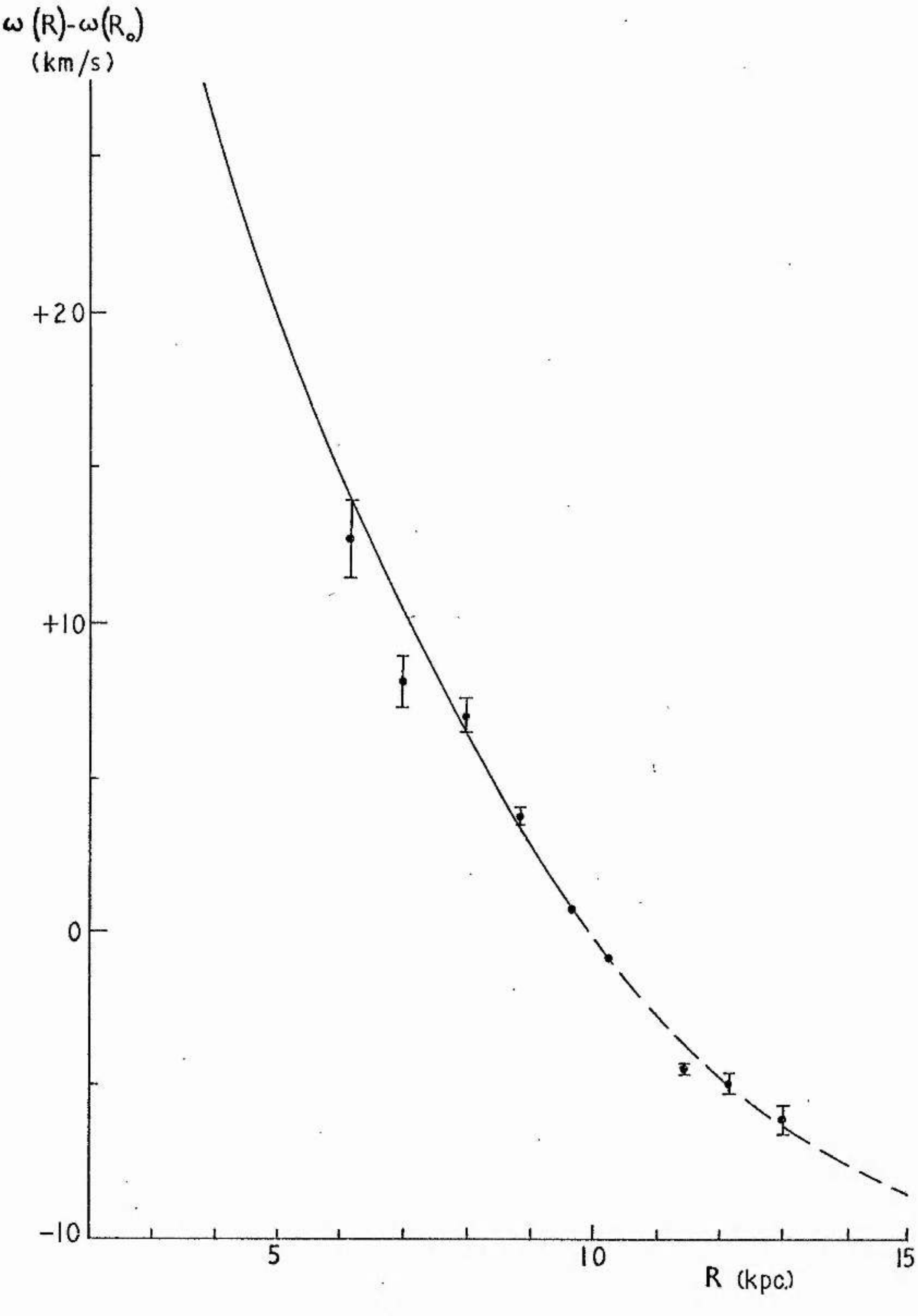

Fig. A6 Galactic rotation curve (Schmidt-Kaler, 1967). The solid line represents the Leiden 21-cm. rotation curve and the broken line is an extension based on the Schmidt (1965) mass model. Filled circles are Feast & Shuttleworth (1965) B star results with adjusted reddening corrections by Schmidt-Kaler (1967).

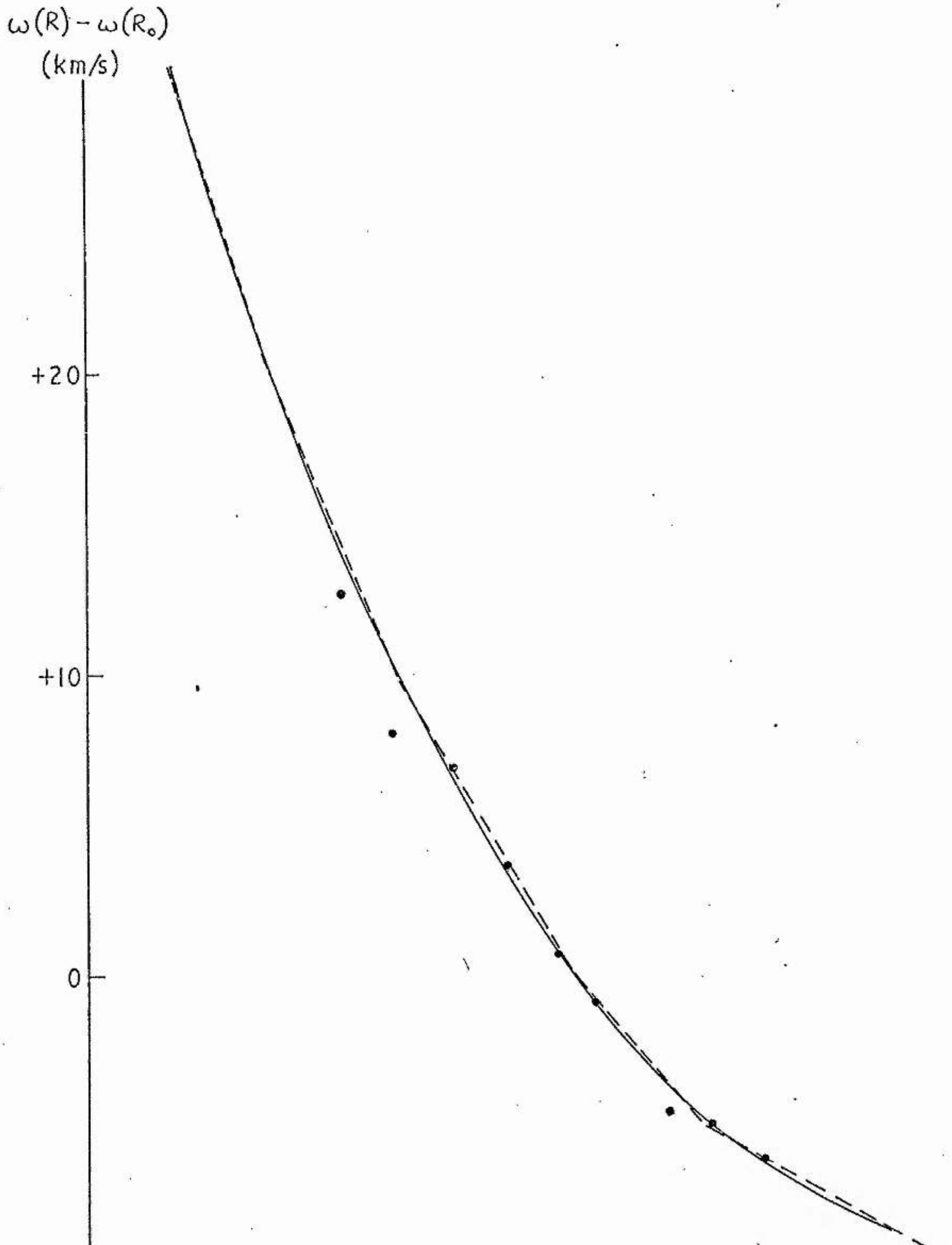

Fig. A7 Linear approximation to the rotation curve. Solid line and filled circles are from fig.A6 . Broken lines indicate the five straight lines approximating the curve in computation.

$$\begin{aligned}
R &< 5 \text{ kpc} & \omega &= -6.45\,R + 52.45 \\
5 \leqslant R &< 7 \text{ kpc} & \omega &= -4.88\,R + 44.40 \\
7 \leqslant R &< 10 \text{ kpc} & \omega &= -3.33\,R + 33.33 \\
10 \leqslant R &< 12 \text{ kpc} & \omega &= -2.50\,R + 25.00 \\
12 \leqslant R & & \omega &= -1.16\,R + 8.93
\end{aligned} \qquad (A5)$$

R is the galactocentric distance in kiloparsecs and $\omega = \omega(R) - \omega(R_o)$. For $R < 4$ and $R > 15$ kpc the function is uncertain, being dependent on theoretical models; the linear approximations will also be unreliable.

With equations (A5) substituted in (A4), corrections for the effect of differential galactic rotation can be applied to programme star radial velocities. Also, V_{BA} in equation (A4) can be sketched for constant values of r, the distance from the sun, to show the expected distribution in galactic longitude of observed radial velocities. Figure A8 shows results for r = 1, 2, 3 and 4 kpc with R_o = 10 kpc and is the well known "double wave" when sketched for all longitudes. Asymmetry of the wave for large r is already noticeable at r = 2 kpc. Figure A8 was useful as an overlay for plots of programme star velocities.

4. <u>Correction of proper motion for differential galactic rotation</u>

In a similar manner to the derivation of equation (A4) we can obtain equations for observed tangential velocities due to differential rotation of a distant standard of rest and the local standard of rest about the galactic centre. In galactic orientation of proper motion co-ordinates we obtain

$$t_l = R_o\,[\omega(R) - \omega(R_o)] \cos l - r.\omega(R) \cos b$$
$$t_b = -V_{BA} \tan b$$

where the function $\omega(R, z)$ is again approximated by $\omega(R)$. These equations can be re-written

$$Kr\,\mu_l \cos b = R_o\,[\omega(R) - \omega(R_o)][\cos l - \frac{r \cos b}{R_o}] - \omega(R_o) r \cos b$$
$$Kr\,\mu_b = -R_o\,[\omega(R) - \omega(R_o)] \sin l \sin b \qquad (A6)$$

giving $\mu_l \cos b$ and μ_b in arcseconds per annum. The function $\omega(R) - \omega(R_o)$

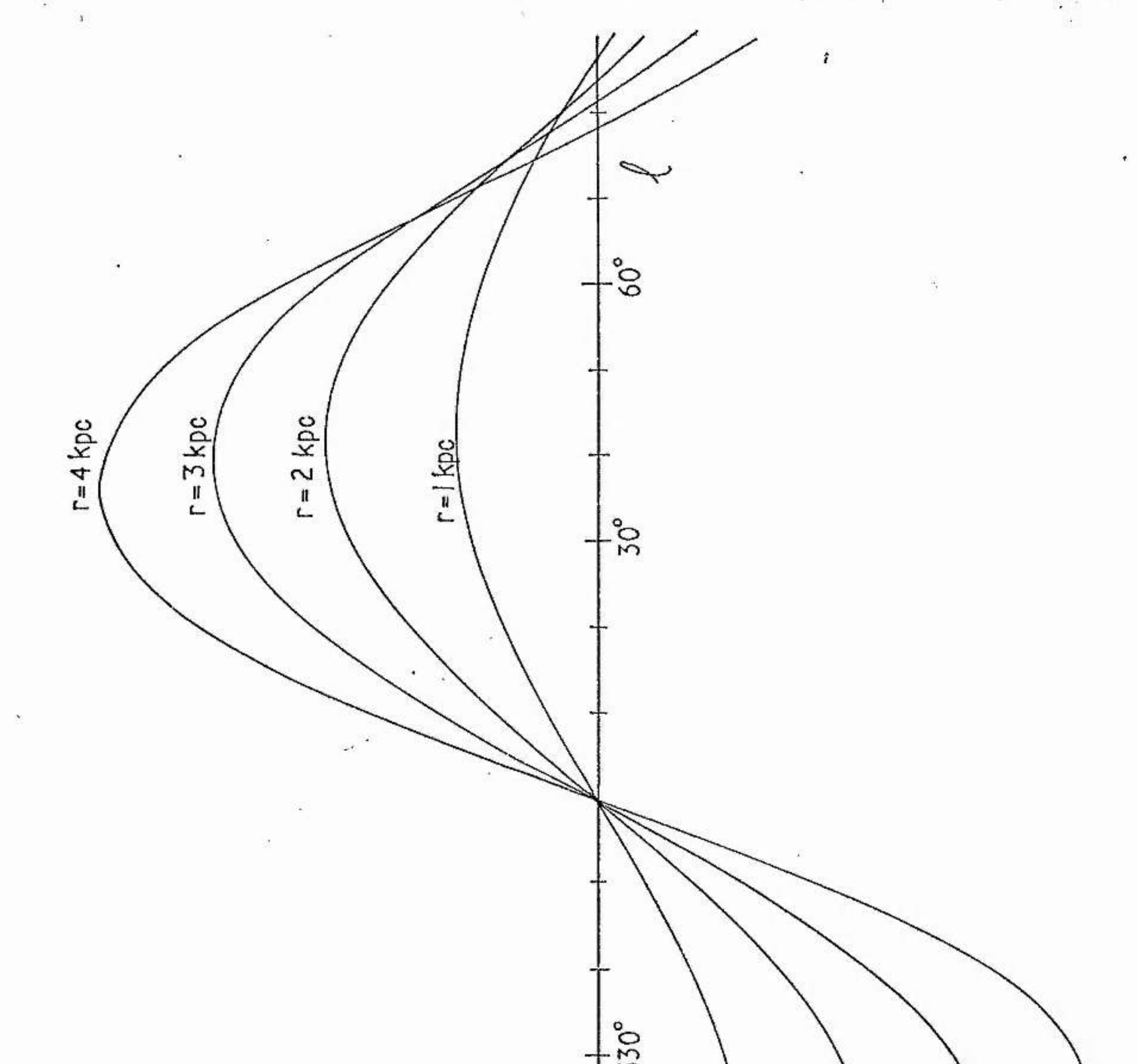

Fig. A8 Effect of differential galactic rotation on radial velocities.

is as described in section 3. With standard values for R_o and the circular velocity at R_o of 10 kpc and 250 km/s respectively, then $\omega(R_o)$ = 25 km/s/kpc for the last quantity in the expression for μ_l. Figure A9 illustrates the effect of differential galactic rotation on μ_l for stars in the galactic plane at distances of 0.5, 2.5 and 5 kpc from the sun, computed with the first of equations (A6). It can be seen that the effect is smaller than the standard deviation of the proper motion for a typical early-type star.

The effect can be converted from galactic to equatorial components of proper motion. By resolution of components sketched in fig. A10 (a) we have

$$\begin{aligned} \mu_\alpha &= \mu_l \cos b \cos\phi - \mu_b \sin\phi \\ \mu_\delta &= \mu_l \cos b \sin\phi + \mu_b \cos\phi \end{aligned} \qquad \text{(A7)}$$

where μ_α is in arcseconds. ϕ is sometimes referred to as the galactic parallactic angle and is the angle between north galactic and north celestial poles at the star under consideration (fig A10). From the spherical triangle NCP–NGP–S in fig. A10 (b), the cosine formula gives

$$\cos\phi = \frac{\sin\delta_o - \sin\delta \sin b}{\cos\delta \cos b} \qquad \text{(A8)}$$

where $\delta_o = +27^\circ.4$ is the declination of the north galactic pole. Equations (A6) determine corrections μ_b and μ_l cos b which, when substituted with (A8) into (A7), give the required corrections to the observed proper motion components μ_α and μ_δ .

5. A Fortran IV programme

The short programme following this section is a simplified version of the original but contains the essential corrections described in this appendix. Input is star number, equatorial co-ordinates for the epoch 1950.0, galactic co-ordinates, star distance in parsecs, radial velocity corrected to the sun and proper motion components μ_α and μ_δ in

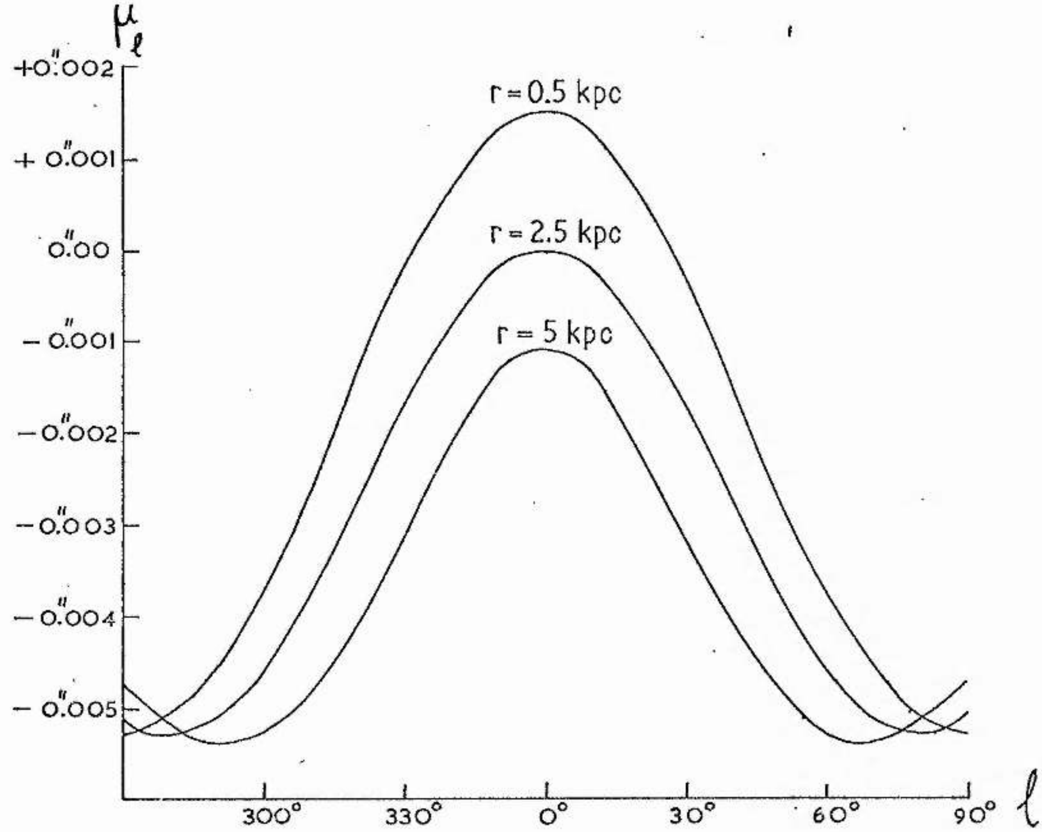

Fig. A9 Effect of differential galactic rotation on galactic longitude proper motion component.

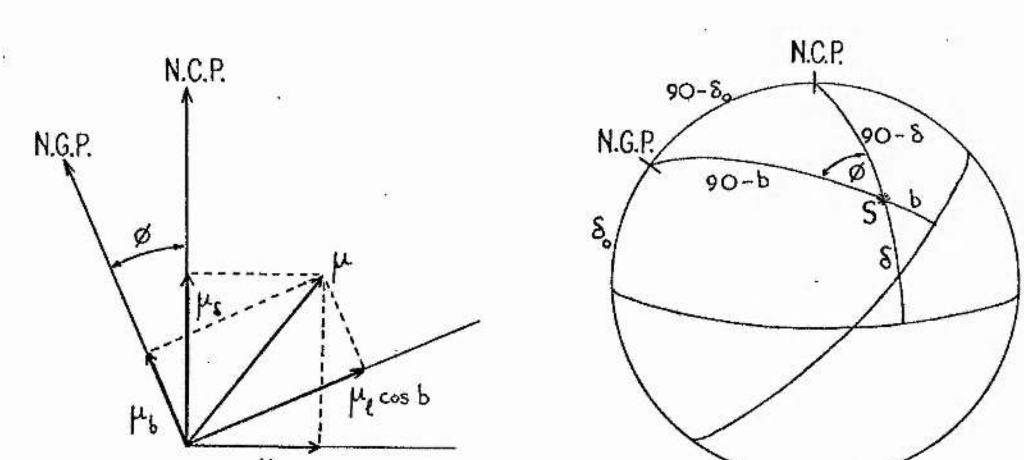

Fig. A10 Conversion from equatorial to galactic proper motion components.

arcseconds. The programme converts equatorial and galactic co-ordinates into radians and calculates the sine and cosine of α, δ, l and b using standard library trigonometric functions (statements 18 - 35). The distance of the star projected on to the galactic plane and distance from the plane are computed and, with the assumption $R_\odot = 10$ kpc, the galactocentric distance of the star is determined (43 - 47). Statements 51 - 55 correct the radial velocity to the local standard of rest using the solar motion derived by Feast & Shuttleworth (1965). The function $\omega(R) - \omega(R_o)$ is determined in statements 66 - 70, which are equivalent to equations (A5), and the corrected radial velocity is computed (71). Statements 78 and 79 represent equations (A6) for the effect of differential galactic rotation on proper motion components μ_l and μ_b. The sine and cosine of the galactic parallactic angle are found (78 - 83) and the corrections to μ_α and μ_δ are determined and applied (84 - 93). Tangential velocities are computed (97, 98), then the matrix corresponding to equations (A1) is formed and multiplied by the 3 x 3 matrix in (A3) to give the space motions U, V and W (100 - 131). The subroutine MATRIX simply multiplies a 3 x 1 matrix with a 3 x 3 matrix and returns the product 3 x 1 matrix to the main programme. The total space motion is calculated (133 - 136) and the remainder of the programme is output control.

The original programme input was star number, equatorial co-ordinates (1950.0), observed magnitude and colours (UBV), $(B-V)_o$, absolute magnitude, radial velocity and proper motion components. It had a subroutine to compute galactic co-ordinates and, after correcting V-magnitude for interstellar extinction, computed U, V and W velocity components for a range of absolute magnitudes including the input value. This was done with and without proper motion components for each case. The programme in this form was very useful for investigating stars in detail, testing the effect of different distance moduli on the kinematical properties of high velocity stars, possible subdwarfs and other interesting stars.

```
      IMPLICIT REAL*8(A-H,O-Z)
      DIMENSION NAME(3),SE(3,3),EG(3,3),VEL(3),XYZ(3),UVW(3)
C
   98 WRITE(6,99)
   99 FORMAT('1',1X,'HD/CPD',4X,'L',6X,'B',4X,'DIST',2X,'VEL',3X,'MU(A)'
     *,2X,'MU(D)',' R', '     GCD',3X,'RVC',3X,'MU(A)C', 1X,'MU(D)C',6X,'U
     *',7X,'V',7X,'W',4X,'SPACE',/)
      ICOUNT=0
  100 READ(5,150) ID,IHR,RAM,IDG,MIN,GII,BII,IR,IRV,C,UA,UD,MC
  150 FORMAT( 2X,I7,1X,I3,F5.1,I4,I3,2X,2F6.2,I5,2X,I4,A1,2F8.3,A2)
      IF(ID.GT.1000000) GO TO 899
      IF(IR.EQ. 0) GO TO 100
  180 CONTINUE
      ICOUNT=ICOUNT+1
      R=DFLOAT(IR)
      RV=DFLOAT(IRV)
C
      IF(IDG.LT.0) MIN=-MIN
      DEC=60.0D0*DFLOAT(MIN+(60*IDG))
      MIN=IABS(MIN)
      RAT=60.0D0*(RAM+DFLOAT(60*IHR))
      RA=15.0D0*RAT
      A= RA/206264.806
      D=DEC/206264.806
      RB2=(BII*3600.0D0)/206264.806
      RL2=(GII*3600.0D0)/206264.806
C
      SA=DSIN(A)
      CA=DCOS(A)
      SD=DSIN(D)
      CD=DCOS(D)
      SL=DSIN(RL2)
      CL=DCOS(RL2)
      SB=DSIN(RB2)
      CB=DCOS(RB2)
```

```
C
C     RO = GALACTOCENTRIC DISTANCE OF SUN IN PARSECS (RO = 10000)
C     R  = SUN - STAR DISTANCE (DIRECT)
C     RS = SUN - STAR DISTANCE PROJECTED ONTO GALACTIC PLANE
C     RC = GALACTOCENTRIC DISTANCE OF STAR PROJECTED ONTO GALACTIC PLANE
C     RZ = DISTANCE OF STAR FROM GALACTIC PLANE
C
      RS=R*CB
      RZ=R*SB
      RO=10000.0D0
      RQ=RS*RS+RO*RO-2.0D0*RS*RO*CL
      RC=DSQRT(RQ)
C
C     CORRECTION FOR SOLAR MOTION RELATIVE TO LOCAL STANDARD OF REST
C
      UO=10.0D0
      VO=13.0D0
      WO=6.0D0
      CORR=UO*CL*CB+VO*SL*CB+WO*SB
      RW=RV+CORR
C
C     CORRECTION FOR DIFFERENTIAL GALACTIC ROTATION
C
      RK = R/1000.0D0
      RSK=RS/1000.0D0
      RCK=RC/1000.0D0
      ROK=RO/1000.0D0
      MARK=0
      IF(RCK.LT.4.0) MARK=1
      IF(RCK.GT.15.0)MARK=2
      IF(RCK.GE. 0.0.AND.RCK.LT. 5.0) OMEGA=-6.45*RCK+52.25
      IF(RCK.GE. 5.0.AND.RCK.LT. 7.0) OMEGA=-4.88*RCK+44.40
      IF(RCK.GE. 7.0.AND.RCK.LT.10.0) OMEGA=-3.33*RCK+33.33
      IF(RCK.GE.10.0.AND.RCK.LT.12.0) OMEGA=-2.50*RCK+25.00
      IF(RCK.GE.12.0)                 OMEGA=-1.16*RCK+ 8.93
      RVP=RW-ROK*OMEGA*SL*CB
```

```
C
      IC=IDINT(RC)
      IZ=IDINT(RZ)
      IVP=IDINT(RVP)
      ICO=IVP-IRV
C
      RKUL=(ROK*OMEGA*(CL-RSK/ROK))-25.0D0*RSK
      RKUB=-(ROK*OMEGA*SL*SB)
      UL=RKUL/(4.738*R)
      UB=RKUB/(4.738*R)
      CPHI=(0.4602-SD*SB)/(CD*CB)
      SPHI=DSQRT(1-CPHI*CPHI)
      UAC=UL*CPHI-UB*SPHI
      UDC=UL*SPHI+UB*CPHI
C
      IF(UA.NE.0.0.OR.UD.NE.0.0) GO TO 300
  301 UAC=0.00
      UDC=0.00
  300 CONTINUE
C
      UAP=UA-UAC
      UDP=UD-UDC
C
C     CONVERSION OF PROPER MOTIONS TO VELOCITIES
C
      TA=4.738*UAP*R
      TD=4.738*UDP*R
C
      VEL(1)=TA
      VEL(2)=TD
      VEL(3)=RVP
      SPVEL=DSQRT(TA*TA+TD*TD+RVP*RVP)
```

```
C
C     CONVERSION FROM OBSERVED TO EQUATORIAL VELOCITY AXES
C
      SE(1,1)=-SA
      SE(1,2)=-CA*SD
      SE(1,3)=CA*CD
      SE(2,1)=CA
      SE(2,2)=-SA*SD
      SE(2,3)=SA*CD
      SE(3,1)=0.0D0
      SE(3,2)=CD
      SE(3,3)=SD
C
      CALL MATRIX(SE,VEL,XYZ)
C
C     CONVERSION FROM EQUATORIAL TO LOCAL GALACTIC VELOCITY AXES
C
      EG(1,1)=-0.066989
      EG(1,2)=-0.872756
      EG(1,3)=-0.483539
      EG(2,1)=+0.492729
      EG(2,2)=-0.450347
      EG(2,3)=+0.744585
      EG(3,1)=-0.867601
      EG(3,2)=-0.188375
      EG(3,3)=+0.460200
C
      CALL MATRIX(EG,XYZ,UVW)
C
```

```
      US=UVW(1)
      VS=UVW(2)
      WS=UVW(3)
      SPUVW=DSQRT(US*US+VS*VS+WS*WS)
C
      WRITE(6,500) ID,GII,BII,IR,IRV,C,UA,UD,MC,IC,IVP,UAP,UDP,US,VS,WS,
     *SPUVW
  500 FORMAT(I8,2F7.2,I6,I5,A1,2F7.3,A2,I7,I6,2X,2F7.3,4F8.1)
      IF(MARK.EQ.0) GO TO 600
      WRITE(6,550)
  550 FORMAT('+',111X,'***')
  600 CONTINUE
C
      IF(ICOUNT.EQ.40) GO TO 98
      GO TO 100
  899 WRITE(6,900)
  900 FORMAT('1')
      STOP
      END

      SUBROUTINE MATRIX(A,B,C)
C
C     MATRIX MULTIPLICATION : C(3*1)=A(3*3)*B(3*1)
C
      IMPLICIT REAL*8(A-H,O-Z)
      DIMENSION A(3,3),B(3),C(3)
C
      DO 1 K=1,3
      C(K)=A(K,1)*B(1)+A(K,2)*B(2)+A(K,3)*B(3)
    1 CONTINUE
C
      RETURN
      END
```

Acknowledgements

I am indebted to my supervisor, Dr.P.W.Hill, for advice and encouragement and for assistance with observation at the Radcliffe and European Southern Observatories. I am most grateful to the directors and staffs of St. Andrews University Observatory, The Royal Observatory, Cape Town, Radcliffe Observatory and the European Southern Observatory. In each establishment I found useful advice freely given and assistance with matters academic and non-academic on many occasions. It is a pleasure to record thanks to Mr.J.B.Alexander , my acting supervisor at the Cape, for guidance and personal kindness, and to Dr.D.L.Crawford of Kitt Peak National Observatory who has communicated pre-publication results of his Hβ photometry on several occasions. This material has been invaluable to my own research.

I am grateful to the Large Telescope Users Panel for observing time on the Radcliffe (Pretoria) and Elizabeth (Cape) telescopes and to the Astronomischen Institute der Ruhr-Universität Bochum for a generous observing allocation on their telescope at the E.S.O. site in Chile. I should like to thank Prof. Schmidt-Kaler for suggesting I apply for time on the latter instrument which provided valuable narrow band data.

My work for this dissertation was supported by a research studentship from the Science Research Council and later by a scholarship from the University of St. Andrews. My visits to South Africa and Chile were financed by S.R.C. travel and subsistence allowances. I am indebted to the S.R.C. and University Awards Committee for the various grants which made observation and research possible.

I am grateful to Miss S.Easton for typing the final draft of the thesis.

References

Abt, H.A. & Biggs, E.S. (1972) "Bibliography of Radial Velocities" Kitt Peak National Observatory

Abt, H.A. & Golson, J.C. (1962) Ap.J. 136 , 363

Abt, H.A. & Osmer, P.S. (1965) Ap.J. 141 , 949

Allen, C.W. (1963) "Astrophysical Quantities" 2nd ed., Athlone

Alter, G., Balázs, B. & Ruprecht, J. (1970) "Catalogue of star clusters and Associations" 2nd ed., Budapest

Alter, G. & Ruprecht, J. (1963) "The system of open star clusters and our Galaxy.Atlas of open clusters", Praha

Bappu, M.K.V., Chandra, S., Sanwal, N.B. & Sinvhal, S.D. (1962) M.N.R.A.S. 123 , 521

Barbaro, G., Dallaporta, N. & Fabris, G. (1969) Pub.Oss.Padova 154

Becker, W. (1964) Z.Astr. 58 , 202

Becker, W. & Fenkart, R. (1963) Z.Astr. 56 , 257
(1970) I.A.U. Symposium 38 , 205

Beer, A. (1962) M.N.R.A.S. 123 , 191

Berger, J., Fringant, A-M. & Rebeirot, E. (1970) Comptes R. Acad. Sci. Paris 273 , 271

Bertiau, F.C. (1958) Ap.J. 128 , 583

Blaauw, A. (1961) B.A.N. 15 , 265
(1963) in "Basic Astronomical Data" p.383 , Chicago

Blaauw, A., Gum, C.S., Pawsey, J.L. & Westerhout, G. (1960) M.N.R.A.S. 121 , 123

Blanco, V.M., Demers, S., Douglass, G.G., & FitzGerald, M.P. (1968) Pub. U.S. Naval Obs. 2nd series, vol. 21

Bok, B.J., Bok, P.F. & Graham, J.A. (1964) P.A.S.P. 75 , 514

Butler, H.E. & Seddon, H. (1958) Pub.R.Obs.Edinburgh 2 , 111

Cannon, A.J. & Pickering, E.C. (1918-24) Ann. Harvard Obs 91 - 99

Courtès, G. (1967) I.A.U. Symposium 31 , 221

Cousins, A.W.J. (1966) M.N.A.S.S.A. 25 , 100
(1967a) Cape Mimeogram: "Mean magnitudes and colours of bright stars south of +10° declination"
(1967b) M.N.A.S.S.A. 26 , 151

Cousins, A.W.J. & Stoy, R.H. (1962) R. Obs. Bull. 49
(1963) R. Obs. Bull. 64

Crampton, D. & Byl, J. (1971) Pub. Dom. Astr. Obs. 13 , 427

Crawford, D.L. (1958) Ap.J. 128 , 185
(1960) Ap.J. 132 , 66
(1964) I.A.U. Symposium 24 , 170
(1972) I.A.U. Symposium 54 , (in press)

Crawford, D.L., Barnes, J.V. & Golson, J.C. (1970) A.J. 75 , 624

Crawford, D.L. & Mander, J. (1966) A.J. 71 , 114

Cruvellier, P. (1967) Ann. Astrophys. 30 , 1072

Edlèn, M.B. (1955) Trans. I.A.U. 9 , 220

Evans, D.S., Menzies, A. & Stoy, R.H. (1959) M.N.R.A.S. 119 , 638

Feast, M.W. & Shuttleworth, M. (1965) M.N.R.A.S. 130 , 245

Feast, M.W., Stoy, R.H., Thackeray, A.D. & Weeselink, A.J.
(1961) M.N.R.A.S. 122 , 239

Feast, M.W. & Thackeray, A.D. (1958) M.N.R.A.S. 118 , 125
(1963) Mem.R.A.S. 68 , 173

Feast, M.W., Thackeray,A.D. & Wesselink, A.J.
(1955) Mem.R.A.S. 67 , 51
(1957) Mem.R.A.S. 68 , 1

Fernie, J.D. (1965) A.J. 70 , 575

FitzGerald, M.P. (1970) Astronomy & Astrophysics 4 , 234

Gill, D. & Kapteyn (1899) Ann. Cape Obs. iv & v

Graham, J.A. (1964) I.A.U. Symposium 20 , 71
(1967) M.N.R.A.S. 135 , 377
(1970) I.A.U. Symposium 38 , 262

Greenstein, J.L. (1971) I.A.U. Symposium 42 , 46

Gum, C.S., Kerr, F.J. & Westerhout, G. (1960) M.N.R.A.S. 121 , 132

Hagen, G.L. (1970) Pub. David Dunlap Obs. 4 "An atlas of open cluster colour-magnitude diagrams"

Hardie, R.H. (1964) I.A.U. Symposium 24 , 243

Hardie, R.H. & Crawford, D.L. (1961) Ap.J. 133 , 843

Herrick, S. (1935) Lick Obs. Bull. 470

Hill, P.W. (1964) M.N.R.A.S. 127 , 113
(1965a) M.N.R.A.S. 129 , 137
(1965b) Observatory 85 , 41
(1968) Observatory 88 , 163
(1969a) I.A.U. Inf. Bull. on var. stars No. 357
(1969b) M.N.A.S.S.A. 28 , 45
(1970) M.N.R.A.S. 150 , 23
(1971) Mem.R.A.S. 75 , 1

Hill, P.W. & Hill, S.R. (1966) M.N.R.A.S. 133 , 305

Hiltner, W.A. & Johnson, H.L. (1956) Ap.J. 124 , 367

Hoffleit, D. (1967) Trans. Astr. Obs. Yale vol. 28
(1968) Trans. Astr. Obs. Yale vol. 29

Hoffleit, D., Eckert, D., Lü, P.K. & Paranya, K.
(1970) Trans. Astr. Obs. Yale vol. 30

Hoyle, F. (1960) M.N.R.A.S. 120 , 22

Iben, I. (1967) Ann. Rev. Astr. & Astrophys. 5 , 571
(1972) I.A.U. Colloquium 17
(1972) in "Stellar Evolution" p.62 , M.I.T.

Isserstedt, J. (1968a) Veröff. Astr. Inst. Univ. Bochum 1 , 1
(1968b) Veröff. Astr. Inst. Univ. Bochum 1 , 121

Jackson, J. (1951) Nature 167 , 169

Jaschek, C., Conde, H. & de Sierra, A.C. (1964) "Catalogue of stellar spectra classified on the Morgan-Keenan system" , La Plata

Johnson, H.L. (1958) Lowell Obs. Bull. 4 , 37
(1968) in "Nebulae and Interstellar matter" p.167

Johnson, H.L. & Iriarte, B. (1958) Lowell Obs. Bull. 4, 47

Johnson, H.L. & Morgan, W.W. (1953) Ap.J. 117 , 313

Kepner, M. (1970) Astr. & Astrophys. 5 , 444

Kerr, F.J. (1970) I.A.U. Symposium 38 , 95

Kraft, R.P. & Schmidt, M. (1963) Ap.J. 137 , 249

Kwee, K.K., Muller, C.A. & Westerhout, G. (1954) B.A.N. 12 , 221

Lindholm, E.H. (1957) Ap.J. 126 , 588

Lü, P.K. (1971) Trans. Astr. Obs. Yale vol. 31

Lundmark, K. (1926) Upsala Obs. Medd. No.12

McCuskey, S.W. (1970) I.A.U. Symposium 38 , 189

Mihalas, D. (1964) Ap.J.Suppl. 9 , 321

Morgan, W.W., Code, A.D. & Whitford, A.E. (1955) Ap.J.Suppl 2 , 41

Morgan, W.W., Harris, D.L. & Johnson, H.L.(1953) Ap.J. 118 , 92

Morgan, W.W., Keenan, P.C. & Kellman, E. (1943) "An atlas of stellar spectra" , Chicago

Morgan, W.W., Whitford, A.E. & Code, A.D. (1953) Ap.J. 118 , 318

Neubauer, F.J. (1943) Ap.J. 97 , 300

Oort, J.H. (1927) B.A.N. 3 , 275
(1928) B.A.N. 4 , 269
(1960) B.A.N. 15 , 45

Pearce, J.A. (1932) Trans. I.A.U. 4 , 187

Petrie, R.M. (1953a) Pub. Dom. Astr. Obs. 9 , 251
(1953b) Pub. Dom. Astr. Obs. 9 , 297
(1956a) Pub. Dom. Astr. Obs. 10 , 287
(1956b) Vistas in Astronomy 2 , 1346
(1958) M.N.R.A.S. 118 , 82
(1962) M.N.R.A.S. 123 , 501

Plaskett, J.S. & Pearce, J.A. (1931) Pub. Dom. Astr. Obs. 5 , 99

Rohlfs, K. (1967) Z.Astr. 66 , 225

Ruprecht, J. (1964) Trans. I.A.U. 12B , 347

Schmidt, M. (1965) B.A.N. 13 , 15

Schmidt, H. & Diaz Santanilla, G. (1964) Veroff.Astr.Inst.Bonn 71

Schmidt-Kaler, Th. (1964a) Z.Astr. 58 , 217
(1964b) Veröff. Astr. Inst. Univ. Bonn 71
(1965) in "Numerical data and functional relationships in science and technology" Group VI, Vol. 1, p.307, Springer-Verlag.
(1967) I.A.U. Symposium 31 , 161
(1968a) Veröff. Astr. Inst. Univ. Bochum 1 , 80
(1968b) Veröff. Astr. Inst. Univ. Bochum 1 , 144
(1971) in "Structure and Evolution of the Galaxy" p.85 , Reidel

Schmidt-Kaler, Th. & Dachs, J. (1969) E.S.O. Bull. 5

Searle, L., Sargent, W.L.W. & Jugaku, J. (1963) Ap.J. 137 , 278

Smith, L.F. (1968) M.N.R.A.S. 141 , 317

Smithsonian Astrophysical Observatory Star Catalogue (1966) U.S. Govt.

Stephenson, C.B. & Sanduleak, N. (1971) Pub. Warner & Swasey 1 , 1

Stock, J. (1969) Vistas in Astronomy 11 , 127

Stoy, R.H. (1964) M.N.A.S.S.A. 23 , 56
(1966) Ann. Cape Obs. 21

Thackeray, A.D. (1954) M.N.R.A.S. 114 , 93
(1962) Observatory 82 , 72
(1966) Mem.R.A.S. 70 , 33

Thackeray, A.D. & Wesselink, A.J. (1952) Observatory 72 , 248

Thackeray, A.D., Tritton, K.P. & Walker, E.N. (1973) in press

Torgard, I. (1961) Ann. Obs. Lund 15

Trumpler, R.J. & Weaver, H.F. (1953) "Statistical Astronomy", Calif.

Wackerling, L.R. (1970) Mem.R.A.S. 73 , 153

Walker, M.F. (1957) Ap.J. 125 , 636

Wallis, R.E. & Clube, S.V.M. (1968) M.N.A.S.S.A. 28 , 59

Weaver, H. (1970) I.A.U. Symposium 38 , 126

Whitford, A.E. (1958) A.J. 63 , 201

Willstrop, R.V. (1965) Mem.R.A.S. 69, 93

Wilson, R. (1956) Pub. R. Obs. Edinburgh 2 , 3